

Editorial Board

Dr. Mohammad I. Malkawi

Associate Professor, Department of Software Engineering

Jordan

Dr. Kaveh Ostad-Ali-Askari

Assistant Professor, Department of Civil Engineering, Isfahan (Khorasgan) Branch,

Iran

Dr. Mohammed A. Akour

Associate Professor in the Department of Software Engineering,

Jordan

Dr. Mohammad mehdi hassani

Faculty of Computer Engineering

Iran

Prof.Ratnakaram Venkata Nadh (Ph.D)

Professor & Head - Chemistry Department, Dy. Director - Admissions

India

Dr. SIDDIKOV ILKHOMJON KHAKIMOVICH

Head of the Department of “Power Supply Systems”,

Uzbekistan

Dr.S.DHANASEKARAN

Associate Professor in the Department of Computer Science and Engineering,

India

Younes El Kacimi, Ph. D.

Science Faculty, Depatment of Chemistry Kénitra

Morocco

Denis Chemezov

Lecturer, Vladimir Industrial College, Vladimir

Russia

RICHARD O. AFOLABI, Ph.D.

Department of Petroleum Engineering,

Nigeria

Volume 6 ISSUE 1

January-February 2022

On Direct Determination of Shear Force Taken UP By Concrete in Oblique Cross-Sections of Reinforced Concrete Structures **01-10**

Aleksei N. Morozov

Effect of Tool Pin Profile of Underwater Friction Stir Welding of Dissimilar Materials Aa5083 and Aa6061-T6 **11-18**

MUHAMMED ZAKARIYA Hasnol || MOHD FARIDH Ahmand Zaharuddin || SAFIAN Sharif || SEHUN Rhee

Analysis of Passenger's Interest on Transportation of the Urban Environment in Tuban Indonesia **19-29**

Sugiyanto || Cicik Nur Indah

The Contribution of LCA Applications to the Development of National Ecolabel Criteria for the Personal Care and Cosmetic Sector **30-40**

Nilgün Kiran Ciliz || Cennet Degirmen || Merve Uzun || Ceyda Kalipçioğlu || Iman Abdulkadir Ahmed ||

Mehmet Emin Birpınar || Mehrali Ecer || Eyüp Kaan Morali || Serkan Atay || Ömer Ulutas || Zeynep Aki ||

Kemal Dag || Yahya Kesimal

Categorization of recommender system methods **41-48**

Chiheb Eddine Ben Ncir

A Comparative Study between Semi-Analytical Iterative Schemes for the Reliable Treatment of Systems of Coupled Nonlinear Partial Differential Equations **49-69**

Liberty Ebiwareme

Optimization of Dressing Conditions When External Cylindrical Grinding to Minimize Surface Roughness **70-74**

Tran Phuong Thao

Thermal Properties of Chemically Prepared Emeraldine-Base Form Polyaniline **75-82**

AMER N. J AL-DAGHMAN

On Direct Determination of Shear Force Taken UP By Concrete in Oblique Cross-Sections of Reinforced Concrete Structures

Aleksei N. Morozov

Research Institute of Construction, Estonian State Committee, Tallin, Estonia

ABSTRACT

A method has been presented for the direct determination of shear force in oblique cross-sections of reinforced concrete structures using a classic formula $Q=bz\tau$, when the main problems of determining the shear force in oblique cross-sections are related to finding cleaving stresses in concrete and the shape of a stress-block of normal stresses in the design section, with no principles of practical division between the forms of failure in oblique sections due to concrete compression or shear. This work incorporates a criterion for dividing the forms of failure due to concrete compression or shear, based on the assumed shape of a compression stress-block with a segment cut away in a normal section, passing through the top of an inclined crack. The height of the compressed area in this normal section is defined from simultaneous solution of the equations of equilibrium in the moments in normal and oblique sections, from testing the experimental beams made of concrete and gas-concrete. This work deals with seeking the approaches for solving the above-mentioned problems in practice. The data of testing beams from gasconcrete and heavy-weight concrete have been used. Strain gauges were used to measure concrete and reinforcement deformities, computer processed thereafter. The studies have been considered on determination of cleaving stresses in oblique sections, further verified according to this method on certain alternative schemes of their application. A practical method for finding the shear force depending on the value of a shear span has been proposed. The work can encourage active discussion of this computation method.

Keywords: Direct determination of shear force in oblique cross-sections; Height of a compressed zone; Reinforced concrete elements in oblique sections; Lateral forces; Shear strength

I. INTRODUCTION

Although the known formula,

$$Q_b = bz\tau \quad (1)$$

for determining the shear force in oblique cross-sections, taken up by concrete, was derived about 100 years ago, it has not found any direct application so far, except for a constraint on its value. Thus, in the existing norms, where $z=h_0$ ($z=0,9h_0 - \tau_{max}=2,8R_{bt}$). One of the problems in using formula (1) lies in complexity of finding cleaving stresses – τ . If compression and tensile strength are defined by standard

tests, cleaving strength is very difficult to determine due to a complex strain-stress state (SSS) of heterogenous concrete in oblique cross-sections. Hence, behind the experimental data to develop this method for direct determination of the shear force in oblique sections were the results of testing beams made of gas-concrete (Morozov, 2018; 2019a, 2019b) without coarse aggregate, that makes SSS substantially heterogeneous and has low plasticity, what allows more accurate estimates of stresses to be made. The entire practice of experimental studies on this problem indicates that the SSS of the normal section, passing through the top of a critical inclined crack, is highly reflective of the shear force. Previously, the SSS of this section was considered in detail by A.S. Zalesov (1977a, 1977b, 1989) and other his works. The problem of using this section in practice as a design one is constrained by the shape of a stress-block for normal stresses therein. Thus, the simplest triangular shape of a stress-block of normal stresses in concrete is assumed in formula (1) and other works, devoted to the studies of the concrete SSS in oblique cross-sections.

Based on our works (Morozov, 1992, 2015), the closest to experimental data curve of normal stresses in concrete with a cut-out oriented towards the top of an inclined crack (see Figure 1) was assumed. According to this stress-block, there has been derived a formula of normal stresses

$$\sigma_b = \left(\frac{x_2^2}{x_0^2} - 1 + 2\omega\right)R_b \quad (2)$$

where $x_2 = x_0 - x_1$. Shear stresses from shear forces are calculated using formula (1) $\tau = \frac{Q}{bz}$ and are obtained from a balance of difference in normal stresses, acting in two parallel sections with distance dl between them. If this condition is considered for a point with the x_2 ordinate,

$$\int_{x_2}^{x_0} b dx_2 d\sigma_b = \tau b dl \text{ can be written. At } R_b = \frac{M}{\omega b x_0 z} \text{ taking (2) into account, we obtain -}$$

$$\sigma = \frac{M}{\omega b x_0 z} \left(\frac{x_2^2}{x_0^2} - 1 + 2\omega\right), \text{ from whence at } Q = \frac{dM}{dl} \tau b dl = \frac{Q_b dl}{\omega x_0 z} \int_{x_2}^{x_0} \left(\frac{x_2^2}{x_0^2} - 1 + 2\omega\right) dx_2 \text{ and}$$

$$\tau = \frac{Q_b}{bz} \left[\frac{1}{2\omega} \left(1 - \frac{x_2^2}{x_0^2}\right) + \left(2 - \frac{1}{\omega}\right) \left(1 - \frac{x_2}{x_0}\right) \right] \quad (3)$$

As per this formula, most failures in oblique cross-sections occur due to concrete compression, and maximum cleaving (shearing, when the SSS is plane) stresses correspond to the neutral axis, i.e. at $x_2 = 0$ and the expression in square brackets of formula (3)

$$m_0 = \frac{4\omega - 1}{2\omega} \quad (4)$$

which is a correction factor for formula (1) and at $\omega=0.5$ formula (4) is transformed into (1). When maximum shearing stresses are at the top of an inclined crack, i.e., at the x_2 ordinate, it corresponds to failure in oblique sections from concrete shear and the expression in square brackets of formula (3) - m_2 . Thus, the formula of shear force is as follows

$$Q_b = b z m \tau \quad (5)$$

It follows from the figure

$$\omega = 0.5 \left(1 + \frac{\sigma_b}{R_b} - \frac{x_2}{x_0} \right) \quad (6)$$

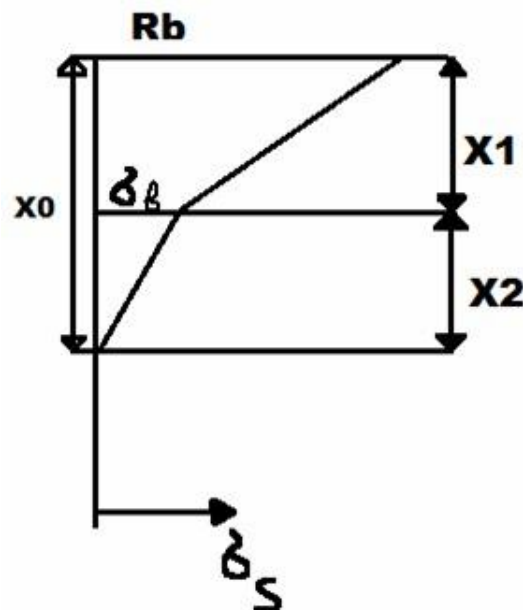


Figure 1. Design diagram of the normal section

(Morozov, 2019a, 2019b) present a comparison between the experimental values of completeness of a stress-block of normal stresses, computed using this formula, and measured values of this rate in (Morozov, 1985). Due to a low plasticity of gas-concrete, it was not taken into account at the last stages of loading, and measured deformities were accounted for. This comparison demonstrated their satisfactory convergence $\omega/\omega_{act} = 0.94 - 1.35$, – mean $\omega/\omega_{act} = 1.06$, $\sigma = 0.23$, what indicates that the assumed design model is appropriate. When oblique sections are broken up due to concrete compression, an equilibrium equation of moments of longitudinal and lateral forces (in normal and oblique crosssections) can be composed for a design section:

$\xi_0 \omega b h_0 R_b z = b z m \tau a$ from whence:

$$\xi_0 = \frac{x_0}{h_0} = \frac{\xi_R}{\omega} = \frac{m \tau a}{\omega R_b h_0} \quad (7),$$

what relates this calculation to the relative shear span $\frac{a}{h_0} = \frac{M}{Q h_0}$. Equilibrium equation of moments in the design section can be derived for a tensile area as well - $A_s \sigma_s z = b z m \tau a$, from whence $\mu \sigma_s = m \tau \frac{a}{h_0}$, what, when substituting into (6), gives $\xi_0 = \frac{\sigma_s \mu}{\omega R_b}$ and provides the results absolutely equal to (6), but requires that

$$\sigma_s = \frac{m \tau a}{\mu h_0} \quad (8)$$

is further determined.

These are the initial conditions for direct calculation of shear force in oblique sections.

The problems of computing the strength of oblique sections of reinforced concrete structures had started to be studied even at the onset of their use. Thus, in 1909 F. Talbot (1909) put forward an idea of transforming a beam with inclined cracks into a restraining system. In 1925, R. Saliger expressed an opinion that the beams with inclined cracks can be considered as bowstring girders. E. Mersch in 1927 proposed a method of so-called truss analogy, considering the compressed zone of concrete as a top chord of a truss, and tensile reinforcement as its bottom chord, compressed concrete of the wall as brace struts. It should be noted that E. Mersch was among the first to derive a classic formula (1). G. G. N. I. Kani (1966) thoroughly explored the effect of the value of a relative shear span in beams on the strength of oblique sections and found that their minimum strength corresponds to $a/h_0 = 2.5$, and when the values of this rate are lower than one and higher than 5-6, the strength of oblique sections becomes equal to the strength of normal sections. Among homeland works, devoted to the problems of strength of oblique crosssections, of note are fundamental works of A. A. Gvozdev (1949) and M. S. Borishanskiy (1946), based on which the norms of calculating strength in oblique cross-sections of reinforced concrete structures were developed. Writings of A. S. Zalesov (1977a) and other his publications were an extension of these works. Among the last publications on the problem in question, the works should be noted of A. S. Silantiev (2012a, 2012b), who studied shearing SSS of concrete in beams and the effect of longitudinal reinforcement on the strength of oblique sections, Y. V. Krasnoschekov (2009), who examined the strength of oblique sections, when lateral forces and moments act, I. N. Starishko (2016), who tested the strength of beams in oblique sections with different cross section forms. Among recent foreign studies, noteworthy are works (Hosein et al., 2020; Qin et al., 2020; Naderpouret al., 2020).

II. MATERIALS AND METHODS

The main experimental data were obtained when testing beams of gas-concrete with the volume weight of 600 – 700 kg/m³ and beams made of heavy-weight concrete with . The beams were loaded with two or one symmetrically located concentrated forces. Strain gauges measured changes in concrete deformities, with strain gauges with 5mm base applied for gas-concrete since there was no coarse aggregate in rosettes. Strain gauges were glued on both concrete, and tensile reinforcement in certain cases. Computers had processed the results of measurements. Gas-concrete beams were 0.15–1.19% reinforced for tensile reinforcement.

III. RESULTS AND DISCUSSION

As it has been stated above, one of the problems of computations by formula (1) lies in determining cleaving-shearing stresses in concrete, related to the action of shear forces. They are difficult to define due to complexity of estimating the concrete SSS. In practice, they are compared with shearing stresses, associated with the action of longitudinal forces, and, most commonly, with readily determined concrete tensile strength. E. Mersch (1927) suggested that the concrete shear value should be determined by formula $R_{sh} = \sqrt{R_b R_{bt}}$. The formula was further revised in various ways (mostly based on the Mohr's theory) and such its form has been used up to now. According to Stolyarov Y.V. (Stoletov, 1941) $R_{sh} = 1.5\tau$, $\tau = 2R_{bt}$ and

$$\tau = \frac{\sqrt{R_b R_{bt}}}{1.5} \quad (9)$$

As per A. S. Zalesov (1989) $R_{sh} < 0.5R_b$. Taking into account that the maximum ratio between tensile $R_{bt}/R_b = 0.10$, and if strength and compression strength relates to low grades of concrete and for B15

$\tau_{max} = 2.5R_{bt}$, $R_{sh} < 2\tau_{max}$. According to A. S. Silantiev (2012a) $R_{sh} = 4 - 5R_{bt}$ and, therefore,

$$\tau = 2R_{bt} \quad (10)$$

can be assumed, as Stolyarov Y.V. recommends. In (Morozov, 2015, 2019b) $\tau = 0.185R_b$ was derived for gas-concrete, what provides $\tau = 1.5R_{bt}$ for B2.5. In (141)(142) of SNiP 2.03.01-84, formation of critical inclined cracks is defined that coincides with the last stages of loading the beams, based on which in (Morozov, 2019a, 2019b) a formula of τ_{max} was derived for a neutral axis

$$\tau = \frac{R_{bt}}{a - R_{bt}/R_b} \quad (11)$$

where $a=0.2+0.01B$, where, according to (Morozov, 2018, 2019a) strength class B can be equated to the experimental values of prism strength, and computations by (141)(142) are made using the rated parameters of concrete strength, and (10) should be at least 0.5. Table 1 presents the options for standard values of shearing stresses.

Table 1. Values of shear stresses.

Concrete class	B15	B20	B25	B30	B35	B40	B45	B50
$\tau_1 MPa$	2.75	3.29	3.72	4.16	4.11	4.00	3.90	3.90
$\tau_2 MPa$	2.32	3.00	3.57	4.13	4.69	5.20	5.65	6.20
$\tau_3 MPa$	2.20	2.70	3.10	3.50	3.90	4.20	4.50	4.90

The table contains τ_1 as per (10), τ_2 as per (8), $\tau_3 = 2R_{bt}$ (9). It is seen from the table that maximum values of shearing stresses are in line with formula (9), the values of which are refined by many researchers, τ_2 and τ_1 approximately correspond to each other down to B40. In this case, τ_1 from B35 ceases rising, what is illogical. Hence, when calculating shear force using formula (5) τ_1 can be assumed down to B35, τ_3 and τ_2 - within the entire range of concrete strength classes. Table 2, based on experimental data of A.S. Silantiev (2012a), presents the results of computing by formula (5). Since in (Silantiev, 2012a) in most beams without compressed reinforcement according to (Morozov, 2019b), a coefficient of completeness of compression stress-block ω using the considered method is close to $\omega = 0.33$, we will take this value of it, to which $m=0.5$ corresponds as per (3) and $\beta = 0.25$. Only in two beams No.9 and 10 $\omega = 0.6$, to what $m=1.17$ and $\beta=0.37$ correspond. At

$$\omega \leq 0.5 \quad \beta = \frac{1+6\omega}{12} \quad (12),$$

and at $\omega \geq 0.5$

$$\beta = \frac{1+2\omega}{6} \quad (13)$$

$z = (1 - \beta\xi_0)h_0$, and the values of shearing stresses are as per (9) and (10). To assume more precise initial conditions, more experimental data are needed. Table 2, based on experimental data (Silantiev, 2012a), presents the results of direct determination of load-carrying capacity of beams according to the accepted initial conditions.

Table 2. Results of calculating strength of beams

Beam No.	1	4	5	6	7	8	9	10
Q kN	23.11	21.5	48.4	50.69	31.44	42.66	74.85	85.00
R_b MPa	30.5	18.5	29.0	29.0	22.0	22.0	20.5	20.5
R_{bt} MPa	2.22	1.60	2.19	2.19	1.82	1.82	1.72	1.72
b, cm	10.3	10.0	10.2	10.4	10.0	10.3	14.9	15.1
cm	2.3	2.3	2.0	2.0	1.7	1.7	1.9	1.9
τ_1 (10) MPa	5.17	3.86	5.26	5.26	4.37	4.37	3.94	3.94
τ_2 (9) MPa	4.44	3.20	4.38	4.38	3.64	3.64	3.44	3.44
Q_1 kN	36.4	25.3	41.8	43.6	46.8	49.6	70.7	78.2
Q_2 kN	32.0	21.8	35.8	35.6	34.8	36.5	59.1	65.1
h_0	16.0	16.0	18.0	18.0	21.4	22.0	15.0	14.8

 a/h_0

In the table, Q_1 corresponds to τ_1 and Q_2 – to τ_2

The calculation results given in the table, demonstrate that the design values of shear force according to (4) with specified initial parameters approximately correspond to each other and experimental values of this force (by mean values $q^1/q = 1.04$, and $q^2/q = 0.85$). Here, preference should be given to the computation with shearing stresses by (10) with concrete strength classes down to B35. A similar approach shall also be employed to our experimental data from beams of gas-concrete (Morozov, 1985), what is presented in Table 3, where there are also the results of computing stresses in tensile reinforcement (compressed zone is not reinforced). Stresses were calculated by formulas -

$$\sigma_{s1} = \frac{m\tau}{\mu} \frac{a}{h_0}$$

(7) and

$$\sigma_{s2} = 600\omega \left(\sqrt{1 + \frac{R_b}{300\mu k}} - 1 \right) \quad (14),$$

which was derived in (Morozov, 2018). In this case, coefficient $k = x/x_0$ is the ratio between the height of compressed zone, in line with the hypothesis of plane sections – $x - \frac{\varepsilon_b}{\varepsilon_s + \varepsilon_b} h_0$, and actual height of this zone, which for gas-concrete beams upon their failure across normal sections is less than one – reaches 0.9 – 1.0, and upon their failure across oblique sections is more than one (about 1.14 on an average, and, in certain cases prior to failure or probably at its onset reaches $\kappa=1.7$). This fact significantly complicates the estimate of the concrete SSS. Since the presented data relate to only weak and highly deformable gasconcrete, and there are no such data found for the heavy-weight concrete, in this work $\kappa=1$ is assumed.

Table 3. Calculation of shear force and stresses in reinforcement.

Beam No.	BK-1	BK-2	B14-1	B18-1	B18-2		
R_b MPa	2.55	2.46	3.00	2.95	3.47	2.16	2.55
R_{bt} MPa	0.35	0.31	0.39	0.37	0.39	0.27	0.32
μ %	0.27	0.10	0.980	0.733	0.707	0.767	0.772
b cm	15.0	15.0	15.6	15.7	16.2	15.5	15.4
h_0 cm	20.0	20.5	20.7	20.3	20.5	20.0	20.0
a/h_0	2.50	2.46	2.44	1.99	1.97	3.12	3.12
Q_1 kN	7.9	7.3	9.5	9.6	10.8	6.3	7.4
Q_{act} kN	8.5	8.3	8.5	10.0	12.5	6.5	7.0
σ_{s1} MPa	139.6	124.8	97.1	100.9	109.7	111.9	132.6
σ_{s2} MPa	107.0	106.2	84.3	106.0	125.7	78.5	89.9
σ_{act} MPa	102.9	138.4	65.9	72.0	95.2	86.6	79.2

BD-1

BD-2

Table 3 presents the data on the strength of gas-concrete beams in oblique cross-sections. Here, $\omega = 0.33$, $m=0.5$, $\tau = 2R_{bt}$ were assumed as the initial calculation parameters likewise for heavy-weight concrete beams. Shear force is calculated by formula (5). Moreover, the table presents the results of computing across the tensile zone with determination of stresses in longitudinal reinforcement using formulas (8) and (13). The last formula was derived in (Morozov, 2018) allowing for distortion of normal sections, what both makes more accurate and complicates the estimate of concrete SSS in design sections. It can be seen from the table that the design values of shear force correspond well to their actual values.

Thus, mean ratio and their measured values for formula (8) is 1.31 on an average at $\sigma = 0.24$, and as per (13) 1.12 and 0.23, respectively. As pointed out above, no distortion of sections was taken into account – $\kappa=1$. The above-stated suggests that the assumed initial parameters for both compressed and tensile zone can be preliminarily used to directly determine the shear force. In Y.V. Krasnoschekov (2009) estimated the experimental data of (Zalesov&Ilyin, 1977a) according to the existing norms, and in (Morozov, 2019b) these data were supplemented by a direct calculation of shear force with the initial calculation parameters, somewhat different from those assumed in this work, and their values were greater by a third than the analogous rates for norms. Table 4 presents the results of calculation using the initial data for beams without compressive reinforcement.

$Q_1/Q_{act} = 0.97$, $\sigma = 0.09$. The ratio between mean values of reinforcement stresses

Table 4. Results of direct calculation of shear force

Beam No.	In cm	h_0 cm	B MPa	R_b MPa	R_{bt} MPa	Q_1 kN	Q_2 kN
1	15.2	27.0	20	11.5	0.9	27.7	32.9
2	15.4	25.8	20	11.5	0.9	26.8	31.8
3	15.5	26.0	20	11.5	0.9	27.2	32.2
6	15.5	26.7	28	16	1.14	35.4	42.1
7	15.5	26.8	28	16	1.14	35.5	42.3
8	14.5	26.8	28	16	1.14	33.2	39.7
9	14.7	26.6	28	16	1.14	32.4	39.9
14	14.4	27.3	42	23.2	1.42	41.9	50.7

In the table: Q_1 – shear force according to existing norms (Krasnoschekov, 2009), Q_2 – shear force when determined directly.

It can be seen from the Table that, at the level of design resistances of concrete, the values of the shear force when determined directly by formulas (4) (5) (7) (10) (12) with $\omega=0.333$, $\frac{a}{h_0} = 2$, $\tau =$

$$2R_{bt}, \xi_0 = 6 \frac{R_{bt}}{R_b}, Q_b = bh_0 (1 - 0.25\xi_0)2R_{bt}0.5$$

are higher by 20% than the values of the shear

force, computed using the existing norms. The problems of calculating strength of oblique sections should involve a division between the forms of their failure (compression or shear). With this method, this question is addressed through detailed consideration of experimental data on the design model according to the figure, comparing m_2 with m_0 and when the first indicator is exceeded, shearing failure should be expected. Although the work of A. S. Silantiev (2012a) relates to examining concrete shearing failure in oblique sections, judging by the observed limit concrete compression deformities, some beams are likely to fail from its compression. However, the direct computation of shear force with assumed initial parameters has shown its compliance with experimental data. It suggests the potential application of direct determination of shear force for both cases of failure in oblique cross-sections. The problem lies in finding correct initial design parameters for ω and τ , using experimental data. According to the assumed option in

$$(4) m\tau = R_{bt}.$$

IV. CONCLUSIONS

The method for direct determination of shear force taken up by concrete in oblique cross-sections, is based on a stress-block of normal stresses with a cut-out, oriented towards the top of an inclined crack.

The standard formula for determining shear force (1) is supplemented with correction factor m (m_2 or m_0).

The direct determination of shear force is made through simultaneous solution of the equations of equilibrium in the moments in normal and oblique sections (moments of normal and lateral forces) for both compressed and tensile zone of normal section, passing through the top of an inclined crack, what, in the last case provides a way of estimating stresses in tensile reinforcement.

The design values of shear force directly determined by the assumed initial design rates ω and τ , in both current and previously conducted works, corresponds to the measured values of this force in experimental beams.

Reaching maximum shearing stresses and the respective coefficient m_2 (2) near the top of an inclined crack (the x_2 ordinate) is a criterion for concrete shear failure in oblique cross-sections.

From a balance of flexural moments along the tensile zone of the design normal section, passing through the top of an inclined crack, and in oblique cross-section, a formula has been derived of stresses in tensile reinforcement (8). The stresses in tensile reinforcement computed using this formula are in compliance with its measured values in gas-concrete beams.

Deviations of design section from the hypothesis of plane sections were not accounted for in this work – $\kappa=1$.

To practically determine shear force, the initial design parameters should be made more precise based on experimental data. $\omega=0.333$ and $\tau = 2R_{bt}$ can be preliminarily assumed.

According to the assumed design data, in the conducted works the values of shear force, taken up by concrete, exceed its values, calculated according to the existing norms, by 20-30 %.

REFERENCES

- [1.] Borishanskiy, M. S. (1946). *Computation of unbent rods and clamps in bended reinforced concrete elements at the destruction stage*. Moscow: Stroyizdat.
- [2.] Gvozdev, A. cvA. (1949). *Computation of load carrying capacity of structures using the limit equilibrium method*. Moscow: Stroyizdat.
- [3.] Kani, G. N. I. (1966). Basic Facts Concerning Shear Failure. *Journal of ACI*, 63(6), 675-692.
- [4.] Krasnoschekov, Y. V. (2009). Strength of reinforced concrete elements in oblique sections when shear forces and moments act jointly. *Bulletin of the Siberian State Automobile and State University*, 3(13), 4650.
- [5.] Mersch, E. (1927). Nochmals zur Frage der Schubsicherung. *Beton und Eisen*, 7, 24
- [6.] Morozov, A. N. (1985). *The study of strength of structures from cinder-shale gas-concrete in oblique sections*. Construction Research Institute of the ESSR, Moscow: Gosstroy.
- [7.] Morozov, A. N. (1992). *On new approaches to the theory of strength of gas-concrete elements in oblique sections*. Construction studies. Tallinn: Estonian Construction Research Institute. pp. 10 – 25.
- [8.] Morozov, A. N. (2015). On some concepts of calculating strength of reinforced concrete elements in oblique sections with acting shear forces (by an example of examining gas-concrete behaviour). *Problemy sovremennoy nauki i obrazovaniya (Problems of modern science and education)*, 4, 41–51.
- [9.] Morozov, A. N. (2018). On the strength theory of reinforced concrete elements in oblique sections. *Promyshlennoye i grazhdanskoye stroitelstvo*, 2, 53 – 59.
- [10.] Morozov, A. N. (2019a). Direct definition of cross-sectional force in sloping sections of reinforced concrete structures. Problems of modern science and education. *Problemy sovremennoy nauki i obrazovaniya (Problems of modern science and education)*, 11, 33 – 39.
- [11.] Morozov, A. N. (2019b). Calculation of shear force taken up by concrete in oblique sections of reinforced concrete elements (to be discussed). *Promyshlennoye i grazhdanskoye stroitelstvo (Industrial and civil construction)*, 12, 30 – 34
- [12.] Naderpour, H., & Mirrashid, M. (2020). A novel definition of damage states for structural elements in framed reinforced concrete building. *Journal of Building Engineering*, 32, 101479. doi:
10.1016/j.job.2020.101479
- [13.] 10.1016/j.job.2020.101479
- [14.] Qin, F., Zhang, Zh., Yin, Zh., Di, J., Xu, L., Xu, X. (2020). Use of high strength, high ductility engineered cementitious composites (ECC) to enhance the flexural performance of reinforced concrete beams. *Journal of Building Engineering*, 32: 101746. <https://doi.org/10.1016/j.job.2020.101746>

- [15.] Said, M., Adam, M. A., Arafa, A. E., & Moatasem, A. (2020). Improvement of punching shear strength of reinforced lightweight concrete flat slab using different strengthening techniques. *Journal of Building Engineering*, 32, 10749. doi: 10.1016/j.jobbe.2020. 101749
- [16.] Silantiev, A. S. (2012a). Strength of bended reinforced concrete elements without clamps in oblique sections with allowance for longitudinal reinforcement parameters. *MSUCE Bulletin*, 2, 163-169.
- [17.] Silantiev, A. S. (2012b). Experimental study of the effect of longitudinal reinforcement on resistance of bended reinforced concrete elements without shear reinforcement in oblique sections. *Promyshlennoye e grazhdanskoyestroitelstvo*, 1, 58-61.
- [18.] Starishko, I. N. (2016). Results of experimental studies of the effect of main factors on the load carrying capacity in oblique sections of bended reinforced concrete rectangular- and T-shape beams. *MSUCE Bulletin*, 7, 18-32.
- [19.] Stoletov, Ya. V. (1941). *Introduction to the theory of reinforced concrete*. Moscow: Stroyizdat.
- [20.] Talbot, F. (1909). Tests of Reinforced Concrete Beams: Resistance of Web Stresses. *Bulletin University of Illinois Experiment Station*, No. 29
- [21.] Zalesov, A. S., & Ilyin, O. F. (1977a). *Resistance of reinforced concrete beams to the action of shear forces*. Moscow: Stroyizdat.
- [22.] Zalesov, A. S., & Klimov, Y. A. (1989). *Strength of reinforced concrete structures when shear forces act*. Kishinev: Budivel'nyk.
- [23.] Zalesov, A. S., Ilyin O. F. (1977b). *Experience of developing a new theory of the strength of beams in the area of action of shear forces*. Moscow: Stroyizdat.

Effect of Tool Pin Profile of Underwater Friction Stir Welding of Dissimilar Materials Aa5083 and Aa6061-T6

MUHAMMED ZAKARIYA Hasnol¹, MOHD FARIDH Ahmand Zaharuddin¹, SAFIAN Sharif¹

¹School of Mechanical Engineering, Faculty of Engineering
Universiti Teknologi Malaysia
81310 UTM Johor Bahru, Johor, Malaysia

SEHUN Rhee²

²Department of Mechanical Engineering
Universiti Hanyang,
17 Haengdang-dong, Seongdong-gu. Seoul 133-791, Korea

ABSTRACT

Underwater friction stir welding (FSW) is a primary joining process for welding aluminium, magnesium, and other metals in which no dissolving occurs and joining occurs below the material's melting point, resulting in a high-quality weld. This welding process was developed to be exceptionally effective, with no filler material used and no gas emitted, making the operation ecologically benign. This research aims to look at how shape and rotational speed relate to different materials during the joining process. It investigates the interaction between the tool pin profile and rotating speed underwater. In this context, the effect of underwater circumstances on tool pin profile and rotational speed concerning the mechanical properties and microstructure of the tool is discussed. This research aims to investigate the hypothesis that better mixing of dissimilar metals happens when the tool rotates faster throughout the weld path. AA5083 and AA6061-T6 were used to develop three different tool profiles. Several defects, such as voids in the weld zone, are apparent during welding. The study's findings indicated that changes in tool pin profile and welding conditions had a significant impact on determining the welded joints' mechanical properties. With ideal welding settings of 900 rpm, 60 mm/min, and tapered cylinder pin profile, the maximal hardness value attained was about 75 HV. These findings imply that different tool profiles have other impacts on the generation of faults during welding. As a result, the tool pin profiles should be considered while building an experimental underwater friction stir welded joint.

Keywords—underwater friction stir welding, aluminium alloy, tool pin, mechanical properties, microstructures

I. INTRODUCTION

Friction stir welding (FSW) is a solid-state joint technology that produces high-quality, low-distortion, high-strength butt, or lap joints in a wide variety of industrial applications [1] [2]. The tool consists of a pin and tool shoulder, which have a relevant influence on heat generation. Heat is generated when the shoulder contacts the base material [3]. Numerous pin tools are available, including straight-cylinder, threaded cylinders, tapered cylinders, and enclosed cylindrical threads. Due to plastic's severe deformation, these are the most efficient elements for metallic grain refinement in significant microstructure development [4]. Excessive material softening promoted sliding conditions due to a reduction in frictional force induced by precipitate dissolving or coarsening, resulting in defects in weld nugget and poor welded joint quality [5]. It was discovered that by using water cooling conditions in various solid-state joining processes, the mechanical properties could be improved the joint performance [6]. Due to its fast circulation and high heat absorption, the method applied water-cooling has a cooling effect on the samples during the friction stir process. As the pin rotation speed increases,

the speed of the shoulder increases, creating tremendous heat in the stir zone, which produces approximately 95% of heat input underneath the tool shoulder[7]. In the water environment, the dynamic heat was influenced by the action of tool pin to dissimilar weldment joints and impacted the heat dissipation of an underwater weld [8]. Furthermore, water cooling can give a more refined grain than air cooling [9].

It was proved that there is a correct combination of the weldment formed by strength and hardness in metallurgical bonding at varying rotational speeds (700 to 900 rpm) and transverse speeds (40 to 80 mm/min) on the FSW of Al-alloy [10]. The rotating tool speed and tool pin shape significantly impacted the strength and microstructure of dissimilar weldments [11]. The effect of process elements on weldment quality was influenced by tool design, material flow, and welding conditions. Through these qualities of alloying element addition on their samples, heat extraction rate may also improve the thermal stability of joints [12]. Structural metallic alloys' quality and microstructure properties exhibit different cooling rate techniques [13]. Mechanical properties demonstrated that the alloy had the same strength as the welded zone AA6111 alloy's base material [14]. Because of porosity, the softening zone is related to the heat generated by the FSW process, and the onion ring was formed when the welding speed increased [15]. Mechanical testing was performed on several tool pin profiles to determine the micro-hardness distribution of the FSW. It was validated in the association between temperature and hardness. Furthermore, frictional forces and material flow stirring produced heat production had a notable augmenting influence on the hardness value for varied tool pin profiles during FSW [16].

A tool shoulder analysis considers numerous profiles with crucial features for given material and welding parameters. Due to a better dynamical-static volume ratio [17], the suitable probe was built from the design triangular pin. The tool flat shoulder design is straightforward; however, interrupted material flowing beneath the surface must be avoided. The welding parameter modification employed a concave 10 mm diameter shoulder produces higher heat resulting in homogenous stirring flow[18]. The conical probe on the concave shoulder tool agitated with three grooves had considerable results compared to other tools [19]. The process parameter combination was proposed to represent the attributes between material output and input parameters during the FSW process [20]. The high friction input supplied additional heat during the welding across the recrystallisation temperature to form the welds, resulting in the optimal mechanical properties [21]. The influence of tool pin profiles on FSW of AA6061-AA5086 joints was studied. The threaded cylindrical shape resulted in good flowability and a free sound weld [22]. The strong combination resulted in the behaviour of tool pin threaded with surface mixing flow[23]. Furthermore, research on FSW keeps on studying how to increase the quality of joints and eliminate defects created for better weldment joints and strength.

II. MATERIALS AND METHODS

A. Experimental Procedure

The material for the workpiece are AA5083 and AA6061-T6 aluminium alloys. The AA6061-T6 is widely used in various applications due to its favourable characteristics, such as high resistance towards corrosion due to seawater and atmospheric condition. AA5083 also shows good corrosion resistance towards seawater. The plates to be joined were in the dimension of 150 mm x 65 mm x 6 mm. Table 1 shows the chemical composition of both AA5083 and AA6061-T6.

Table 1. The chemical composition of aluminum alloy, reproduced from [24,25].

Weight (%)	Si	Fe	Cu	Mn	Mg	Zn	Ti
AA6061-T6	0.6	0.34	0.26	0.07	0.8	0.01	0.01
AA5083	0.40	0.40	0.1	0.2	0.4	0.1	0.15

B. Design of Experiment Setup

Taguchi L9 factorial design was used to investigate the experiment. In this work, dissimilar joints, Taguchi technique was adopted to optimise process parameters in quality control, Taguchi L9 optimisation method was utilised in this experimental study that the component has pointed out the quality of viewing it as the setup of three internal display elements (speed, feed, and type of tool pin

profile). Table 2 shows the experimental level with a variety of parameters. In addition, several trial tests were carried out by adjusting the trial experiments' rotational tool speed (600rpm to 1200rpm) and welding speed (30 mm/min to 90 mm/min). The specimens utilised in this investigation were AA5083 and AA6061-T6 plates.

The FSW procedure was carried out on a vertical milling machine. The tool was made of H13 steel and was designed for single-pass butt welding. Strap clamps were used to secure the plates to the machine table. Four clamps were utilised to secure the plates at the edges. Two extra strap clamps were added to the sidewalls of the plates to guarantee that the plates did not separate during the FSW process. Figure 1 shows the experimental setup of FSW whereas Figure 2 shows variation of the tool pin profiles. The tool is manually inserted into the materials to a depth of 4 mm. Once the pin is fully inserted, and the shoulder is in contact to the plates. The spinning tool is rotated at 30 mm/min, 60 mm/min, and 90 mm/min speeds. The machine table is moved along the welding line at 100 mm per run to make a weld of the same length. Once the tool travel distance of 100 mm was reached, the tool was rotated and drawn out of the welded plating. The machine was only turned off after the tool had been entirely removed. For this investigation, there are nine weld joints built from dissimilar AA6061-T6 and AA5083.

Table 2. The level process of parameters.

Parameters	Notation	Levels of factors		
		1	2	3
Speed	RPM	600	900	1200
Feed	Mm/min	30	60	90
Type of tool pin profile	TTPP	CS	CT	TC

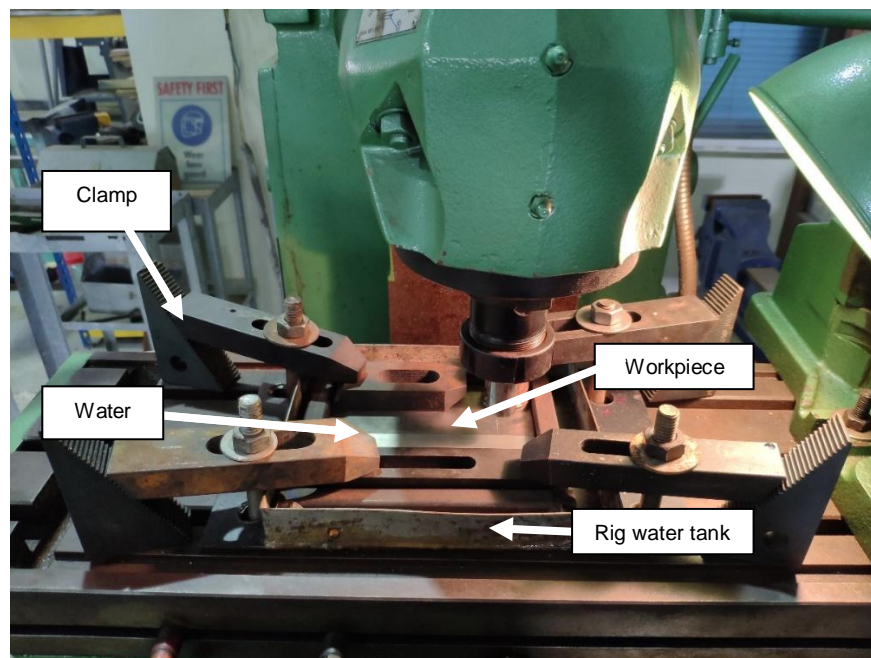


Figure 1. Experimental setup of FSW of butt joint between AA5083 and AA6061-T6 in the water environment.

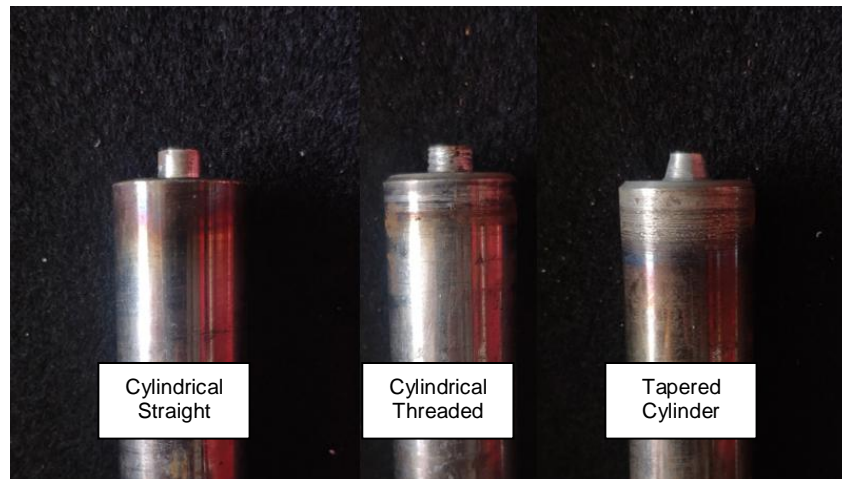


Figure 2. Different experimental tools pin profile.







After welding, the weld was placed on examining the cross-section of each sample. The macrostructure profile assessed the joints; the welding state was polished and etched in 10 to 30 seconds using a reagent containing methanol (25ml), nitric acid (25ml), hydrochloric acid (25ml), and hydrofluoric acid (1 Drop) and inspected under an optical microscope. Vickers hardness testing was also performed on welded joints using a hardness machine with a force of 10kgf and a dwell period of 15s along the perpendicular to the cross-section.

III. RESULTS AND DISCUSSIONS

3.1 Effect of tool pin profiles

The findings include a visual evaluation of the weld surface and a distribution of hardness. Table 3 shows the top view of the welded junction for three distinct tool pin profiles. The stirring behaviour on the top surface exhibits ripples and flashes on the welding line. Welded specimens were visually evaluated for any faults developed at the welded surface of different materials. Under these conditions, the pin produced noticeable onion rings in the cross-sectional region. Three distinct specimens have an unpleasant appearance keyhole surface on the welded surface with flashes. This defect demonstrates that the insufficient heat input in the stir zone caused by the tools resulted in low material flow in the base material. Excessive flashes developed on the surface of both the advancing and retreating sides at 1200 rpm while utilising a threaded tapered cylinder and a cylindrical threaded tool. Tunnel flaws arise when the area of all tool pin profiles is impacted by a greater 600 rpm. This was caused by the FSW tool's low heat input.

Table 3. Macrograph of joint cross-section.

Rotational Speed (rpm)	Tool pin profile	Welding line	The cross-sectional joint of welded joint	Observation
600	Cylindrical Straight			Tunnel defect at the mid thickness and insufficient heat input
900	Cylindrical Threaded			Tunnel defect at the mid thickness and insufficient heat input
1200	Tapered Cylinder			Tunnel defect at the mid thickness and insufficient heat input

The study chooses an experimental sample run for a tapered cylinder pin profile with 900 rpm rotational speeds and 60 mm/min welding speed. This is because the growth of onion rings in the stir zone was not seen in the flow of materials in the mid thickness area. Figure 3 shows the cross-sectional area subjected to macrostructure examination. Microscopy photographs show the stir zone and the characteristics of the aluminium joints and an optical lens to explain the grain structure at surface cross-sections. The material's transfer behaviour controls the significant effect of tool pin profile and welding speed in the welding joint underwater environment and grain refinement process. Underwater FSW was used on various pin profiles, and more excellent thermal dissipation reduces welding temperature. These advantages for process cooling rate produce fine microstructure, which increases weld durability and strength. Figure 4 shows a 5X, and 20X magnification picture of the stir zone and TMAZ region welded of tapered cylinder pin profile on AA5083 and AA6061-T6 joints, respectively. Strong plastic deformations are caused by the mechanical combination of manufacture from the stirring tool pin to the stir zone. Significant product diffusion occurs because of the cumulative impact of higher temperatures and plastic solid deformation, contributing to the homogenisation of elementary components between the specimens. Furthermore, the water environment has a cooling effect on the samples due to its heat absorption capability.

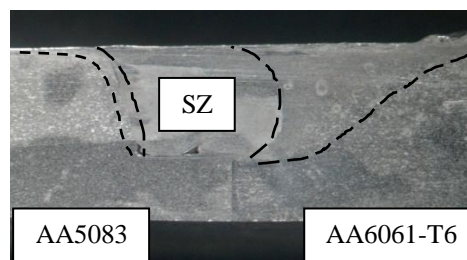


Figure 3. The cross-sectional area of sample 5 (900rpm and 60 mm/min).

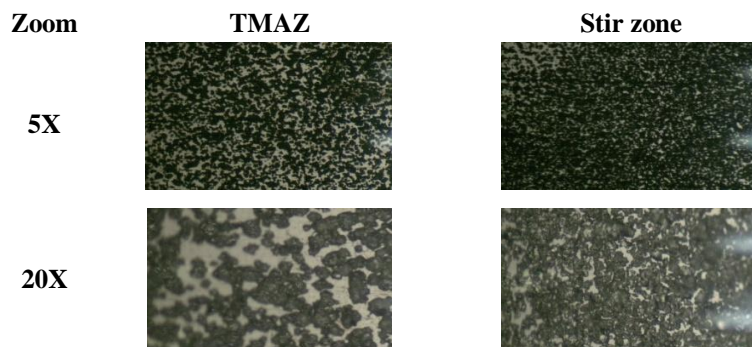


Figure 4. Magnification image at 900 rpm and 60mm/min.

Figure 5 a) shows an onion ring layering formed when the components in the weld nugget are well combined. The material flow starts to develop the banded structure (white circle). The onion ring generated illustrates that the stirring action of the pin profiles is homogenous in the stir zone while welding at a consistent speed of 60 mm/min. Changes in water temperature influence the production of dissimilar weldment junctions in the weld nugget zone. Figure 5 b) shows the dwell time was significantly impacted temperature variations; insufficient heat was generated due to slower welding rates and poor material consolidation, resulting in void defects on the advancing side.

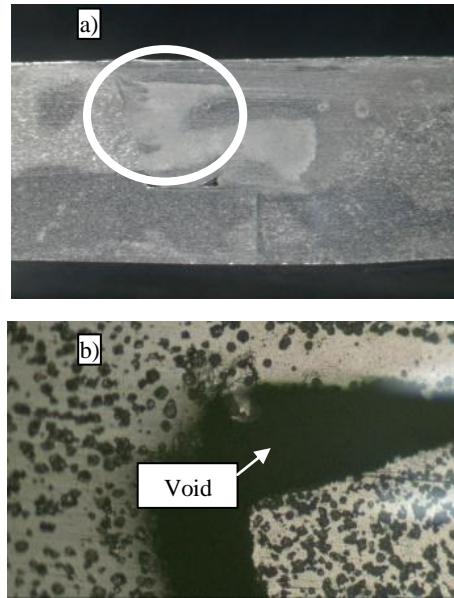


Figure 5. Cross-section of the joint created at a) material flow at advancing side and b) void defect at advancing side.

3.2 Effect On Hardness Value.

The current study found that quick cooling rate was connected to grain size, which was impacted by the water environment. This might be because the grains did not have enough time to germinate in the softened zone. Even though fast cooling reduced the HAZ in the softened area, it enhanced the hardness value reached on both sides of the dissimilar weldments. This significantly influences joint strength and hardness, which is tightly linked to the strengthening stages. Therefore, the water environment enhances hardness variation and keeps the excellent welded joint samples above room temperature. Figure 6 shows both hardness profiles, with no discernible symmetrical trend due to physical and mechanical properties differences, particularly in the stir zone, which consists of dissimilar joints on opposing advancing and retreating sides. The resulting hardness profile is shown over distance in 6 mm thick dissimilar weldment joints. When the feed rate increase to a higher rotational speed, the minimum hardness value in the dissimilar joint increases. It exhibits softening behaviour when the rotation speed increases due to heat generated during FSW.

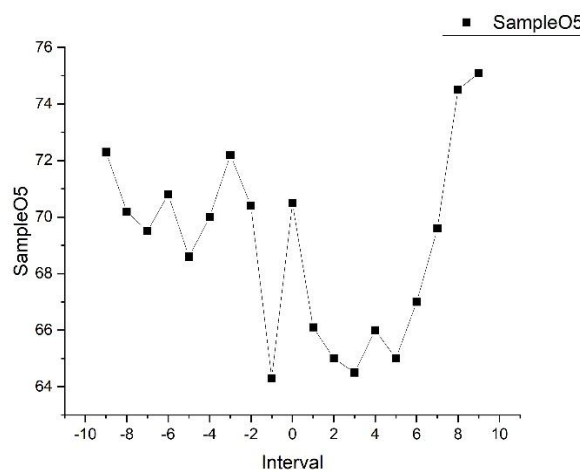


Figure 6. Microhardness for tapered cylinder (900rpm and 60 mm/min).

The minimum hardness value of all places in the relevant weldment AA5083 joint. The advancing side of AA5083, on the other hand, has a rising hardness value since it is close to the centre of the welds. Tool rotation triggered the rising hardness values, while a tapered cylinder pin supplied adequate stirring at all feed rates. At 30mm/min, the maximum hardness was 75Hv. Because the material mixes

with another well and proper heat generation during the welding process, the lowest feed speed corresponds to the highest hardness.

Table 4 shows the summary for hardness value; both cylindrical straight and tapered cylinder pin profiles have a higher hardness value than cylindrical threaded in the stir zone. Figure 6 shows a microhardness plot of a tapered cylinder pin profiled at the weld nugget zone at 900 rpm and 60 mm/min feed rate. The hardness profiles of AA5083 and AA6061-T6 show a sharp drop at the weld nugget zone. The primary concern in the welding zone is the hardness distribution, which is heavily influenced by water cooling changes in the microstructure. A softening region identified the lowest hardness under the pin throughout the stir zone, which was more profound in the TMAZ sections where the production process of observed tunnel flaws was discovered. When the rotation speed is increased, the material transfer distribution of the advancing side (AA5083) in TMAZ is smaller than the material deformation ability of the retreating side (AA6061-T6).

Table 4. Summary data for hardness value.

Experimental Run	Speed	Feed	Pin	Hardness
1	600	30	CS	75
2	600	60	CT	70
3	600	90	TC	73
4	900	30	CT	68
5	900	60	TC	72
6	900	90	CS	65
7	1200	30	TC	75
8	1200	60	CS	74
9	1200	90	CT	63
Average				71

IV. CONCLUSIONS

Different tool profiles influence differently on the formation of defects at welds. For threaded straight cylindrical, the tunnel defect formed at the mid-bottom part of the stir zone, and the size is relatively more significant, while for tapered cylindrical tool, the void formed at the stir zone AA5083, and the size is smaller. The onion ring can also be observed with less dissimilar materials in the welded zone. For tapered cylindrical tools, the size of the tunnel defect is much smaller at 900 rpm and 30 mm/min. It was due to the lack of heat generated at the tool.

All in all, threaded tools provide lower material flow as there is a decrease in hardness at the advancing side of welds. On the other hand, cylindrical straight and tapered cylinder produced joints have the highest hardness value and better mixing based on the hardness distribution. In addition, the higher tool rotational speed produces underwater welded joints with higher hardness value and less defect formation.

ACKNOWLEDGEMENT

This material is based upon work supported by the Ministry of Higher Education (MOHE), Malaysia and Research Management Centre of Universiti Teknologi Malaysia for the financial support through the RUG funding R.J130000.7851.5F382.

REFERENCES

- [1] M. Aissani, S. Gachi, F. Boubenider, and Y. Benkedda, "Design and optimisation of friction stir welding tool," *Materials and Manufacturing Processes*, vol. 25, pp. 1199–1205, 2010.
- [2] M.S. Rao, B.V.R Kumar, and M. Hussain, "Experimental study on the effect of welding parameters and tool pin profiles on the IS:65032 aluminium alloy FSW joints," *Materials Today: Proceedings.*, Vol. 4, pp. 1394–1404, 2017.

- [3] M. A Wahid, Z. A Khan, A.N and Siddiquee, "Review on underwater friction stir welding: A variant of friction stir welding with great potential of improving joint properties", Transactions of Nonferrous Metals Society of China (English Edition), Vol. 28(2), pp.193–219, 2018.
- [4] G. Liu, L.E Murr, C. S Niou, J. C McClure, and F. R Vega,"Microstructural Aspects of the friction-stir welding of 6061-T6 aluminium," Scripta Materialia, Vol. 37, pp. 355–361. 1997.
- [5] W. A Baeslack, K. V Jata, T. J and Lienert T. J, "Structure, properties and fracture of friction stir welds in a high-temperature Al-8.5Fe-1.3V–1.7Si alloy (AA-8009)," Journal of Materials Science, Vol 41(10), pp.2939–2951, 2010.
- [6] D. Sakurada, K. Katoh and H. Tokisue., 2002. "Underwater friction welding of 6061 aluminium alloy," Journal of Japan Institute of Light Metals, Vol. 52(1), pp. 2–6, 2002.
- [7] S. M Bayazid, M.M Heddad, and I. Cayiroglu,"A review on friction stir welding, parameters, microstructure, mechanical properties, post-weld heat treatment and defects," Material Science & Engineering International Journal, Vol. 2. 2018
- [8] M. A Mofid, A. Abdollah-Zadeh, F. M Ghaini and C. H Gür, "Submerged friction-stir welding (SFSW) underwater and under liquid nitrogen: An improved method to join Al Alloys to MG Alloys,"Metallurgical and Materials Transactions A, Vol. 43, pp. 5106–5114. 2012.
- [9] Y. B Tan, X. M Wang, M. Ma, J. X Zhang, W. C Liu, R. D Fu, and S. Xiang, "A study on microstructure and mechanical properties of AA 3003 aluminium alloy joints by underwater friction stir welding," Materials Characterization., Vo.127,pp. 41–52. 2017.
- [10] S. S Sivachidambaram, G. Rajamurugan, Amirtharajand Divya, "Optimising the parameters for friction stir welding of dissimilar aluminium alloys AA 5383/AA 7075," ARPN Journal of Engineering and Applied Sciences, Vo. 10, pp. 5434-5437, 2015.
- [11] R. Palanivel, P. K Mathews, N Muruganand I. Dinaharan, "Effect of rotational tool speed and pin profile on microstructure and tensile strength of dissimilar friction stir welded AA5083-H111 and AA6351-T6 aluminium alloys," Materials & Design, Vol. 40, pp. 7–16, 2012.
- [12] P. Pietrusiewicz, K. Bloch, M. Nabialek. and S. Walter. "Influence of 1% addition of NB and W on the relaxation process in classical Fe-based amorphous alloys,"Acta Physica Polonica A, Vol. 127, pp. 397–399, 2015.
- [13] M. Nabialek, "Influence of the quenching rate on the structure and magnetic properties of the Fe-based amorphous alloy," Archives of Metallurgy and Materials., Vol. 61, pp. 439–444, 2016.
- [14] W. Gan, K. Okamoto, S. Hirano, K. Chung, C. Kim. and R.H Wagoner, "Properties of friction-stir welded aluminium alloys 6111 and 5083," Journal of Engineering Materials and Technology, Vol.130, 2008.
- [15] S. A Khodir, and T. Shibayanagi, "Friction stir welding of dissimilar AA2024 and AA7075 aluminium alloys," Materials Science and Engineering: B, Vol.148, pp. 82–87, 2008.
- [16] A. Emamikhah, A. Abbasi, A. Atefatand MK Givi, "Effect of tool pin profile on friction stir butt welding of high-zinc brass (CUZN40)," The International Journal of Advanced Manufacturing Technology, Vol. 71, pp. 81–90, 2013.
- [17] K. Elangovan, V. Balasubramanianand S. Babu, "Developing an empirical relationship to predict tensile strength of friction stir welded AA2219 aluminium alloy," Journal of materials engineering and performance, 17 (7), pp. 820–830, 2008.
- [18] Q. Wang, Y. Zhao, K. Yan, and S. Lu,"Corrosion behaviour of spray formed 7055 aluminium alloy joint welded by underwater friction stir welding," Materials & Design, Vol. 68, pp. 97–103, 2015.
- [19] JH Aval, and A. Loureiro, "Effect of reverse dual rotation process on properties of friction stir welding of AA7075 to AISI304," Transactions of Nonferrous Metals Society of China, Vol. 29(5), pp. 964–975, 2019.
- [20] M. Yunus, and M.S SAlsoufi, "Mathematical Modelling of a Friction Stir Welding Process to Predict the Joint Strength of Two Dissimilar Aluminium Alloys Using Experimental Data and Genetic Programming," Modelling and Simulation in Engineering, 2018, pp. 1–18, 2018.
- [21] A. Chandrashekar, H.N Reddappa, and B.S Ajaykumar,"Influence of Tool Profile on Mechanical Properties of Friction Stir Welded Aluminium Alloy 5083,"World Academy of Science, Engineering and Technology International Journal of Materials and Metallurgical Engineering, Vol. 10(1), 2016.
- [22] M. Ilangovan, S. R Boopathy, and V. Balasubramanian, "Effect of tool pin profile on microstructure and tensile properties of friction stir welded dissimilar AA6061-AA5086 aluminium alloy joints," Def. Technol, 11, pp.174–184, 2015.
- [23] R. M Reza-E-, W. Tang, and A.P Reynolds, "Effects of thread interruptions on tool pins in friction stir welding of AA6061,"Sci. Technol. Weld. Join, Vol. 23, pp. 114–124, 2018.
- [24] M. Hasan, R. Abdi, and M. Akbari, "Modelling and Pareto optimisation of mechanical properties of friction stir welded AA7075 / AA5083 butt joints using neural network and particle swarm algorithm,"Materials and Design, Vo. 44. pp. 190–198. 2013.
- [25] J. Fathi,P. Ebrahimzadeh, R. Farasati and R. Teimouri, "Friction stir welding of aluminium 6061-T6 in the presence of water-cooling: Analysing mechanical properties and residual stress distribution," International Journal of Lightweight Materials and Manufacture., Vol. 2, pp. 107–115, 2019.

Analysis of Passenger's Interest on Transportation of the Urban Environment in Tuban Indonesia

Sugiyanto & Cicik Nur Indah

*Civil Engineering Study Program, Faculty of Engineering, SunanBonang University
Tuban East Java Indonesia*

ABSTRACT

This study aims to determine how much influence the interest of urban environmental transport passengers in the city of Tuban, Indonesia. The interest is measured using 5 research variables consisting of transportation fares, transportation routes, waiting time for transportation orders, transportation driver services and transportation driving safety. The results of the evaluation of the outer model have met the results of the validity and reliability tests. The validity test was conducted to test whether the questions contained in the questionnaire given to the respondents were valid and able to explain the latent variables, while the reliability test was used to measure the reliability of the confidence level of the model generated in this study. The results of the evaluation of the inner model showed that the correlation number of the variable waiting time for environmental transportation messages was the most influential variable (88%), followed by vehicle driving safety by 23% and environmental transportation routes by 18%, while the other variables with the lowest effect consisted of environmental transportation driver services 2% and transportation fares have an effect on reducing by -3%.

Keywords: *Interest, respondents, outer model and inner model.*

I. INTRODUCTION

In today's dynamic development, transportation is a very important (vital) need for humans, both for individual and social interests. In reality, humans need movement from one location to another, from various origins to various destinations in order to distribute products (goods) to reach consumers' locations. This mobility is carried out by using various modes of transportation, namely by means of land, river, sea, or air transportation.

The growing need for variants of transportation modes is no exception in the city of Tuban, Indonesia in accordance with the current situation and conditions. This is due to the increasing number of residents, especially in the urban environment of Tuban, thus increasing the number of needs for flexible transportation levels. As we all know, the movement of people or goods can occur due to various interests, including making a living (drivers and delivery services), tourism, services and so on. Therefore, the movement of goods for both people and goods is required to always be able to serve the various interests needed and its nature will always change both the means of transportation and the accessories to satisfy all parties.

The Tuban Regency Government through Regional Owned Enterprises in collaboration with the Department of Transportation in 2018 launched a vehicle called environmental transportation for urban areas and non-route public transportation tourism. The existence of this transportation is expected to further complement the needs of public transportation in the Tuban Regency area, especially in the development of tourism potential in the City of Tuban. The advantage of this transportation compared to other modes of transportation is that it can reach people who live in narrow alleys, residential areas, tourist destinations, can be ordered as desired and can even reach villages with a charter system from within the city to outside the city.

The emergence of urban environmental transportation is a type of transportation with the desired breakthrough is that it can be used by the community because it is practical, economical, effective, safe and comfortable. Because this transportation is non-route, the direction of destination of the users can be according to their choices and needs without having to wait long on the streets because they can be ordered directly from the homes of each user. Based on investigations and surveys in the field, it can be informed that the users are dominated by mothers and students. Some of them even use this mode of transportation with a subscription system and a shuttle system.

Based on the increasing growth of urban environmental transportation which is marked by more and more people choosing to use this transportation for various destinations, then of course there are several driving

force factors for the interest in using these services. In connection with the phenomenon that occurs, it is deemed necessary to conduct research on the analysis of passenger interest in urban environmental transportation in the City of Tuban, Indonesia.

II. RESEARCH METHODS

The research area consists of urban areas in Tuban consisting of: Gedongombo Village, Panyuran Village, Ronggomulyo and Sendangharjo Villages, Karang Villages and Bogorejo Villages. Based on these locations can be shown on the map as follows:

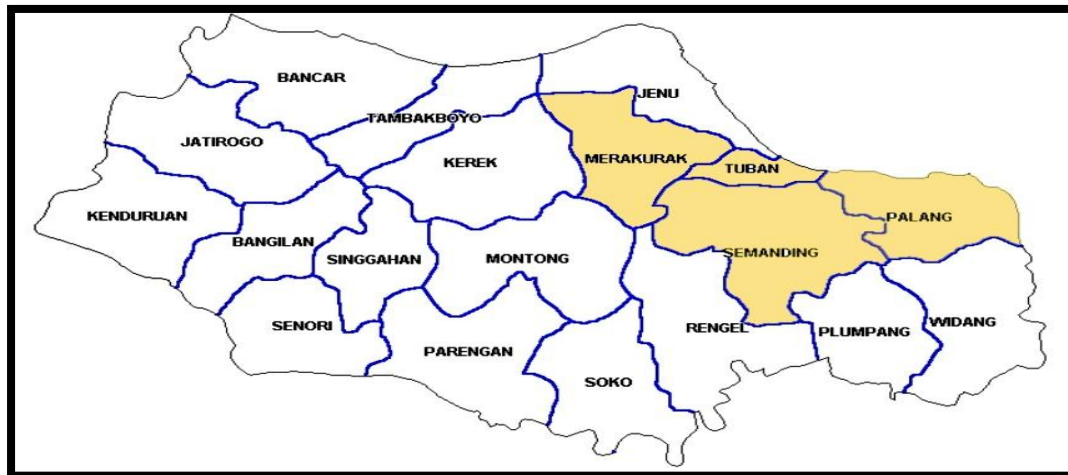


Figure 1. Map of research location

The method of data collection in the implementation of this research was carried out by distributing questionnaires to respondents. Participants who are selected to be respondents will be given a list of questions related to data that can measure passenger interest in the existence of urban environmental transportation in the areas that have been selected for research data collection. To support accuracy in data collection using a likert scale (Sugiyono, 2018). This scale is used to measure the attitudes, opinions, and perceptions of passengers about this transportation service, with a scale of 1 to 5 consisting of:

- Scale 1: Very disinterested in urban environmental transportation
- Scale 2: Not interested in urban environmental transportation
- Scale 3: Hesitating (between not interested and interested) with urban environmental transportation
- Scale 4: Interested in urban environmental transportation
- Scale 5: Very interested in urban environmental transportation

Based on the scale above, it is used to analyze the assessment of variables consisting of:

1. The independent variables (X) and the indicators used include:
 - a. Urban environmental transportation tariffs (X1), namely the nominal amount of money paid by users in using transportation services, the indicators consist of:
 - 1) Cheap, namely the cost of transportation services is considered cheap because even though more than 1 person only pays the cost of 1x trip (TA1).
 - 2) Easy, namely the way to pay is easy because you don't have to use an application, just cash is enough, so it's easier for people who are technology savvy, especially for those aged 40 and over (TA2).
 - 3) Prices are stable, namely tariffs that apply to services do not fluctuate, even if you become a subscriber you still get a discounted price (TA3).
 - 4) Prices are negotiable, namely the price for using transportation services can be negotiated based on an agreement, especially for rental or charter purposes (tourism) back and forth (TA4).
 - b. Urban environmental transportation routes (X2), namely areas that can be passed by transportation, the indicators consist of:
 - 1). Flexible, namely the area that can be reached by transportation can adjust to user needs (RA1).
 - 2) Route knowledge, namely the driver has good knowledge of the route (understanding the road) or the area intended by transportation users (RA2).

- 3) Shorter travel time (shortest route), where the driver looks for the fastest route and avoids traffic jams that are prone to congestion (RA3).
- 4) Route coverage, which can pass through non-route routes according to the wishes of transportation service users, even narrow alleys, residential areas and other areas (RA4).
- c. The service of an urban environment transportation driver (X3), namely the attitude of courtesy, patience and friendliness of the transportation driver in serving users, the indicators consist of:
 - 1) Friendly, namely the driver serves transportation users in a friendly and non-surly manner (PS1).
 - 2) Polite, namely the driver is polite in speaking and in serving users of transportation services (PS2).
 - 3) Responsiveness, which is the response or alertness of the driver to changes in routes or others from transportation service users (PS3).
 - 4) Patience, namely the attitude of the transportation driver in serving the needs of users of transportation services, including being able to wait and help carry the luggage of transportation service users (PS4).
- d. Waiting time for urban environmental transport messages (X4), which is the time required for the arrival of transportation according to the location ordered by users of transportation services, the indicators consist of:
 - 1) Arrival time, which is the time taken from the time ordered until the transportation vehicle arrives at the customer's location (WT1).
 - 2) Directly to the location, namely because the transportation is private so it can come directly to serve because it does not stop or hang at certain places. The driver will immediately come to pick up passengers (WT2).
 - 3) Waiting in a relaxed manner, namely the ability of transportation that can pass through narrow alleys and residential locations, so the customer can relax and wait at their respective homes (WT3).
 - 4) Coming directly to the road, namely the time required by transportation service users when the vehicle arrives on the road and does not need to wait for other passengers or full load (WT4).
- e. Driving safety of urban environmental transportation vehicles (X5), namely the way the driver drives transportation vehicles in order to create a sense of security for users of transportation services, the indicators consist of:
 - 1) Obedient to traffic, namely transportation drivers always obey traffic signs and be disciplined in driving transportation vehicles (KM1).
 - 2) Not reckless, namely the driver drives the vehicle at a moderate speed (normal), is not emotional and maintains a safe distance from other vehicles (KM2).
 - 3) Attitude in driving, namely the mental attitude of the driver in driving the vehicle to concentrate (focus) and not mess with the applications available on cell phones (KM3).
 - 4) Completeness of attributes and vehicle documents, namely the availability of complete attributes of transportation vehicles along with documents that must be fulfilled such as STNK, kir books and so on (KM4).
2. The dependent variable (Y), namely passenger interest in urban environmental transportation is measured based on the following indicators:
 - a. The desire to use transportation services, namely the intention to use transportation services (K1).
 - b. Possibility of using transportation services, namely seeking information about urban environmental transportation and at some point being interested in using it (K2).
 - c. Repeat orders, namely users of transportation services can several times to fulfill their needs using transportation services (K3).
 - d. Distribution between users, namely the users of transportation services feel helped and can enjoy it so that they notify others to be able to use the transportation service (K4).

In this study, in the selected area, the respondent criteria were determined, consisting of:

1. Male and female gender
2. Age 30-60 years old
3. Place of residence in the City of Tuban, Indonesia
4. The lowest education is SMK/MA/SMA
5. Urban environmental transport users

In Solimun et al (2017) it is stated that to be able to meet the rules in determining the number of samples, it can be used to calculate sample requirements as below:

$$\text{Number of samples (M)} = 50 + 8 (n)$$

Where:

M : Number of variables studied
N : Number of variables samples

Thus, because the variables studied consist of 6 variables, the results of the calculations can be seen as follows:

$$\begin{aligned}\text{Number of samples (M)} &= 50 + 8 (6) \\ &= 98\end{aligned}$$

Based on the distribution of respondents' residences in Gedongombo Village, Panyuran Village, Ronggomulyo Village, Karang Village, Sendangharjo Village, and Bogorejo Village, the number of 16-17 respondents each village is determined so that the number of samples needed is 100 respondents.

The data analysis used to measure passenger interest in urban environmental transportation in the City of Tuban consists of:

1. Descriptive analysis method

For the purposes of this analysis method, Microsoft Excel computer software is used to process input into the data tabulation, calculate the amount, determine the average value and others.

2. Quantitative analysis method

This quantitative analysis method uses partial least squares (PLS) with the application of the WarpPLS 7.0 software program, which is very suitable for conducting multivariate analysis of the influence of independent variables on the dependent variable.

III. RESULTS AND DISCUSSION

1. Characteristics of Research Respondents

Based on the information collected from the respondents, it was found that the characteristics of the respondents, consisting of age, education level, gender and type of work; as can be observed in Table 1 below:

Table 1. Characteristics of respondents

No	Respondent data	Characteristics of respondent	Total	Percentage
1	Age	16-19 years	5 peoples	5%
2		20-25 years	15 peoples	15%
3		26-30 years	14 peoples	14%
4		31-35 years	16 peoples	16%
5		36-40 years	14 peoples	14%
6		> 40 years	36 peoples	36%
Total			100 peoples	100%
1	Level of education	Primary school	4 peoples	4%
2		Junior high school	24 peoples	24%
3		Senior high school	62 peoples	62%
4		Graduated from university	10 peoples	10%
Total			100 peoples	100%
1	Gender	Man	32 peoples	32%
2		Woman	68 peoples	68%
Total			100 peoples	100%
1	Job status	Student	6 peoples	6%
2		University student	6 peoples	6%
3		Private sector employees	30 peoples	30%
4		Entrepreneur	5 peoples	5%
5		Government employees	4 peoples	4%
6		Housewife	49 peoples	49%
Total			100 peoples	100%

Source: Processed data (2021)

Based on the information in Table 1 above, the characteristics of the respondents can be explained that the most age is > 40 years old 62%, the highest education level is SMA 62%, the sex is mostly female 68% and the type of work is mostly housewives 49%.

2. Data Analysis and Modeling

Ghozali (2014) explains that the Partial Least Square (PLS) method is an analysis technique of all variables (multivariable) that can be used to describe the simultaneous linear relationship between observational variables, which are called latent variables consisting of independent variables and dependent variables. The independent variables consist of fare, route, driver service, message waiting time, and driving safety; while the dependent variable is the passenger's interest in environmental transportation.

Based on the involvement of the latent variables used, path analysis (block diagrams) can be performed to locate the independent variables with their dependent variables, as can be seen in Figure 2 below:

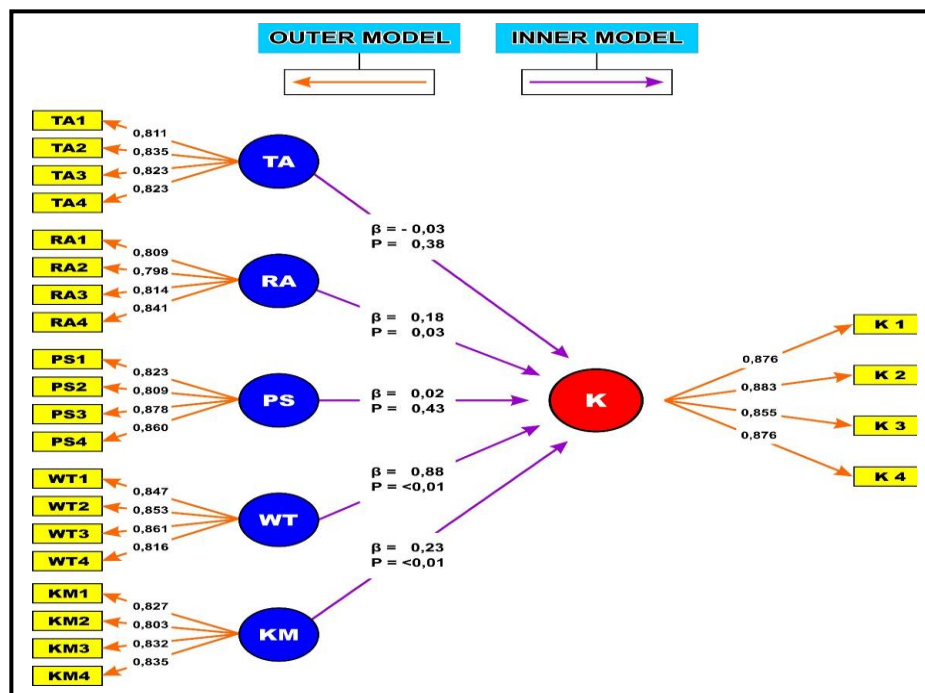


Figure 2. Results of partial least squares data processing

Based on the results of the partial least square method data processing using the WarpPLS 7.0 software as shown in Figure 2, an evaluation of the modeling obtained will then be carried out. In this study, the evaluation model formed consists of the outer model (measurement model), which explains the relationship (correlation) between the indicator and its construct and the inner model (structural model), which explains the relationship between the independent variable and the dependent variable.

3. Evaluation of the Outer Model (Measurement Model)

In Ghozali (2014) it is explained that the outer model is often called the outer relation or measurement model, which describes the relationship between each indicator and its latent variables. This model is also called the measurement model, which measures the depth of the relationship (correlation) between the indicators used in the study and the variables used. By getting a sufficient number of correlations (outer loading), it will be possible to generate how the indicators used are adequate or not to be used to measure research variables (constructs).

Ghozali (2014) explains that the outer model explains the relationship between construct indicators and latent variables. In this relationship, it can be evaluated based on the correlation value indicated by the value of the loading factor or outer model of the construct indicator in constructing the latent variable. From the output loading factor values, all of which are > 0.5, it can be said that they have good convergent validity. Meanwhile, based on a review of the cross-loading numbers, it can be stated that the indicators used have good discriminant validity as well. This can be identified based on the correlation value of the indicator to the construct, which is the

highest number compared to the correlation between the indicator and other constructs. From the loading factor value, the ability of construct indicators can be tested in explaining the latent variables. Therefore, the evaluation of this model involves testing consisting of a validity test and a reliability test as described below:

1. Validity Test

This test was conducted to test whether the questions contained in the questionnaire given to the respondents were valid and able to explain the latent variables. In conducting the validity test, it is determined by the following 2 (two) things:

a. Convergent Validity

The results of the indicator validity test in this study have a loading factor number that can be used to validate the latent construct. In this study, there are 6 latent constructs with a total of 24 indicators using a likert scale with an interval rating of 1 to 5. Based on the test results, the loading factor value can be seen in Table 2 below:

Table 2. Testing the value of loading factor

Variables	Code	Indicators	Loading factor
Rate (X1)	TA1	The cost of transportation services is considered cheap because even if more than 1 person only pays for 1x trip only	0.811
	TA2	How to pay, you don't have to use an application, just cash is enough, so for people who are technology stuttering it's easier, especially for those aged 40 and over	0.835
	TA3	The rates that apply to services do not fluctuate, even if you become a subscription you still get a discount	0.823
	TA4	Prices for using transportation services can be negotiated based on an agreement, especially for rental or charter purposes (tourism) back and forth	0.823
Travel route (X2)	RA1	The area covered by transportation is flexible enough to adapt to user needs	0.809
	RA2	The driver has good knowledge of the route (understands the road) or the area targeted by transportation users	0.798
	RA3	Shorter travel time (shortest route) looking for a route that is prone to congestion	0.814
	RA4	Route coverage can pass through non-route routes according to the wishes of transportation service users, even entering narrow alleys, residential areas and other areas.	0.841
Driver service (X3)	PS1	The driver serves transportation users in a friendly and not sour face	0.823
	PS2	The driver is polite in speaking and acting in serving transportation service users	0.809
	PS3	Responsiveness or the readiness of the driver to change routes or others from users of transportation services	0.878
	PS4	The attitude of the transportation driver in serving the needs of service users is quite patient, including being able to wait and help carry the luggage of service users	0.860
Waiting time (X4)	WT1	Arrival time required from ordering until the vehicle arrives at the customer's location	0.847
	WT2	Transportation is personal so it can come to serve immediately because it does not stop or hang at certain places. The driver will immediately come to pick up the passengers	0.853
	WT3	The ability of transportation that can pass through narrow alleys and residential locations, so customers can relax and wait in their respective homes	0.861
	WT4	The time required by service users when the vehicle arrives on the road and does not need to wait for other passengers or a full load	0.816
Driving safety (X5)	KM1	Transport drivers always obey traffic signs and be disciplined in driving vehicles	0.827
	KM2	The driver drives the vehicle at a moderate (normal) speed without being reckless, unemotional and maintaining a safe distance from other vehicles	0.803
	KM3	The mental attitude of the driver in driving the vehicle to concentrate (focus) and not play with cell phones	0.832

	KM4	Availability of completeness of vehicle attributes along with documents that must be fulfilled such as vehicle registration certificate, vehicle test books and so on	0.835
Passenger interest (Y)	K1	Desire to use urban environmental transportation services	0.876
	K2	Looking for information about environmental transport and interested in using it	0.883
	K3	Repeat orders or users of environmental transportation services can use environmental transportation services several times	0.855
	K4	The users of transportation services feel helped and can enjoy it so that they tell others to be able to use these transportation services	0.876

Source: Processed data (2021)

From a review of the loading factor figures, it can be identified how strong the relationship between the indicators is to each latent construct (latent variable). In another sense, it can be explained that the loading factor value describes how strong the correlation between construct indicators and latent variables is. Based on the results of data processing (output) as shown in Figure 2 about the model in this study and Table 2 about testing the loading factor value, it can be shown that all indicators have a loading factor value above 0.6. With the acquisition of the values obtained, it means that all indicators show valid validity test results (Ghozali, 2014). Thus, the interpretation of the question indicators used in the questionnaire is valid because it is relevant because it can explain and be able to measure the latent variables.

b. Discriminant Validity

A review of discriminant validity figures is needed to identify significantly the highest loading factor number in the resulting construct compared to the loading factor with other constructs. Ghozali (2014) provides guidelines on the inner model with reflective indicators tested using cross loading numbers. The mechanism is by knowing the magnitude of the effect (correlation) of the variable (construct) if it has a higher correlation test result than other variables, then this proves that the variable can measure its own block better than other blocks, as shown in Table 3 below:

Table 3. Cross loading value between latent variables

The value of the loading factor of the variables used in the study						
Code	X1	X2	X3	X4	X5	Y
TA1	0.811	-0.566	-0.286	0.433	0.616	-0.407
TA2	0.835	-0.054	0.178	-0.369	0.099	0.118
TA3	0.823	0.446	0.041	-0.001	-0.463	0.225
TA4	0.823	0.165	0.061	-0.051	-0.244	0.057
RA1	-0.062	0.809	0.238	0.085	0.143	-0.066
RA2	-0.121	0.798	-0.110	-0.378	0.410	-0.110
RA3	0.176	0.814	-0.349	0.182	-0.123	-0.116
RA4	0.004	0.841	0.213	0.100	-0.408	0.279
PS1	0.120	0.056	0.823	-0.016	-0.172	0.042
PS2	0.027	-0.001	0.809	-0.314	0.395	-0.196
PS3	-0.120	-0.267	0.878	0.190	0.151	0.073
PS4	-0.018	0.220	0.860	0.117	-0.362	0.070
WT1	-0.004	0.109	0.119	0.847	-0.238	-0.036
WT2	0.099	-0.029	-0.142	0.853	-0.261	0.063
WT3	0.137	0.075	0.086	0.861	0.085	-0.225

WT4	-0.244	-0.161	-0.065	0.816	0.430	0.210
KM1	-0.039	0.094	0.364	-0.480	0.827	0.224
KM2	-0.081	0.065	-0.612	0.443	0.803	-0.127
KM3	0.185	0.168	-0.061	0.033	0.832	-0.314
KM4	-0.067	-0.323	0.289	0.016	0.835	0.214
K1	0.122	-0.003	-0.048	0.005	-0.029	0.876
K2	-0.023	-0.129	-0.134	0.051	0.050	0.883
K3	-0.197	0.050	0.196	0.373	-0.007	0.855
K4	0.093	0.084	-0.008	-0.420	-0.015	0.876

Source: WarpPLS7.0 data processing output (2021)

Based on the data information in Table 3 above, it can be shown from the evaluation of the comparison of the cross loading values resulting in good discriminant validity because the correlation value of the indicator to the construct is higher than the correlation value of the indicator with other constructs. Thus, it can be explained that an indicator that is already a member of a certain variable, may not be a member of another variable.

2. Reliability Test

Reliability test is used to measure the reliability of the confidence level of the resulting model on the results of research data processing. In the reliability test, there are 3 parameter benchmark values to determine whether they are reliable or not, which consist of composite reliability, cronbach's alpha and average variance extracted (AVE). Based on these test parameters, the modeling generated in the implementation of this research can be explained as follows:

a. Composite reliability and cronbach's alpha

Based on the results of data processing, in the evaluation of the outer model, construct reliability tests can be carried out based on the value of composite reliability and cronbach's alpha from the indicator block that measures the construct. The following are the results of testing composite reliability and cronbach's alpha from the WarpPLS 7.0 output presented in Table 4 as follows:

Table 4. Composite Reliability and Cronbach's Alpha

Construct (Latent Variables)	Composite Reliability	Cronbach's Alpha
Rate (X1)	0.894	0.841
Travel route (X2)	0.888	0.832
Driving service (X3)	0.907	0.864
Waiting time (X4)	0.909	0.866
Driving safety (X5)	0.894	0.843
Passenger interest (Y)	0.927	0.895

Source: WarpPLS7.0 data processing output (2021)

Based on Ghazali (2014), a guideline is given that a construct is said to be reliable if it has a composite reliability value above 0.70 and cronbach's alpha above 0.60. Based on the results of data processing output using WarpPLS7.0 presented in Table 4, it was found that all constructs in this study had a composite reliability value above 0.70 and cronbach's alpha above 0.60. Thus, the indicators used in the questionnaire are reliable (reliable). A more in-depth interpretation can be explained as follows:

- 1) Based on the composite reliability value above 0.7, it shows that the latent variables used in this study have reliable reliability to test the research hypothesis.
- 2) Based on cronbach's alpha value above 0.6, it shows a fairly good level of consistency of answers from respondents to the questions in the questionnaire distributed to all respondents.

b. Average variance extracted (AVE)

The WarpPLS7.0 output results show the average variance extracted (AVE) value shown in Table 5 as follows:

Table. 5. Average variance extracted (AVE) value

Construct (Laten Variables)	AVE Value	AVE Benchmark Value	Description
Rate (X1)	0.677	0.5	Reliable
Travel route (X2)	0.665	0.5	Reliable
Driving service (X3)	0.711	0.5	Reliable
Waiting time (X4)	0.713	0.5	Reliable
Driving safety (X5)	0.679	0.5	Reliable
Passenger interest (Y)	0.761	0.5	Reliable

Source: WarpPLS7.0 data processing output (2021)

Based on the output of the AVE value as shown in Table 5, all construct variables showed values above 0.50. With the achievement of these parameter values, the results of the evaluation of the outer model show that it meets the reliability test (reliable) Ghazali, (2014). The interpretation in more depth can be explained that the indicators in this study have met the criteria for discriminant validity, in the sense that if certain indicators are included in certain variables, it is unlikely that they will become part or members of other variables (mutually exclusive).

4. Evaluation of the Inner Model (Structural Model)

Ghozali (2014) states that the inner model which is sometimes also called the inner relation, structural model or substantive theory describes the relationship between latent variables, which can be evaluated as follows:

1. Structural model testing (influence test)

The structural model in WarpPLS7.0 is evaluated based on the value of the regression coefficient (β) for the dependent variable and the path coefficient value for the independent variable which is then assessed for significance based on the P value of each path. In the inner model, this is also known as the influence test, in the sense of how the independent variable (independent variable) affects the dependent variable (dependent variable). Besides that, whether this influence can be proven significantly (significant) or not by looking at the p value compared to the p value table. As for explaining the structural model in this study, it can be seen through the WarpPLS7.0 output in Table 6 below:

Table 6. Influence test based on regression coefficient value (β)

Construct (Laten Variables)	Regression Coefficient Value(β)	Influence Percentage
Rate (X1)	- 0.03	-3%
Travel route (X2)	0.18	18%
Driving service (X3)	0.02	2%
Waiting time (X4)	0.88	88%
Driving safety (X5)	0.23	23%

Source: WarpPLS7.0 data processing output (2021)

Based on the value of the regression coefficient (β) obtained in this study as shown in Table 6, the parameter values for all constructs have 1 negative value and 4 positive values. With the achievement of the majority of positive coefficient values, it can be seen that there is an increasing effect on the factors of passenger interest in urban environmental transportation. Because of this, a more in-depth interpretation can be explained as follows:

- Urban environmental transport fares have an effect of -3% lowering the interest of the passengers.
- Urban environmental transportation routes have an increasing effect of 18% on passenger interest.
- The service of an urban environment transportation driver has an effect of increasing by 2% on the interest of its passengers.
- Waiting time for urban environmental transportation messages has an increasing effect of 88% on passenger interest.
- Driving safety of urban environmental transportation vehicles has an increasing effect of 23% on the interest of its passengers.

Based on the results of testing the structural model as described above, it can be concluded that the regression equation is as follows:

$$\text{Passenger interest (Y)} = -3\% \text{ Transport fare (X1)} + 18\% \text{ Transport route (X2)} + 2\% \text{ Driver service (X3)} + 88\% \text{ Transport order waiting time (X4)} + 23\% \text{ Vehicle driving safety (X5)}$$

2. Test the significance of the effect

In testing the structural model, it can be proven that there is an influence on all factors of passenger interest in environmental transportation in Tuban City. Based on the test results, further testing is still needed to obtain more convincing information whether the effect is significant (real) or only pseudo (not significant). In another sense, whether there is an effect indicated by a correlation value will need to be proven again whether the influence is real or is it just a coincidence. To test the significance of the effect of the independent variable on the dependent variable in the study, it can be shown in Table 7 as follows:

Table 7. Test the significance of the effect based on P Value

Construct (Latent Variables)	P Value	Test level			Significance test results
		$\alpha=10\%$	$\alpha=5\%$	$\alpha=1\%$	
Rate (X1)	0.38	0,1	0,05	0,01	Not significant
Travel route (X2)	0,03	0,1	0,05	0,01	Significant
Driving service (X3)	0.43	0,1	0,05	0,01	Not significant
Waiting time (X4)	< 0.01	0,1	0,05	0,01	Significant
Driving safety (X5)	< 0.01	0,1	0,05	0,01	Significant

Source: WarpPLS7.0 data processing output (2021)

The significance test can be done by looking at the comparison of the P value with the value of (test level) at the error rate =10%, =5% and =1%. Based on the P value obtained in the inner model of the data processing results in this study, if the parameter value is smaller than the value, it can be said that the influence of the independent variable in explaining (affecting) the dependent variable is significant (real) (Ghozali, 2014). As shown in Table 7 above, at the error test level =10% and =5% it can be seen that the construct (latent variable) that can be proven is passenger interest in urban environmental transportation, has a significant effect consisting of: variable transportation routes, waiting times and driving safety. As for the variable of transportation tariffs and driver services, the effect is not significant (not real or pseudo).

Based on the results of the influence test obtained, the results of the analysis can be used to test the research hypothesis, as can be observed in Table 8 below:

Table 8. Research Hypothesis Test Results

Research Hypothesis	Effect Test Results	Description
H1: Urban environmental transportation fares have a significant effect on passenger interest	Nosignificant effect	Rejected
H2: Urban environmental transportation routes have a significant effect on passenger interest	Significant effect	Accepted
H3: The service of an urban environment transportation driver has a significant effect on the interest of its passengers	Nosignificant effect	Rejected
H4: Order waiting time has a significant effect on the interest of urban environment transportation passengers	Significant effect	Accepted
H5: The safety of driving an urban environment transportation vehicle has a significant effect on the interest of its passengers	Significant effect	Accepted

Based on the results of hypothesis testing in this study as can be observed in Table 8 above, the interpretation can be explained as follows:

1. The effect of the transportation fare factor on the interest of urban environmental transportation passengers (H1 is rejected), showing the test results are not significant, in the sense that the influence of these factors cannot be proven and is not real (pseudo).
2. The influence of the transportation route factor on the interest of urban environmental transportation passengers (H2 is accepted), shows the test results of a significant effect, in the sense that the influence of these factors can be proven and is real.
3. The influence of the service factor of the urban environment transportation driver on the interest of the passengers (H3 is rejected), showing the test results are not significant, in the sense that the influence of these factors cannot be proven and is not real (pseudo).

4. The effect of the waiting time factor for ordering on the interest of urban environmental transport passengers (H4) is accepted, showing a significant effect test result, in the sense that the influence of these factors can be proven and is real.
5. The influence of the safety factor of driving an urban environment transportation vehicle on the interest of its passengers (H5 is accepted), shows the test results of a significant effect, in the sense that the influence of these factors can be proven and is real.

IV. CONCLUSION

Based on the analysis of passenger interest in urban environmental transportation in Tuban Indonesia, conclusions can be drawn:

1. Based on the evaluation of the outer model, the indicators and variables used meet the validity and reliability tests. This means that the questions contained in the questionnaire given to the respondents are valid and able to explain the latent variables and can be used to measure the reliability of the resulting model's confidence level.
2. Based on the results of the analysis of passenger interest in urban environmental transportation (evaluation of the inner model) it was found that message waiting time was the most influential variable, namely 88%, followed by driving safety 23% and route 18%, while the lowest influential variable consisted of driver service 2 % and the rate of effect decreases by -3%.

REFERENCES

- [1.] Ghozali, I. (2014). Structural Equation Modeling:Metode Alternatif dengan Partial LeastSquare (PLS). Fourth edition. Diponegoro University Publishing Agency, Semarang Indonesia.
- [2.] Solimun, Achmad; Reinaldo Fernandes and Nurjannah. (2017). Metode Statistika Multivariat: Pemodelan Persamaan Struktural (SEM)-Pendekatan WarpPLS (1st edition.). Brawijaya University Press, Malang Indonesia.
- [3.] Sugiyono. (2018). Metode Penelitian Kuantitatif, Kualitatif, dan R&D.Alfa Beta Publishing, Bandung Indonesia.

The Contribution of LCA Applications to the Development of National Ecolabel Criteria for the Personal Care and Cosmetic Sector

Nilgün Kıran Cılız¹, Cennet Değirmen¹, Merve Uzun¹, Ceyda Kalıpçioğlu¹, İman Abdulkadir Ahmed¹, Mehmet Emin Birpınar², Mehrali Ecer², Eyüp Kaan Morali², Serkan Atay², Ömer Ulutaş², Zeynep Aki², Kemal Dağ², Yahya Kesimal²

*¹Boğaziçi University, Institute of Environmental Sciences
Boğaziçi University Sustainable Development and Cleaner Production Center
Istanbul, Turkey*

*²Turkish Ministry of Environment, Urbanization and Climate Change
General Directorate of Environmental Impact Assessment, Permit and Inspection
Ankara, Turkey*

ABSTRACT

One of the industries which cause negative environmental impacts throughout the supply chain is the personal care and cosmetic products industry. The development of national ecolabelling criteria has been considered necessary to decrease the environmental pollution originating from the production and consumption of these products. This research was conducted for specific types of personal care and cosmetic products (bar soap, liquid soap, shampoo, hair conditioner, shower gel, hand and body cream, shaving soap, and shaving foam) that are produced and consumed in Turkey. Consumers have begun to look for more environmentally friendly products due to the increase in plastic and chemical pollution. This creates a need for companies to promote the green nature of their products to comply with the environmental awareness of consumers and their demands. Within this framework, the sector's approach to environmentally friendly products and ecolabeling was evaluated by applying life cycle assessment (LCA) as the decision-making mechanism. In addition to that, internationally recognized ecolabel standards, which are mainly used by countries with high import and export capacity, were analyzed. As a result of LCA studies, national environmental label criteria have been developed for personal care and cosmetic products. The environmental and socio-economic aspects of the products are evaluated based on sustainable production and consumption principles. Apart from the environmental benefits, it is expected that the implementation of the Turkey Ecolabel System, which is on a voluntary basis, will increase the market shares of products and the competitive abilities of the companies.

Keywords—Personal care and cosmetic products; LCA; Ecolabel standards; National criteria development

I. INTRODUCTION

Cosmetics and personal care products have been used for generations, and their existence in modern times has become an integral component of human life and more specifically sanitation. In addition to the need for personal hygiene, the desire to look young and well-groomed has also enabled the cosmetics industry to grow at an undeniable rate in the last decade. The size of the personal care and cosmetics market has reached approximately 500 billion dollars as of 2017 globally. According to data from the same year, it is observed that EU countries (77.6 billion euros), the USA (67.2 billion euros), and China (43.4 billion euros) have the highest shares in the consumption of personal care and cosmetic products based on retail sales prices (1). In 2020, the European cosmetics and personal care

market, which is the world's largest cosmetics market, was expected to be worth 76.7 billion euros at retail sales price. Among the European countries, the share of Germany (14 billion euros), France (11.5 billion euros), the United Kingdom (9.8 billion euros), and Italy (9.7 billion euros) have corresponded to more than half of the total capacity (2). The cosmetics industry exports of Turkey have also increased to 70.8 million dollars in 2019 while the imports decreased by 10.3% to that of 1 billion dollars (3). Moreover, the export capacity of Turkey was estimated to be 136.5 million dollars by October 2020 with the main export markets being the USA, Iraq, England, Russia, and the Netherlands, respectively. From the total export value, hair product has the highest percentage with 11.6%, followed by soap products at 5.3%, body lotions and creams at 3.1%, and shaving products at 1.7% (4).

The cosmetic industry is an interesting area to look into as certain synthetic chemicals, which are also defined as environmentally persistent, bioactive, bioaccumulative, and endocrine-disrupting compounds and which exist in the formulations of personal care and cosmetic products, pose a significant threat to ecological and human health (5). Increasing awareness about the environment and human health within different sectors has led to changes in consumption habits and the cosmetic industry is no exception. Consumers who want to reduce their environmental footprint by cutting the purchase of products made of synthetic chemicals have shown interest in more environmentally friendly products and services. Several studies examining consumer behavior reveal that environmentally friendly products are preferred more than conventional products and a growing interest in responsible consumption and production, which is one of the critical issues determined within the context of the Sustainable Development Goals (SDGs), have been observed (6)(7)(8). In the light of these data, it is foreseeable that companies will be steering towards innovative and sustainable alternatives in their value chains, especially in product formulations by taking strategic decisions to obtain an environmental label since ecolabel application plays a key role in guiding consumers to eco-friendly products (9).

The concerns regarding the environmental impacts of personal care and cosmetic products have been increasing tremendously, especially due to the unqualified selection of raw materials, which worsens the biota of aquatic environments (10). The consumption stage in the life cycle, which directly affects the wastewater stream, along with packaging selection and waste management are the specific processes that were considered necessary to be standardized in terms of environmental sustainability. A managerial and technical roadmap was developed by prioritizing environmental sustainability parameters according to the life cycle evaluations of the products in the project and is carried out in cooperation with the Turkish Ministry of Environment, Urbanization and Climate Change and Boğaziçi University with the aim of developing environmental label criteria with LCA principles. Life cycle assessment (LCA) is a decision-making mechanism that evaluates the environmental impacts of any process, system, or product by analyzing them via special software, which comparatively interprets these impacts to the "cradle to grave" approach and used that to provide fundamental information for policy development. The hot spots with the highest environmental impacts are determined by evaluating the relevant impact categories for each step of the process. Determination of hot spots and related impact categories with the LCA methodology provides an advantage of a better understanding of ecolabel indicators (11).

This study, which is highly significant in directing attention to eco-labeled products in the market, is expected to encourage several companies in taking a step in developing products with lower environmental impact, improving their environmental performance, and increasing consumer demand by providing environmentally labeled products to their customers. Furthermore, an effective governance system which includes guiding stakeholders; making the applicability of environmental label criteria valid for companies using various chemicals transported from all over the world; and considering issues such as government interventions, market requirements, and consumer awareness, is expected to encourage stakeholders to participate in the process of reducing the environmental impact of the product.

II. LITERATURE

Personal care or cosmetic products comprise multiple chemical components that are divided into various categories based on the value that they add. For instance, the group of chemicals that are used to add odor are called fragrance, whereas the group of chemicals that are used to extend the shelf life of a product and act as antimicrobials, antioxidants, etc. are called preservatives (12). Surfactants that have emulsifying, thickening, and conditioning effects, especially in hair products, are another example of chemical components that are frequently used (13).

Some of these chemical components are known to have a damaging impact on human and ecological health. For example, there are 26 fragrance agents defined as allergen chemicals according to the Food and Drug Administration (FDA). Hexyl cinnamal, citronellol, linalool, and limonene, which are included in many products in the market, are among these allergen fragrances. The use of these fragrances in the cosmetic industry was prohibited by the European Commission since 2019. Other fragrance agents that are known by their trade names are lylal (hydroxyisohexyl 3-cyclohexene carboxaldehyde; HICC) and lilial (butylphenyl methylpropional). These are classified as toxic substances for reproduction per the CLP Regulation and their use has been revised by the International Fragrance Association and will possibly be banned starting from March 2022. Furthermore, triclosan, which is one of the preservatives used in dental care products, has been debated upon its benefits towards the users. However, a survey conducted has shown high concentrations of triclosan in Japanese rivers (14) where it can then turn into chlorinated compounds which shows poisonous characteristics in water bodies (15). Thirdly, the synthetic surfactants such as sodium lauryl sulphate (SLS), cocamidopropyl betaine, and cocamide diethanolamine (DEA), which are commonly included in hair products, are known to cause both health damages like eye irritation and environmental damages due to their non-biodegradable structures in water and soil (12).

Ecolabel system is, hence, helpful as it gives correct and clear information to consumers regarding the environmental sustainability of products or services. It also provides an advantage for producers in terms of the market competition as it claims to offer environmentally more efficient and safer products (16). Ecolabel standards have been developed in an attempt to reduce the environmental impacts of chemicals and to integrate more sustainable methods in agricultural production activities. Encouraging environmentally friendly consumption and sustainable production techniques in the industry will improve the ecological and environmental aspects and performance of a product, raise awareness among all stakeholders about their responsibilities, and support the growth in institutional capacity, which leads to creating an evaluation system that is more reliable for both producers and consumers (17). Ameliorating the environmental performance of a product, which has been adopted by not only key stakeholders such as manufacturers and buyers but also secondary parties such as intermediary firms and institutions, has already been recognized to have a positive effect by incentivizing the purchase of products made with eco-friendly technologies (18). The development of such products can be achieved by using an integrated approach similar to LCA methodology which aims to diminish potential risks of the product across its entire life cycle. The Turkish Ministry of Environment, Urbanization, and Climate Change aim to support sustainable consumption and production practices by encouraging businesses that follow environmentally friendly processes and has implemented voluntary environmental labeling practices in line with the Environmental Label Regulation (dated: 19.10.2018) and the standard "TS EN ISO 14024:2018 Type 1: Environmental labeling - Principles and methods". Moreover, national environmental label practices are expected to push manufacturers to evaluate their product chain and prioritize issues such as low carbon emissions, waste prevention, energy efficiency, water-saving, and reduced use of harmful chemicals in their products/service.

Environmental labeling and ecolabel system are also related to the life cycle assessment approach and there are a few life cycle assessment studies conducted in the personal care and cosmetic sector. For instance, the impacts of the ecological scenarios that are ameliorated with operational techniques (the use of palmitic/stearic triglycerides, which are produced as a by-product in the olive oil industry, in variable formulations) in comparison to the conventional formulation (caprylic/capric triglyceride) were analyzed in an LCA study performed for hand creams. The results showed that the hand creams

produced with ecological scenarios cause less environmental impacts. Moreover, among these scenarios, it is shown that the use of palmitic/stearic triglycerides in the content of a pre-formulated component is more environmentally advantageous than direct use (19). Another study observed that the type of packing material used in a product's life cycle has also a significant impact on its environmental performance. In this national LCA study, PET packaging of a liquid soap, which was previously used, is compared with HDPE packaging, which is presented as an alternative. The results indicated that the HDPE use leads to a 15.6% decrease in the global warming potential, an 8.2% decrease in the acidification potential, and a 12.6% decrease in both the eutrophication and ozone depletion potentials compared to the PET use (20). Similarly, improvements such as refilling practices and/or the use of recycled materials as much as possible in the production of packaging have been observed to play a role in reducing the overall environmental impact of the product. It has also been determined that the type of energy used and the methods applied in waste management throughout a product's life cycle have a significant impact on the product's environmental performance. Raw material selection and extraction is also another variable that is critical for the environmental performance of the product.

When exploring raw materials within the personal care and cosmetic sector one valuable raw material that is discussed is palm oil. Most cosmetic products commonly contain substances derived from palm oil and its derivatives such as palm stearin and palm kernel oil, fatty acids, esters, fatty alcohols, fatty amines, and glycerin. As an example, fatty alcohols are utilized frequently in cosmetic and pharmaceutical products as a plasticizer, lubricant, and thickening agent (21). However, palm oil cultivation contributes to the greenhouse effect by creating negative impacts such as deforestation as well as methane and nitrogen oxide emissions from nitrogenous fertilizers. Forest trees absorb more carbon dioxide than palm trees; therefore, the destruction of forests and planting palm trees to obtain palm oil results in a drastic reduction in carbon dioxide sequestration. Furthermore, the peat soil in which palm trees grow creates more carbon dioxide when peat oxidation occurs. The milling process also releases methane, which has a negative impact on the environment (22). To minimize these negative impacts, it is critical to obtain palm oil, palm kernel oil, and their derivatives from fields where sustainable agricultural methods are applied.

In addition to raw material selection, one critical factor to look into regarding the environmental impact of products after consumption is their biodegradability which is a process that takes place when organic substances are decomposed into simpler organic and inorganic compounds such as carbon dioxide, water, ammonia by microorganisms in metabolic or enzymatic ways (23). Hence, biodegradation potential informs consumers about the environmental safety of products and assist them in selection of environmentally friendly ingredients (24). The persistent character of chemical substances in nature poses a danger to organisms in the long-term exposure, even in low levels, and causes irreversible potential problems depending on the frequency and concentration of the entrance to water bodies. For instance, when the surface-active agents end up in lakes and rivers, they decrease of oxygen level, disrupt the circulation between air and water, and leads the photosynthesis and aerobic oxidation of the aquatic organisms lower the water quality which result in environmental problems such as eutrophication (25). The prevalence of these substances in nature can be limited through a standardization that sets a framework for the use of biodegradable ingredients (26).

Manufacturers tend to increasingly use synthetic chemicals to both improve their formulations and fulfill consumer demands. The problem arises after these products reach consumers since they are released to aquatic environments after use (27). Thus, critical dilution volume has been considered an important methodology to determine the impact of these chemicals on aquatic bodies. (5). Additionally, personal care and cosmetic products may contain some hazardous chemicals which can have negative impacts even at low concentrations (28). Consequently, the use of these hazardous chemicals is prohibited while the use of other non-hazardous chemicals is permitted but only at certain concentrations. Certain preservatives, colorants, and fragrance compounds are some of the most toxic and banned chemicals in personal care and cosmetic products. Preservatives are important because they enable products to fully perform their functions; however, their use is limited by values such as biological density (BCF)

and octanol-water partition coefficient (log Kow) due to the toxic, irritating, and sensitizing properties of these chemicals (29). Colorant agents can cause both allergic reactions and skin irritation (30). The production of fragrance substances, which can either be natural or synthetic, in a laboratory can cause ethical and safety problems (31).

Energy utilization, which is part of the different operational stages in a product's life cycle, also has an impact on the environment as it contributes to global warming the most (32). For this reason, it is of vital importance to abandon conventional methods and to encourage the use of renewable energy sources to reduce environmental impacts and mitigate climate change. For instance, Aveda has succeeded in being one of the pioneer cosmetic companies for responsible manufacturing by transitioning to green energy via wind power technologies and has reduced its carbon emissions over the past 30 years (33).

Packaging, which has a tremendous effect on the branding of personal care and cosmetic products, and recycling of packaging materials are also highly significant for sustainable and economic development in terms of improving brands' competitiveness on the market. Hence, a shift from the old-fashioned model for production and disposal of plastics to a new model that evaluates the life cycle of plastics from an environmental point of view is essential since the disposal of plastic waste is unsustainable in the long run (34). Therefore, considering the increase in plastic production and the ineffectiveness of waste management, there is a concern that the atmospheric emissions can reach up to 6.5 Gt CO₂-eq. and the cumulative plastic pollution can reach up to 12,000 Mt by 2050 (35)(36). Waste management is also essential in the cosmetics industry as it ensures that waste from the products and packaging materials is prevented from being released to the environment once the product is no longer in use. Moreover, it is used to control that the waste amount is regulated; and that recyclable package is contributing to the economy. It should be noted that the type of waste is not restricted to bottles and tubes; that is, it also involves cardboard and boxes as the secondary packaging so virtually, all the consumer packaging ends up as solid waste after consumption (37).

The demand for organic and natural content in personal care and cosmetics owing to the sensitivity of consumers to both protecting environmental health and ensuring sustainable production has become a factor that directs manufacturers to more environmentally friendly technologies, especially in recent years (38). Organic content means the components in the product formulation are obtained following organic agriculture practices in which there is no use of pesticides, synthetic fertilizers, sewage sludge, genetically modified organisms, and ionizing radiation. On the other hand, natural content refers to ingredients in the product formulation that are mainly derived from plants and/or animal origins (39). It is expected that the consumption of organic products reduces health risks, which stems from, for instance, pesticide residues, and environmental contamination due to the synthetic chemicals used in the product (40).

Fitness for use, which has gained a significant role as the cosmetic industry has an upward trend in the recent decades, shows the product's capacity to accomplish its primary and secondary purposes. Even if personal care and cosmetic products are manufactured by well-known and trustworthy companies, most prevalent beauty products contain various chemical ingredients that may be noxious and cause some allergic reactions in consumers (41). For this reason, some laboratory tests are devised through international guides to prove the efficacy and congruency of the products before releasing them to the market (42). This will also encourage manufacturers to avoid using unsuitable components in their products due to their potential effects. The information written on the ecolabel of personal care and cosmetic products is very determinant in consumers' choices. The implementation of the ecolabels may result in putting too much information on the frame which should be avoided (43). Nonetheless, manufacturers aim to supply reliable and detailed information to make consumers aware of the product's environmental performance and its sustainability aspects (16).

III. METHODOLOGY

A research survey has been conducted to summarize the relevant conditions regarding environmental sustainability and evaluate product compositions in terms of environmental labels within the personal

care and cosmetics sector in Turkey. The survey was done to understand the perspective of the producers in the sector and with the participation of relevant institutions, stakeholders, and reliable brands which has then provided production data on the cosmetics and care products that are discussed in the study of the environmental label system. Evaluation of the obtained survey results was made using the SPSS statistical analysis program. Within the context of life cycle assessment, studies were carried out for personal care and cosmetic products such as liquid and bar soap, shampoo, hair conditioner, shower gel, hand/body cream, shaving soap, and shaving foam and their environmental impacts have been examined at various stages including raw material supply; production; filling (primary packaging); secondary and tertiary packaging; distribution; and use and disposal of wastes (wastewater, packaging waste, etc.) generated. The environmental impact categories that were considered are global warming potential (GWP), acidification potential (AP), eutrophication potential (EP), ozone depletion potential (ODP), freshwater aquatic ecotoxicity potential (FAETP), and photochemical ozone creation potential (POCP). These impact categories are used to frame the impacts of analyzed products on air and water quality.

The life cycle evaluation studies aim to develop national environmental label criteria by identifying the points that need to be highlighted from raw material supply to waste management. The development process of environmental label criteria requires a great deal of research, support mechanisms (life cycle assessment in this study), and input from multiple stakeholders. To develop the national ecolabel criteria, it is required to research the chemicals, resource consumption, and waste generation in the context of the value chain. Moreover, the related national legislation and international standards should be considered in the context of relevance and inclusiveness. As a first step, out of the 66 ecolabel standards that are approved by the international market, 10 widely applied ecolabel standards (EU Ecolabel (44), Blue Angel (45), COSMOS (46), Good Environmental Choice (Bra Miljöval) (47), Nordic Swan (48), Korean Ecolabel (49)(50), Green Seal (51), Ecocert (52), Green Choice Philippines (53)(54), Environmental Choice New Zealand (55)) which are also valid in countries with high export rates were examined. As the support mechanism, GaBi 8.0 software and Ecoinvent databases were utilized to assess the data obtained from industry and literature sources. Throughout the study assumptions ranging between 20% and 30% were made in some cases depending on the quality and adequacy of the available data. The relationship between these international ecolabel standards and the national criteria was taken into consideration in accordance with the information on the national legislation to accurately assess the feasibility, effectiveness, and bindingness of the national criteria.

IV. RESULTS AND DISCUSSION

The national criteria of the ecolabel, which is a voluntary scheme and is developed for personal care and cosmetic products, cover a broad area in terms of sustainability. The ecolabel applications carried out under the coordination of the Turkish Ministry of Environment, Urbanization and Climate Change is an important milestone that encourages companies to pursue sustainability goals and allow them to publish reports and announce the environmental impacts of their products transparently based on LCA studies.

A. Evaluation of Survey Results

The survey that was conducted with the participation of the manufacturers was effective in developing the national ecolabel criteria since it investigated the views of stakeholders, who are active in the sector, on subjects such as ecolabel and LCA. The survey results showed that only 43% of the participants have knowledge about life cycle assessment method, and it was seen that in the LCA studies, the participants mostly focus on the "final product manufacturing" stage of a life cycle (23.5%) followed by "packaging" (21.6%), and "distribution/transportation" (13.7%). Additionally, it was observed that the participants prefer to apply the ecolabel application mostly with the purpose of presenting the products as quality (32%) followed by encouraging consumers to be responsible (23%) and then addressing consumers' demands (18%).

Additionally, the survey reflects how numerous chemicals with multiple purposes are used in the production of personal care and cosmetic products but also explores how certain regulations have

taken effect within the sector. For instance, in the production stage, it was seen that the most-used chemicals are "mineral oils, Vaseline and relevant hydrocarbons" and "synthetic fragrances and aromatic substances" (11.7%). However, phthalates are included in the List of Excluded Substances in Cosmetic Products which is in the Appendix 2 of the Cosmetics Regulation (the Turkish Ministry of Health/Date: 23.05.2005 and No: 25823); therefore, no participant indicates phthalate use in their products.

Finally, the survey also looks into the packaging habits of the participants. Packaging is a tool that protects the product, ensures its distribution to consumers in a safe way, and enables the transportation and storage of the product. It is important for packaging to be reusable and recyclable, and to be considered as secondary raw material in several industries. The survey results showed that the participants mostly prefer PET (21.2%) in packaging followed by PP and PE (both 19.2%).

B. Evaluation of Life Cycle Assessment Results

According to the results, it is observed that the environmental load in global warming and ozone layer depletion impact categories has mostly originated from the distribution process whereas the production process has the highest impact in the other categories. Moreover, although the production process of shower gel creates a greater effect in acidification, eutrophication, and photochemical ozone creation impact categories compared to the consumption phase, the consumption phase in the life cycles of shampoo and hair conditioner has the highest effect in all categories. The reason is that the amount of water used to rinse hair care products and the energy spent to heat the water are too high compared to the water and energy used to wash off shower gel. When it comes to hand and body creams, which are leave-on care products, the production process has a massive impact on acidification, eutrophication, and photochemical ozone creation impact categories, while production process of the primary packaging, on the other hand, affects ozone layer depletion and freshwater ecotoxicity potential and raw material supply affects the global warming potential among the other impact categories. For shaving products, depending on the life cycle stages, it is seen that raw material supply, transportation of products to the consumer, and the transportation of wastes to landfill affects the impact categories of global warming, ozone layer depletion, and photochemical ozone formation potential, while production of both products and primary packaging stages affects the impact categories of acidification, eutrophication and freshwater ecotoxicity potential.

Emissions arising from the fuel used in the transportation of raw materials and delivery of the products to the distribution points; emissions stemming from the unsustainable production of energy sources such as electricity, natural gas or steam used in fundamental processes such as production and/or packaging; and emissions being released as a result of the interaction between chemicals in the mixing phase during the production process have all contributed in developing the aforementioned impact categories. The disposal methods (landfill, incineration, and recycle) of packaging waste generated during the post-consumer phase were also evaluated, and it was concluded that the most beneficial disposal method in terms of environmental performance changes depending on the packaging type.

C. The Criteria of Environmental Label

The environmental, social and economic aspects of the study were carried out in accordance with the United Nations Sustainable Development Goals. Consequently, a feasible national environmental labelling standard for the personal care and cosmetic products, which can be applied on the national scale and is in parallel to the national sustainability priorities, have been developed based on the results of the LCA studies and by considering the international ecolabel standards for the sector and their impacts.

The criteria developed are related to the results of the life cycle study. To be more precise, sustainable supply of palm oil, palm kernel oil and their derivatives, biodegradability, toxicity to aquatic organisms, excluded and limited chemicals, organic and natural content are the specific criteria that are related to raw material acquisition, and consumption stages in the context of the life cycle, whereas energy management, packaging and fitness for use are related with the production process. Due to this direct

relationship between the life cycle assessment and the environmental label criteria, the adverse environmental impacts observed at any LCA stage will be reduced and/or prevented by the criteria established within the scope of the study. The national environmental label criteria, which are created by evaluating the potential effects of personal care and cosmetic products throughout their life cycle, and based on the compatibility of eco-label standards examined on a global scale with national legislation, are listed below.

- Sustainable Supply of Palm Oil, Palm Kernel Oil, and Their Derivatives: Cultivation and supply of palm oil cause adverse effects on the environment. Obtaining the palm oil used in environmentally labeled products from fields operating with sustainable methods is a necessary criterion to minimize these negative effects.
- Biodegradability: All surfactants are expected to be readily biodegradable both aerobically and anaerobically as the biodegradability of surfactant is important. However, the organic substances in cosmetic products might contain substances that are considered to be aerobically and/or anaerobically non-biodegradable in limited amounts within the context of national environmental labeling criteria.
- Toxicity to aquatic organisms: Preventing the release of synthetic chemicals into the environment as they do not degrade in nature is a more ideal and easier solution than finding new ways to remove these chemicals from the water bodies.
- Excluded and limited chemicals; Some of the fragrances, colorants, and preservatives, the use of which was restricted are also evaluated within the scope of this criterion in addition to the chemicals that are excluded in the formulations (alkylphenol ethoxylates and other alkylphenol derivatives, trisodium nitrilotriacetate, formaldehyde and formaldehyde separators, parabens, etc.) and harmful chemicals with at least one hazard statement.
- Energy Management: It aims to alleviate the pressure on climate change by encouraging the use of renewable and clean energy sources. Most of the emissions released into the atmosphere during the production of personal care and cosmetic products are due to energy use. For this reason, energy management has also been evaluated among the criteria that are regarded as necessary for the environmental label.
- Packaging: In accordance with international guidelines which cover primary and secondary packaging design criteria and aim to minimize the environmental impacts of packaging, this criterion has been given priority in the national environmental labeling system of Turkey, as well.
- Waste management: The packaging material of each product poses a waste potential. Organic chemicals exist in cosmetics and personal care products create a trace in nature both during the use of the product and after the product is finished due to the disposal of the packaging and the residual product in it. Recycling of plastic material is an integral part of the circular economy. Therefore, waste management is among the criteria deemed necessary for the national environmental label.
- Organic and natural content: This criterion requires that the components within the product which are extracted from plants and/or animals to be obtained without disturbing the function of the ecosystem in any way, or without further endangering the endangered/at risk species, or without making a possible negative contribution to environmental pollution.
- Fitness for use: Companies' reliability and preferability are enhanced when information regarding the product's potential effects is presented to the consumer in an honest and transparent manner. For this reason, manufacturers who want their products to have an environmental label, are responsible for having the conformity tests required by this criterion.
- Information written on the ecolabel: It is a criterion that considers it to be necessary to inform the consumer about the product and its highlighted environmental and sustainable aspects. The information that is included in the environmental label is expected to be presented in a clear, concise,

and understandable manner such as "reduced impact on aquatic ecosystems", "production and packaging with environmentally friendly techniques".

V. CONCLUSION

With the increase in the utilization of personal care and cosmetics products, producers have found themselves manufacturing synthetic chemicals in lieu of those obtained naturally as these chemicals help producers to meet the increase in demand. Nevertheless, there is a considerable amount of evidence indicating that such chemicals are harmful to both human health and the environment since they may be toxic and bioaccumulate or may cause some long-term damage. Hence, consumers are provided with options such as having access to products with an environmental label that expresses the quality and sustainability of a product which in turn helps consumers to be informed about their choices daily.

In this study, the national ecolabel criteria have been developed for the selected personal care and cosmetic products (bar soap, liquid soap, shampoo, hair conditioner, shower gel, hand and body cream, shaving soap, and shaving foam). During this process, several national and international regulations, declarations, standards, and guides were examined to ensure that the criteria would be as comprehensive, reasonable, and feasible as possible. Life cycle assessment (LCA) methodology was applied to establish a relationship between the set of criteria and the impacts resulting from each life cycle stage. Another important thing to state is that assistance is provided by the Turkish Ministry of Environment, Urbanization and Climate Change throughout the study, and technical feedback and/or evaluations were delivered by the Technical Committee and the industry itself. Government support, market demand, and consumer awareness along with the business ethics approach for loss of biodiversity and needs of future generations will accelerate the interest for supplying the ecolabel criteria content. The ecolabel will provide transparency which is the key to assist stakeholders in making decisions.

ACKNOWLEDGMENT

This project was funded by Turkish Ministry of Environment, Urbanization and Climate Change.

REFERENCES

- [1] S. Özden, M. Saygılı, and N. Sütütemiz, "Kozmetik ürünlerin tüketiminde sağlık bilincinin rolü," IBANESS Congress Series, 2019, pp. 790-802.
- [2] Cosmetic Europe, "Cosmetic and personal care industry overview," Personal Care Association, 2021.
- [3] The Turkish Ministry of Trade, "Cosmetics sector, sectoral reports," Republic of Turkey, Ministry of Trade, Ankara, Turkey, 2021.
- [4] D. Yücesan, "Kozmetik sektörü raporu," İstanbul, 2020.
- [5] A. Chavoshani, M. Hashemi, M. Mehdi Amin, S. C. Ameta, "Personal care products as an endocrine disrupting compound in the aquatic environment, in: Micropollutants and Challenges. Elsevier Inc., 2020, pp. 91–144, doi: 10.1016/B978-0-12-818612-1.00003-9.
- [6] M. Bekk, M. Spörrle, R. Hedjasie, and R. Kerschreiter, "Greening the competitive advantage: Antecedents and consequences of green brand equity," *Quality and Quantity*, 50(4), pp. 1727–1746, 2016, doi: 10.1007/s11135-015-0232-y.
- [7] I. Mufidah, B. C. Jiang, S. C. Lin, J. Chin, Y. P. Rachmaniati, and S. F. Persada, "Understanding the consumers' behavior intention in using green ecolabel product through Pro-Environmental Planned Behavior model in developing and developed regions: Lessons learned from Taiwan and Indonesia," *Sustainability (Switzerland)*, 10(5), pp. 1–15, 2018, doi:10.3390/su10051423.
- [8] A. Kahraman and İ. Kazaçoğlu, "Understanding consumers' purchase intentions toward natural-claimed products: A qualitative research in personal care products," *Business Strategy and the Environment*, 28(6), pp. 1218–1233, 2019, doi: 10.1002/bse.2312.
- [9] Y. Chakravarthy, A. Potdar, A. Singh, S. Unnikrishnan, and N. Naik, "Role of ecolabeling in reducing ecotoxicology," *Ecotoxicology and Environmental Safety*, 134, pp. 383–389, 2016, doi: 10.1016/j.ecoenv.2015.09.017.
- [10] N. A. Vita et al., "Parameters for assessing the aquatic environmental impact of cosmetic products," *Toxicology Letters*, 287, pp. 70–82, 2018, doi: 10.1016/j.toxlet.2018.01.015.

- [11] M. Bernardo, "Evaluation of ecolabelling criteria using life cycle assessment," Master's Thesis, Arizona State University, Tempe, Arizona, 2012.
- [12] V. Smith and S. M. Wilkinson, Chapter 23: Cosmetics, in *Quick Guide to Contact Dermatitis*, J. D. Johansen; JP. Lepoittevin; J. P. Thyssen, Eds. Springer, Berlin, Heidelberg, 2016, pp. 257–273, doi:10.1007/978-3-662-47714-4.
- [13] H. L. Brannon, Surfactants in skin and hair products, verywellhealth [Online], 2020. Available: <https://www.verywellhealth.com/surfactant-ingredients-skin-hair-products-1069381>.
- [14] K. Kimura et al., "Occurrence of preservatives and antimicrobials in Japanese rivers," *Chemosphere*, 107, pp. 393–399, 2014, doi: 10.1016/J.CHEMOSPHERE.2014.01.008.
- [15] M. Bilal, S. Mehmood, and H. M. N. Iqbal, "The beast of beauty: Environmental and health concerns of toxic components in cosmetics," *Cosmetics*, 7(1), pp. 1–18, 2020, doi: 10.3390/cosmetics7010013.
- [16] F. Iraldo, R. Griesshammer, and W. Kahlenborn, "The future of ecolabels," *International Journal of Life Cycle Assessment*, 25(5), pp. 833–839, 2020, doi: 10.1007/s11367-020-01741-9.
- [17] V. Prieto-Sandoval, J. A. Alfaro, A. Mejía-Villa, and M. Ormazabal, "Eco-labels as a multidimensional research topic: Trends and opportunities," *Journal of Cleaner Production*, 135, pp. 806–818, 2016, doi: 10.1016/j.clepro.2016.06.167.
- [18] M. Esmaeilpour and E. Bahmiary, "Investigating the impact of environmental attitude on the decision to purchase a green product with the mediating role of environmental concern and care for green products," *Management and Marketing*, 12(2), pp. 297–315, 2017, doi: 10.1515/mmcks-2017-0018.
- [19] M. Secchi, V. Castellani, E. Collina, and N. Mirabella, "Assessing eco-innovations in green chemistry: life cycle assessment (LCA) of a cosmetic product with a bio-based ingredient," *Journal of Cleaner Production*, 129(June 2007), pp. 269–281, 2016, doi: 10.1016/j.jclepro.2016.04.073.
- [20] Istanbul Development Agency, "Faaliyet 5: kişisel bakım ve kozmetik sektöründe ulusal eko etiketleme metodolojisinin oluşturulması - sıvı sabun ydd raporu," Istanbul, Turkey, 2016.
- [21] S. K. Yeong, Z. Idris, and H. Abu Hassan, Palm oleochemicals in non-food applications, in: Lai, O., Tan, C., Akoh, C. C., Eds. *Palm Oil: Production, Processing, Characterization, and Uses*, AOCS Press, 2012, pp. 587–624, doi: 10.1016/B978-0-9818936-9-3.50023-X.
- [22] R. H. V. Corley and P. B. Tinker, *The oil palm*, Wiley Blackwell, 2016.
- [23] J. Alvarez, *Biodegradation: properties, analysis and performance*. Nova Science Publisher Inc., New York, NY, 2016.
- [24] N. Dayan and L. Kromidas, *Formulating, Packaging, and Marketing of Natural Cosmetic Products*. John Wiley & Sons, Inc., 2011, doi: 10.1002/9781118056806.
- [25] A. K. Mungray and P. Kumar, "Occurrence of anionic surfactants in treated sewage: Risk assessment to aquatic environment. *journal of hazardous materials*," 160(2–3), pp. 362–370, 2008, doi: 10.1016/j.jhazmat.2008.03.025.
- [26] OECD, "Phototransformation of Chemicals in Water – Direct Photolysis," *OECD Guideline for the Testing of Chemicals*, (October), pp. 1–53, 2008.
- [27] S. Rainieri, A. Barranco, M. Primec, and T. Langerholc, "Occurrence and toxicity of musks and uv filters in the marine environment," *Food and Chemical Toxicology*, 104, pp. 57–68, 2017, doi: 10.1016/j.fct.2016.11.012.
- [28] C. Su, Y. Cui, D. Liu, H. Zhang, and Y. Baninla, "Endocrine disrupting compounds, pharmaceuticals and personal care products in the aquatic environment of china: Which chemicals are the prioritized ones?," *Science of The Total Environment*, 720, p. 137652, 2020, doi: 10.1016/J.SCITOTENV.2020.137652.
- [29] G. Alvarez-Rivera, M. Llompert, M. Lores, and C. Garcia-Jares, Preservatives in cosmetics: Regulatory aspects and analytical methods, in: Salvador, A., and Chisvert, A., Eds. *Analysis of Cosmetic Products: Second Edition*, Elsevier, 2018, pp. 175–224, doi: 10.1016/B978-0-444-63508-2.00009-6.
- [30] A. Weisz, S. R. Milstein, A. L. Scher, and N.M. Hepp, Colouring agents in cosmetics: Regulatory aspects and analytical methods, in: Salvador, A., and Chisvert, A., Eds. *Analysis of Cosmetic Products: Second Edition*, Elsevier, 2018, pp. 123–157, doi: 10.1016/B978-0-444-63508-2.00007-2.
- [31] A. Chisvert, M. López-Noguerolles, P. Miralles, and A. Salvador, Perfumes in cosmetics: Regulatory aspects and analytical methods, in: Salvador, A., and Chisvert, A., Eds. *Analysis of Cosmetic Products: Second Edition*, Elsevier, 2018, pp. 225–248, doi: 10.1016/B978-0-444-63508-2.00010-2.
- [32] W. Moomaw, F. Yamba, M. Kamimoto, L. Maurice, J. Nyboer, K. Urama, and T. Weir, Introduction, in: Edenhofer, O., Pichs-Madruga, R., Sokona, Y., Seyboth, K., Maatschoss, P., Kadner, S., Zwickel, T., Eickemeier, P., Hansen, G., Schlömer, S., and Von Stechow, C., Eds., *IPCC Special Report on Renewable Energy Sources and Climate Change Mitigation*, NY, USA, 2011, doi: 10.1002/9781119994381.
- [33] M. J. Brady and S. Monani, "Wind power! Marketing renewable energy on tribal lands and the struggle for just sustainability," *The International Journal of Justice and Sustainability*, 17(2), pp. 147–166, 2012, doi: 10.1080/13549839.2011.646966.
- [34] E. J. North and R. U. Halden, "Plastics and environmental health: The road ahead," *Reviews on Environmental Health*, 28(1m), pp. 1–8, 2013, doi: 10.1515/reveh-2012-0030.
- [35] R. Geyer, J. R. Jambeck, and K. L. Law, "Production, use, and fate of all plastics ever made - supplementary information," *Science Advances*, 3(7), pp. 19–24, 2017, doi: 10.1126/sciadv.1700782.
- [36] J. Zheng and S. Suh, "Strategies to reduce the global carbon footprint of plastics," *Nature Climate Change*, 9(5), pp. 374–378, 2019, doi: 10.1038/s41558-019-0459-z.

- [37] C. J. C. Bennett and M. S. Brown, Energy and Waste Management, in: Sahota, A., Ed. Sustainability: How the Cosmetics Industry Is Greening Up, John Wiley & Sons, Incorporated, London, UK, 2013 pp. 158–160.
- [38] C. Barros and R. B. G. Barros, "Natural and organic cosmetics: Definition and concepts," *Journal of Cosmetology & Trichology*, 6(2), 2020, doi: 10.20944/preprints202005.0374.v1.
- [39] C. Villa, Green cosmetic ingredients and processes, in: Salvador, A., and Chisvert, A., Eds. Analysis of Cosmetic Products: Second Edition, Elsevier, 2018, pp. 303–330, doi: 10.1016/B978-0-444-63508-2.00013-8.
- [40] E. Ghazali, P. Chen, D. S. Mutum, and B. Nguyen, "Investigating consumers' values for buying organic personal care products. *journal of retailing and consumer services*," 39(June), pp. 154–163, 2017, doi: 10.1016/j.jretconser.2017.08.002.
- [41] P. Tejal, D. Nishad, J. Amisha, G. Umesh, K. T. Desai, and R. K. Bansal, "Cosmetics and health: usage, perceptions and awareness," *Bangladesh Journal of Medical Science*, 12(4), pp. 392–397, 2013, doi: 10.3329/bjms.v12i4.13330.
- [42] Cosmetics Europe - The Personal Care Association, "Guidelines for the evaluation of the efficacy of cosmetics products," (May), pp. 1–18, 2008.
- [43] J. Thøgersen, P. Haugaard, and A. Olesen, "Consumer responses to ecolabels," *European Journal of Marketing*, 44(11), pp. 1787–1810, 2010, doi: 10.1108/03090561011079882.
- [44] European Commission, EU Ecolabel rinse-off cosmetic user manual, 2016.
- [45] The Federal Ministry of Environment, "Blue Angel, The German ecolabel: shampoos, shower gels, soaps and other so-called 'rinse-off' cosmetic products," Bonn, 2016.
- [46] COSMOS-Standard AISBL, "Cosmetics standard organic and natural cosmetics," France 2020.
- [47] Swedish Society for Nature Conservation, "Criteria for Good Environmental Choice: cosmetics," Gothenburg, 2018.
- [48] The Nordic Council of Ministers, "Nordic Swan ecolabelling of cosmetic products," Nordic Swan Ecolabelling, 2020.
- [49] The Korean Ministry of Environment, "Korea eco-label standards: cosmetic soap," 2014.
- [50] The Korean Ministry of Environment, "Korea eco-label standards: shampoo and rinse," 2014.
- [51] Green Seal, "Green Seal standard for soaps, cleansers, hand sanitizers, and shower products," Washington, DC, 2020.
- [52] ECOCERT Greenlife SAS, "Ecocert standard: natural and organic cosmetics," Organic Natural Living, (May), 2012.
- [53] Philippine Center for Environmental Protection and Sustainable Development Inc., "The ecolabelling program of the Philippines: Green Choice Philippines - bath soap," 2002.
- [54] Philippine Center for Environmental Protection and Sustainable Development Inc., "The ecolabelling program of the Philippines: Green Choice Philippines – hair shampoo," 2002.
- [55] The New Zealand Ecolabelling Trust, "Licence criteria for Toitety products," Auckland, 2020.

Categorization of recommender system methods

Chiheb Eddine Ben Ncir

Management Information System
College of Business, University of Jeddah
Jeddah, Saudi Arabia

ABSTRACT

Recommender systems have become a necessary requirement in several application domains due to information overload. The development of web applications and social networks has made data widely and largely available. Filtering necessary and important data has become a non-trivial task. Recommender systems can help users to filter relevant data and provide them with the best suggestions. To develop such automatic system, several methods have been used to filter data and to build suggestions. Usually, these methods are categorized into three main categories which are: content-based, collaborative-based and hybrid methods. In this paper, we give a new categorization of recommender system methods where methods are categorized into six categories. We add three new categories which are multi-criteria recommendation, context awareness-based recommendation and social network-based recommendation.

Keywords—recommender systems; collaborative filtering; content-based filtering; Hybrid methods

I. INTRODUCTION

The web has become the largest accessible information space in the world [1]. In this space, information in its various forms grows exponentially which results in large amount of data available for users. It becomes more and more difficult for regular Internet-users to successfully find items related to their tastes and preferences. For example, an internet user browsing an online film or movie does not wish to go through thousand of uninteresting movies before finding a preferred one. The increasing number of choices makes it harder for users to find exactly the preferred item. Fueled by this need to combat information overload, recent years have witnessed an increase of research in the area of recommender systems.

Recommender Systems are software tools providing users with suggestions related to their tastes and preferences. They help users to deal with information overload by giving suggested items to a user related to his tastes and expectations. An item can be an article to read, a product to buy, a piece of music to listen to, a movie to watch or a web page to consult. The objective is both to minimize his time spent on research, but also to suggest relevant items that he would not have spontaneously consulted and thus increase his overall satisfaction.

Recommendation systems have become an important research area with the publication of the first articles in the collaborative filtering field. The academic literature has introduced the term collaborative filtering by "Tapestry" [2] system that represents one of the first recommendation systems. It was developed in 1992 by the research center of "Xerox" in the United States. A few years later, with the growth of the Internet, and web applications, there have been a keen interest in recommendation systems that have developed in different areas of application, such as movies recommendation like Netflix or MovieLens [3], Musical titles Recommendation like Last FM, news recommendation like Yahoo! News, products recommendation introduced on e-commerce sites like Amazon [4], bibliographic citations recommendations systems like Tech Lens [5], courses recommendation systems introduced in e-learning sites, friends recommendation systems like Twitter or Facebook.

These applications show that recommender system are receiving an important attention [6] by the research community. Indeed, there has been dedicated conferences and workshops related to this field such as the ACM Recommender Systems (Rec Sys) established in 2007. In addition, sessions dedicated to recommender systems are frequently included in the more traditional conferences in the area of data bases, information systems and adaptive systems. Recent interesting books [7] related to recommender systems has been recently published introducing recommender system's techniques. Moreover, there have been several special issues in academic journals covering research and developments in the recommender system field.

This paper gives an overview of recommender systems methods and techniques which are adopted in several existing systems. We give a classification of these methods based on the approach used to give recommendations. The rest of the paper is organized as in the following: Section II presents main components of recommender systems, then Section III presents main concepts and approaches of recommendation systems while giving a classification of existing methods. Finally Section IV gives conclusions and future works.

II. RECOMMENDER SYSTEMS COMPONENTS

Recommender systems are information processing systems that actively gather various kinds of data in order to build their recommendations [7]. Data is primarily about the items to suggest and the users who will receive these recommendations. In general, these data are dependent to the used recommendation technique. However, data used by recommender systems can refer to three kinds of objects [7]: items, users, and Preferences.

- **Users** : People who accesses the system , entering his demographic information, his interests and other personal information.
- **Items**: Products which the system can recommend are referred to as "items". These items correspond to the need of the user, including any product likely to be seen (movies in online TV sites such as Netflix), sold (book in the e-commerce sites such as Amazon.com), listened (music) or read (such as scientific article in a digital libraries).
- **Preferences**: In order to provide personalized recommendations adapted to the needs of the active users, recommender systems must collect personal preference information. Two categories of preferences data exist, the first is the explicit data [8] expressed by users during their navigation activities. For example, providing a note on a scale of predefined values (notes that users indicate on products they buy on the Internet for example), express an opinion on an object (example of the button "Like" on Facebook), etc. The second category is the implicit data [9] collected by observing user behavior and activity. The activity may be web pages viewed, the user's history of purchases, click-stream data, etc.

III. CATEGORIZATION OF RECOMMENDER SYSTEM METHODS

To get an earlier overview of the different types of recommendation systems, a taxonomy provided by authors in [10] has been considered a benchmark for classifying these systems. Three main methods are defined:

- Content-based recommendation system: The relevance of the recommended items is estimated by the similarity between the features or content of the items, and the profile of the user reflecting its needs in terms of content.
- Collaborative-based recommendation system: The system recommends items seen by other users with similar tastes or common interests.
- Hybrid recommendation system: The system exploits the complementary of the two previous approaches by combining them.

In addition to these recommendation categories, we added new recommendation categories which are multi-criteria recommendation, context awareness-based recommendation and social network-based recommendation. These recommendation system methods are presented in more detail in the following subsections.

A. Content-based recommendation methods

Content-based method tries to recommend items that are similar to items previously liked by a specific user as described in Figure1. To return recommendations, the system needs the following information:

- **item profile**: the item profile is a set of features that represent the content of the recommended item. For example, in a research article recommendation system, the attributes adopted to describe an article are title, author, year, venue, ..., etc. Content-based method depends strongly on the nature of the data to be represented and it finds difficulties for the representation of the items, which decreases its accuracy from one type of resource to another. Textual data is the best represented and with which the method gives the best accuracy, whereas other data types, i.e. non-textual data such as videos and images, give poor precision due to the difficulty in extracting characteristics. Generally, for non-textual data, the approach uses metadata to represent its content.

- **user profile:** The user profile build a description of user needs and preferences. From the user profiles and descriptions of the items to be recommended, this content-based recommender system analyzes their similarity, then it builds a list of suggestions to present to the user.

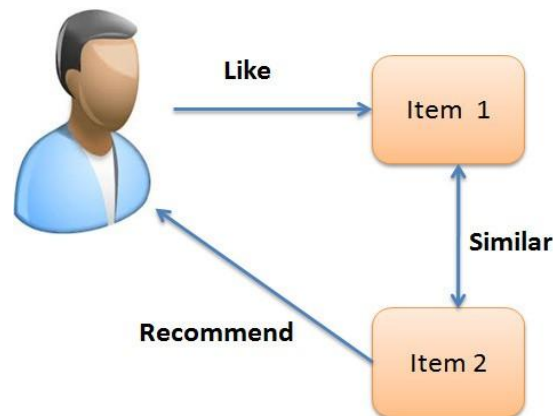


Fig1.Content-based recommendation: recommend items that are similar to items previously preferred by a similar user

One major drawback of the content-based filtering (recommendation) is the new user cold start problem. When a new user requests a recommendation, there is only little information about this user. Therefore, it will be very difficult for the recommender system to produce relevant recommendations. Moreover, content-based filtering usually suffers from the over-specialization problem. The system will infinitely suggest items that are highly matching with the user profile. It will not find unrelated items to the one already appreciated.

B. Collaborative filtering-based recommendation methods

Collaborative filtering is one of the most explored methods in the area of recommendation. The main advantage of this approach is that it doesn't require any description of the items to recommend. Therefore, this method allows to recommend complex objects without having to analyze them, thus most popular online music, and movie recommendation services such as Netflix and Last fm apply it.

The main idea of these methods is to recommend items based on the opinions and the ratings of other similar users. The opinions of users can be obtained explicitly from the existing users or by using some implicit measures. Explicit opinions are directly provided by the user. For example, when a new user logs in, many systems begin by asking the user to note multiple items so that they can subsequently recommend items that match them; this is the case of Amazon recommendation system. It is then possible to note the items. These notes can be:

- binary note : the decision of the user is to choose whether the object is "good" or "bad".
- digital note : generally ranging from 1 to 5; 5 reflects the fact that the object is very pleasing to the user. These notes are often represented by a number of stars as on Amazon system as described in Figure 2.
- ordinal note: the user must choose from a list of terms the one that is the most adapted for his feeling towards the item in question. An example of a list can be "Very good, good, average, bad, very bad".
- descriptive note: the user chooses one or more terms that describe his opinion on the object. For a movie, these terms can be "exciting", "uninteresting", etc.

Implicit opinion gathers all the information that can be extracted from the usage's patterns. For example, the number of visits to a page, the number of views on a video, the time spent on a page (Dwell time) which can reflect the fact that a user has taken the time to read or not the content of this page. In a collaborative filtering system, as described in Figure 3, the data are represented as "User x Item" matrix as described in Figure 3, where the rows represent users (Joe, Dalia, Eric, Helena) and columns correspond to the items (the set of book list: Harry Potter, Springer, Rever.). Users provide their opinions on the items in the form of notes.

According to [11], there are two sub-categories of collaborative filtering: memory-based and model-based algorithms.



Fig2. Explicit user opinion's in amazon recommendation system

The memory-based methods use the entire evaluation matrix and provide recommendations based on the relation- ship between the active user and item and the rest of the rating matrix. On the other hand, model-based methods use the evaluation matrix to fit a parameterized model, which will then be used for predictions. We give in the following basic concepts of each sub-category.

For the first category, Memory-based methods, it can be divided into two kinds: user-based CF and item-based CF [12]. User-based CF explores the relationship between rows(users) in the rating matrix. It firstly calculates the similarities between the active user and the other users. The most popular measures are the Pearson correlation [3] and the cosine-based measure [13] which are described by Equation (1) and Equation (2) where $Cos(u_a, u_b)$ and $CorrP(u_a, u_b)$ designate the similarities calculated respectively with the Pearson correlation coefficient and the cosine-based measure, between two users u_a and u_b , I_a and I_b respectively represent all items rated by u_a and u_b , $v(u_a)$ represents the average of notes of u_a , $v(u_a, i)$ represents the note of u_a on item i and I_c represents the co-noted items between the active user u_a and the user u_b . Users with high similarities are selected as neighbors of the active user. Then the system utilizes the neighbors' ratings on a specific item to calculate the weighted average [3] which is regarded as the predicted rating, treating the respective similarities as weights. This method is described in Equation 3, where $Pred(u_a, i_k)$ is the prediction note of the active user u_a on the item i_k , U_a is the set of nearest neighbors having already noted the item i_k , $Sim(u_a, u_b)$ means the similarity value between u_a and u_b ($u_b \in U_a$) that can be the cosine similarity ($Cos(u_a, u_b)$) or the Pearson correlation similarity ($CorrP(u_a, u_b)$). The recommender system ranks all the items according to their predicted ratings and selects Top-N items as recommendations.

				
 Joe	1	?	3	?
 Dalia	1	?	4	3
 Eric	1	5	?	5
 Helena	5	?	1	1

Fig3. Collaborative filtering matrix: rows represent users and columns represent items

The method based on the memory is concentrated on the items [14]. This method analyzes the matrix “User x Item” to identify the relationships between the items and use these relationships to calculate predictions. The assumption is that the user would be interested in the items similar to items he previously appreciated (similar in terms of ratings assigned by the user). Hence the similarities among items are firstly calculated using the same similarity measures with the user-based CF. After choosing the neighbors for the target item and calculating the weighted average, the predicted rating on this item is obtained.

$$Cos(u_a, u_b) = \frac{\sum_{i \in I_c} v(u_a, i) * v(u_b, i)}{\sqrt{\sum_{i' \in I_a} v(u_a, i')^2} * \sqrt{\sum_{i' \in I_b} v(u_b, i')^2}} \quad (1)$$

$$CorrP(u_a, u_b) = \frac{\sum_{i \in I_c} (v(u_a, i) - \overline{v(u_a)}) (v(u_b, i) - \overline{v(u_b)})}{\sqrt{\sum_{i \in I_c} (v(u_a, i) - \overline{v(u_a)})^2} \sqrt{\sum_{i \in I_c} (v(u_b, i) - \overline{v(u_b)})^2}} \quad (2)$$

$$Pred(u_a, i_k) = \overline{v(u_a)} + \frac{\sum_{u_b \in U_a} Sim(u_a, u_b) * (v(u_b, i_k) - \overline{v(u_b)})}{\sum_{u_b \in U_a} Sim(u_a, u_b)} \quad (3)$$

The advantage of the memory-based methods is the simplicity of the implementation and the integration of new data into the system. However, this approach suffers from the cold start issue. It requires rating data in order provide recommendations. When a new item is added, there is no enough information about that item. Consequently, this item cannot be recommended to anyone before it gets enough ratings. For example, in the online movies, when a new movie is uploaded, there is no rating that is given to that movie. So, this new movie cannot be recommended by the system until collecting enough ratings and evaluations by a group of users. Therefore, this category of methods cannot provide recommendations before a target user has given enough ratings for several items. Data sparsity is also one of the main problem of memory-based methods when the evaluation space is dispersed, it is difficult to identify reliable neighbors (from the co-scored items) and consequently the system performance decreases. For example, considering movie domain, the evaluation matrix

includes thousands of movies and millions of users. However, a given user evaluates only a small number of movies. As a result, the evaluation matrix has many empty cells, which makes it difficult to calculate the similarity between users. In addition, memory-based methods do not allow scaling. Indeed, when the number of users and items in the system becomes large, the generation of recommendations requires a very high processing time.

On the other side, the second subcategory is model-based methods. A variety of model-based recommendation methods were developed to address the scalability and the real time performance problems [15] of user-based methods by using dimensionality reduction techniques or clustering in order to remove users or non-representative items. Therefore, the user-item representation space is smaller, and the missing data rate are less important compared to the original representation space. Model Based algorithms received an important attention by the recommender system community.

C. Hybrid recommendation methods

Each of the presented recommendation approaches has strengths as well as weaknesses [16]. Therefore, hybrid system [17] combines two or more recommendations techniques to address the disadvantages of each technique and take advantage of their strengths. There are various possible combinations which is classified [18] into seven categories:

- **Weighted:** hybrid recommender combines the results of all available recommendation techniques to compute a score for a recommended item.
- **Switching:** the system switches between recommendation techniques depending on the current situation.
- **Mixed:** recommendations from several techniques are presented simultaneously to the user.
- **Feature combination:** features from different recommendation data sources are thrown together into a single recommendation algorithm.
- **Cascade:** one recommender refines the recommendations given by another.
- **Feature augmentation:** the output from one technique is used as an input feature to another.
- **Meta-level:** the model learned by one recommender is used as input to another.

D. Multi-Criteria recommendation method

Single-rating collaborative filtering recommender systems have shown their effectiveness to provide acceptable automatic recommendations. However, they do not include different attributes and dimensions of an item in the process of recommendation. Multi-criteria recommender systems have been proposed to address this issue. Several works show that using multi-criteria ratings, instead of a single rating, can largely improve the performance of the recommender system and may offer a more relevant and reliable recommendation. An example of a multicriteria rating system [19] is Zagat's system that provides three criteria for restaurant ratings (e.g., food, decor and service), "Buy.com" that provides multi-criteria ratings for consumer electronics (e.g., display size, performance, battery life, and cost), and "Yahoo" Movies that show each user's ratings for four criteria (e.g., story, action, direction, and visuals).

E. Context awareness-based recommendation method

One of the most cited definitions of context is the definition of [20] that defines context as "any information that can be used to characterize the situation of an entity. An entity could be a person, a place, or an object that is considered relevant to the interaction between a user and an application, including the user and the application themselves." The context information such as time or location has been recently considered in existing recommender systems. The contextual information provides additional information for recommendation making, especially for some applications in which it is not sufficient to consider only users and items, such as recommending a vacation package. It is also important to incorporate the contextual information in the recommendation process to be able to recommend items to users in specific circumstances. For example, using the temporal context, a travel recommender system might make a very different vacation recommendation in winter compared to summer. Nowadays, when the mobile devices are getting popular and taking part in our lives, this kind of recommender systems are especially urgent. Using GPS, 3G access to internet and other

technologies recommender systems can rapidly get any information about location of a user and the user himself.

F. Social network-based recommendation method

Social network analysis has been used in recommender systems as a result of the important growth of social networking tools in Web-based systems in recent years. Data is automatically collected from social networks is a real source of information for a recommendation system. Such system is based on the presence of a community of users linked by social links. In social platforms, these recommendation systems make it possible to recommend a whole range of information. Examples include users to follow, specific publications, multimedia elements, groups (sub-communities) to integrate.

IV. CONCLUSION

In this paper we presented the main recommendation methods, namely: content-based methods, memory-based and model-based CF, hybrid methods, multi-criteria recommendation methods, context awareness-based recommendation methods and social network-based recommendation methods. There is no method category that is superior to all others or any method that can be successfully applied for any application of recommender systems. Each technique has some advantages but also some disadvantages. The choice of one technique is based on the problematic, the application context and the availability of data. An interesting improvement of this work is to prepare a guide in which we can specify key factors affecting the choice of a recommendation method given a list of different target applications.

REFERENCES

- [1] Akshay Kumar Chaturvedi, Filipa Peleja, and Ana Freire. "Recommender System for News Articles using Supervised Learning". In: arXiv preprint arXiv:1707.00506.2017.
- [2] David Goldberg et al. "Using collaborative filtering to weave an information tapestry". In: Communications of the ACM 35.12.1992, pp. 61–70.
- [3] Jonathan L Herlocker et al. "An algorithmic framework for performing collaborative filtering". In: Proceedings of the 22nd annual international ACM SIGIR conference on Research and development in information retrieval. ACM. 1999, pp. 230–237.
- [4] Greg Linden, Brent Smith, and Jeremy York. "Amazon.com recommendations: Item-to-item collaborative filtering". In: IEEE Internet computing 7.1.2003, pp. 76–80.
- [5] Sean M McNee et al. "On the recommending of citations for research papers". In: Proceedings of the 2002 ACM conference on Computer supported cooperative work. ACM. 2002, pp. 116–125.
- [6] Francesco Ricci, Lior Rokach, and Bracha Shapira. "Introduction to recommender systems handbook". In: Recommender systems handbook. Springer, 2011, pp. 1–35.
- [7] Dietmar Jannach et al. Recommender systems: an introduction. Cambridge University Press, 2010.
- [8] J Ben Schafer et al. "Collaborative filtering recommender systems". In: The adaptive web. Springer, 2007, pp. 291–324.
- [9] Bamshad Mobasher, Xin Jin, and Yanzan Zhou. "Semantically enhanced collaborative filtering on the web". In: Web Mining: From Web to Semantic Web. Springer, 2004, pp. 57–76.
- [10] Gediminas Adomavicius and Alexander Tuzhilin. "Toward the next generation of recommender systems: A survey of the state-of-the-art and possible extensions". In: IEEE transactions on knowledge and data engineering 17.6.2005, pp. 734–749.
- [11] John S Breese, David Heckerman, and Carl Kadie. "Empirical analysis of predictive algorithms for collaborative filtering". In: Proceedings of the Fourteenth conference on Uncertainty in artificial intelligence. Morgan Kaufmann Publishers Inc. 1998, pp. 43–52.
- [12] Kwanghee Hong, Hocheol Jeon, and Changho Jeon. "Personalized research paper recommendation system using keyword extraction based on user profile". In: Journal of Convergence Information Technology 8.16.2013, p. 106.
- [13] Badrul Sarwar et al. Application of dimensionality reduction in recommender system-a case study. Tech. rep. DTIC Document, 2000.
- [14] Badrul Sarwar et al. "Item-based collaborative filtering recommendation algorithms". In: Proceedings of the 10th international conference on World Wide Web. ACM. 2001, pp. 285–295.
- [15] Mukund Deshpande and George Karypis. "Item-based top-n recommendation algorithms". In: ACM Transactions on Information Systems (TOIS) 22.1 2004, pp. 143–177.
- [16] Toine Bogers and Antal Van den Bosch. "Recommending scientific articles using citeulike". In: Proceedings of the 2008 ACM conference on Recommender systems. ACM. 2008, pp. 287–290.
- [17] Robin Burke. "Hybrid recommender systems: Survey and experiments". In: User modeling and user-adapted interaction 12.4 2002, pp. 331–370.

- [18] Robin Burke. “The adaptive web. chapter Hybrid web recommender systems”. In In: Brusilovsky P., Kobsa A., Nejdl W. (eds) The Adaptive Web. Lecture Notes in Computer Science, vol 4321. Springer, Berlin, Heidelberg 2007.
- [19] Gediminas Adomavicius and YoungOk Kwon. “Multi-criteria recommender systems”. In: Recommender Systems Handbook. Springer, 2015, pp. 847–880.
- [20] Anind K Dey, Gregory D Abowd, and Daniel Salber. “A conceptual framework and a toolkit for supporting the rapid prototyping of context-aware applications”. In: Human-computer interaction 16.2 2001, pp. 97–166.

A Comparative Study between Semi-Analytical Iterative Schemes for the Reliable Treatment of Systems of Coupled Nonlinear Partial Differential Equations

Liberty Ebiwareme

Department of Mathematics, Rivers State University, Nkpolu-Oroworukwo, Port Harcourt.

ABSTRACT

This study is aimed at making comparative analysis between three semi-analytical iterative methods viz: Adomian decomposition method, Temimi-Ansari method and Daftardar-Jafari method. The applicability and efficiency of these methods is confirmed by applying them to five different systems of nonlinear partial differential equations. Also, the respective errors of all the methods are ascertained to know the effectiveness and closeness to the exact solution. The results revealed, they all produce solution which is in good agreement with existing literature.

Keywords: Nonlinear PDEs, Iterative schemes, Adomian decomposition method (ADM), Temimi- Ansari-method (TAM), Daftardar-Jafari Method.

I. INTRODUCTION

Systems of partial differential equations comprising both linear and nonlinear have attracted interest from academics the world over especially mathematicians and engineers for decades now and have been extensively studied for analytical and approximate solutions. These systems have numerous useful applications in chemical-reaction diffusion model of Brusselator, Physics, digital image processing, computer science, fluid mechanics, astrophysics, electronic, telecom, computer engineering, evolution equation applied in the propagation of shallow water waves [1-12].

Due to the important nature of these systems, several techniques or methods have been proposed to seek for closed form or numerical solutions. They includes, Homotopy Analysis Method (HAM), Homotopy perturbation method (HPM), Optimal Homotopy Asymptotic method (OHAM), Variational Iteration method (VIM), Differential Transform method (DTM), Laplace Adomian decomposition method (LADM), Aboodh Adomian decomposition method (AADM), Maghoush Adomian decomposition method (MADM), Modified Decomposition method (MDM), Riemann Invariants method (RIM), Fusion of Waveform Relaxation and Multigrid, Periodic multigrid wave form, Tanh-Coth method, Banach Contraction method (BCM), Lattice Boltzmann Method(LBM)[13-23].

Most of the methods produce closed form and approximate solutions but with much tedious computational work before giving solution, others experience inherent difficulty by way of calculating the so-called Adomian polynomial for the nonlinear term and some couldn't give accurate solution but a slowly converging series solution with marked error from the exact solution but time consuming. The Adomian decomposition method (ADM) was proposed by G. Adomian in 1994. This method requires expressing the unknown solution as an infinite decomposition series and the nonlinear term as an Adomian polynomial. This gives the solution elegantly in few steps of a rapidly converging series which matches the exact solution if it exists. The only snag in this method is in the calculation of the Adomian polynomials if the problem contains a nonlinear term. But this difficulty is easily overcome

with tact, experience, and diligence. It has been applied by many researchers to solve diverse problems. [24-33].

Equally, the novel Temimi-Ansari denoted (TAM) was presented by Temimi and Ansari to solve linear and nonlinear ODEs and PDEs. It's an iterative procedure which leads to an approximate solution that converges to the exact solution when the initial condition is satisfied. This method doesn't require linearization, perturbation, discretization, or calculation of Adomian polynomials which is a benchmark that reduce the complications in calculating the polynomial for nonlinear terms. For example, TAM has been applied to the following: Duffing Equation, KDV equation, Chemistry problems, nonlinear thin flow problems, Fokker-Plank's equation and many more. [34-40]. Most recently, the novel Daftardar-Jafari method (DJM) was developed by Daftardar-Gejji and Jafari in 2006 originally with an inspiration from the Banach contraction method. DJM has been extensively applied by academics to successfully solve linear and nonlinear PDEs, fractional dynamics, coupled Burger's equation, nonlinear Abel-type equation, Klein-Gordon equation [41--46].

In this paper, the motivation is to solve system of coupled nonlinear partial differential equations, using the Adomian decomposition method (ADM), Temimi-Ansari method (TAM) and Daftardar-Jafari method (DJM). The methods are easy to implement and doesn't require lengthy calculations as is the case with other methods and less computational time. To confirm the efficiency and reliability of the iterative algorithms of the proposed methods, we solve four examples and compare their results. The work is organized as follows: In chapter 1, the relevant literatures and previous works using the proposed methods is presented in the introduction. Sections 2-4 is devoted to the fundamentals of the ADM, TAM and DJM. Numerical examples of nonlinear systems of PDEs is implemented with the different methods in section 5 and finally in section 6, the conclusion of the study is drawn.

II. FUNDAMENTALS OF ADOMIAN DECOMPOSITION METHOD (ADM)

Consider a general nonlinear differential equation of the form

$$F(u(x)) = g(x) \quad (1)$$

Where F is a nonlinear operator and y, g are both functions of x

Decomposing the nonlinear operator, F into the sum of linear and nonlinear operator.

$$L(u(x)) + R(u(x)) + N(u(x)) = g(x) \quad (2)$$

Where L is the highest order derivative that's invertible, R is the linear differential operator, N is a nonlinear term and g is the source term

Rewriting Eq. (2) for $L[u(x)]$ yield the form

$$L(u(x)) = g(x) - R(u(x)) - N(u(x)) \quad (3)$$

Taking the inverse operator, L^{-1} on both sides of Eq. (3), we get

$$\begin{aligned} y(x) &= L^{-1}g(x) - L^{-1}R(u(x)) - L^{-1}N(u(x)) \\ y(x) &= \phi - L^{-1}R(u(x)) - L^{-1}N(u(x)) \end{aligned} \quad (4)$$

Where ϕ is the term arising from the integration of the source term using the boundary conditions

By the standard Adomian decomposition method, we write the unknown solution as an infinite decomposition series of the form

$$u(x) = \sum_{n=0}^{\infty} u_n(x) \quad (5)$$

Putting Eq. (5) into Eq. (4), we obtain

$$\sum_{n=0}^{\infty} u_n(x) = \phi - L^{-1}R(\sum_{n=0}^{\infty} u_n(x)) - L^{-1}N(\sum_{n=0}^{\infty} u_n(x)) \quad (6)$$

Matching both sides of Eq. (6), we obtain the zeroth order component given by

$$u_0 = \phi$$

Then the recursive relation is given by

$$u_{n+1}(x) = -L^{-1}R(u_n) - L^{-1}N(u_n), n \geq 0 \quad (7)$$

The solution of the problem in Eq. (1) is obtain as limit of the decomposing series

$$u(x) = \lim_{n \rightarrow \infty} u_n(x) \quad (8)$$

Similarly, the nonlinear term can be determined by an infinite series of the Adomian polynomials. That is,

$$N(u_0, u_1, u_2, \dots, u_n) = \sum_{n=0}^{\infty} A_n \quad (9)$$

Then the A_n 's are obtained from the formula

$$A_n = \frac{1}{n!} \frac{d^n}{d\lambda^n} [N(\sum_{k=0}^{\infty} \lambda^k y_k)]_{\lambda=0}, n = 0, 1, 2, 3 \quad (10)$$

Using Eq. (9), the first five Adomian polynomials are given as

$$A_0 = N(u_0)$$

$$A_1 = u_1 N'(u_0)$$

$$A_2 = u_2 N'(u_0) + \frac{1}{2!} u_1^2 N''(u_0)$$

$$A_3 = u_3 N'(u_0) + u_1 u_2 N''(u_0) + \frac{1}{3!} u_1^3 N'''(u_0)$$

$$A_4 = u_4 N'(u_0) + \frac{1}{2} N''(u_0)(2u_1 u_3 + u_2^2) + \frac{1}{2} N'''(u_0) u_1^2 u_2 + \frac{1}{4!} N^{(iv)}(u_0) u_1^4$$

$$A_5 = u_5 N'(u_0) + \frac{1}{2} N''(u_0)(2u_1 u_4 + 2u_2 u_3) + \frac{1}{3!} N'''(u_0)(3u_1^2 u_3 + 3u_1 u_2^2) + \frac{4}{4!} N^{(iv)}(u_0)(u_1^3 u_2) + \frac{1}{5!} N^{(v)}(u_0) u_1^5$$

$$A_6 = u_6 N'(u_0) + \frac{1}{2!} N''(u_0)(2u_1 u_5 + 2u_1 u_4 + u_2^3) + \frac{1}{3!} N'''(u_0)(3u_1^2 u_4 + u_2^3 + 6u_1 u_2 u_3) + \frac{1}{4!} N^{(iv)}(u_0)(4u_1^3 u_3 + 6u_1^2 u_2^2) + \frac{5}{5!} N^{(v)}(u_0) u_1^4 u_2 + \frac{1}{6!} N^{(vi)}(u_0) u_1^6$$

$$A_7 = u_7 N'(u_0) + \frac{1}{2!} N''(u_0)(2u_1 u_6 + 2u_2 u_5 + 2u_3 u_4) + \frac{1}{3!} N'''(u_0)(3u_1^2 u_5 + 3u_1 u_2^3 + 3u_3 u_2^2 + 6u_1 u_2 u_4) + \frac{1}{4!} N^{(iv)}(u_0)(4u_1^3 u_4 + 12u_1^2 u_2 u_3 + 4u_1 u_2^3) + \frac{1}{5!} N^{(v)}(u_0)(5u_1^4 u_3 + 10u_1^3 u_2^2) + \frac{1}{6!} N^{(vi)}(u_0) u_1^5 u_2 + \frac{1}{7!} N^{(vii)}(u_0) u_1^7$$

$$\begin{aligned}
 A_8 = & u_8 N'(u_0) + \frac{1}{2!} N''(u_0)(2u_1 u_7 + 2u_2 u_6 + 2u_3 u_5 + u_4^2) \\
 & + \frac{1}{3!} N'''(u_0)(3u_1^2 u_6 + 3u_4 u_2^2 + 3u_2 u_3^2 + 6u_1 u_2 u_5 + 6u_1 u_3 u_4) \\
 & + \frac{1}{4!} N^{(iv)}(u_0)(4u_1^3 u_5 + 12u_1^2 u_2 u_4 + 12u_1 u_2^2 u_3 + 6u_1^2 u_3^2 + u_2^4) \\
 & + \frac{1}{5!} N^{(v)}(u_0)(5u_1^4 u_4 + 20u_1^3 u_2 u_3 + 10u_1^2 u_2^3) \\
 & + \frac{1}{6!} N^{(vi)}(u_0)(u_1^5 u_3 + 15u_1^4 u_2^2) + \frac{7}{7!} N^{(vii)}(u_0)u_1^6 u_2 \\
 & + \frac{1}{8!} N^{(viii)}(u_0)u_1^8
 \end{aligned}$$

III. BASICS OF THE TEMIMI-ANSARI METHOD (TAM)

Consider the general differential equation in operator form as follows

$$L(y(x)) + N(y(x)) + f(x) = 0, \quad (11)$$

$$B\left(y, \frac{dy}{dx}\right) = 0, \text{ or } y_1(0) = \alpha \text{ and } y_1'(0) = \beta \quad (12)$$

Where x is the independent variable, $y(x)$ is an unknown function, $f(x)$ is a given known function, L is a linear operator, N is a nonlinear operator and B is a boundary operator.

To implement the TAM method, we first assume that $y_0(x)$ is an initial guess that satisfy the problem in Eq. (11) subject to Eq. (12).

$$L(y_0(x)) + f(x) = 0, B\left(y_0, \frac{dy_0}{dx}\right) = 0 \text{ or } y_0(0) = \alpha \text{ and } y_0'(0) = \beta \quad (13)$$

The next approximate solution is obtained by solving the problem

$$L(y_1(x)) + N(y_0(x)) + f(x) = 0, B\left(y_1, \frac{dy_1}{dx}\right) = 0, \text{ or } y_1(0) = \alpha \text{ and } y_1'(0) = \beta \quad (14)$$

The next iterate of the problem become

$$L(y_2(x)) + N(y_1(x)) + f(x) = 0, B\left(y_2, \frac{dy_2}{dx}\right) = 0, \text{ or } y_2(0) = \alpha \text{ and } y_2'(0) = \beta \quad (15)$$

Continuing the same way to obtain the subsequent terms, the general equation of the method becomes

$$L(y_{n+1}(x)) + N(y_n(x)) + f(x) = 0, B\left(y_{n+1}, \frac{dy_{n+1}}{dx}\right) = 0, \text{ or } y_{n+1}(0) = \alpha \text{ and } y_{n+1}'(0) = \beta \quad (16)$$

Then the solution of the problem in Eq. (11) is given by

$$y(x) = \lim_{n \rightarrow \infty} y_n(x) \quad (17)$$

From Eq. (16), each $y(x)$ is considered alone as a solution for Eq. (11). This method easy to implement, straightforward and direct. The method gives better approximate solution which converges to the exact solution with only few members.

IV. DAFTARDAR-JAFARI METHOD (DJM)

Consider the function equation in Eq. (1) in the form

$$L(y(x)) + N(y(x)) + g(x) = 0 \quad (18)$$

With the boundary or initial conditions

$$B\left(y, \frac{dy}{dx}\right) = 0, y(0) = \alpha \text{ and } y'(0) = \beta \quad (19)$$

Where x is the independent variable, $y(x)$ is the unknown function and $g(x)$ is given known function, N is a nonlinear operator, B is the boundary operator and $L(.) = \frac{d^n}{dx^n}$ is the linear operator.

Now applying the inverse operator, $L^{-1}(.) = \int_0^x \int_0^x (.) d\xi d\xi$ to Eq. (18) subject to Eq. (19), we obtain the equivalent form

$$y(x) = \phi(x) + \int_0^x \int_0^x N(y(\xi)) d\xi d\xi \quad (20)$$

Reducing the double integral in Eq. (20), we get the form

$$y(x) = \phi(x) + \int_0^x (x - \xi) N(y(\xi)) d\xi \quad (21)$$

Where $\phi(x)$ is an analytic function that comprises the sum of all initial conditions as well as the integration of the known function. $g(x)$

The solution of Eq. (21) takes the series form

$$y(x) = \sum_{n=0}^{\infty} y_n(x) \quad (22)$$

Now, using the nonlinear term we define the following terms

$$G_0 = N(y_0)$$

$$G_m = N(\sum_{n=0}^{\infty} y_n) - N(\sum_{n=0}^{m-1} y_n), m \geq 1$$

Next, we decompose $N(y)$ as follows

$$N(\sum_{n=0}^{\infty} y_n) = \underbrace{N(y_0)}_{G_0} + \underbrace{[N(y_0 + y_1) - N(y_0)]}_{G_1} + \underbrace{[N(y_0 + y_1 + y_2) - N(y_0 + y_1)]}_{G_2} + \dots \quad (23)$$

In view of Eq. (23), we define a recurrence relation for the problem as follows.

$$y_0 = f \quad (24)$$

$$y_1 = L(y_0) + G_0 \quad (25)$$

$$y_{m+1} = L(y_m) + G_m, m \geq 1 \quad (26)$$

Using the linearity property, since L is a linear operator, we write

$$\sum_{n=0}^m L(y_n) = L(\sum_{n=0}^m y_n), \text{ then we write}$$

$$\sum_{n=1}^{m+1} y_n = \sum_{n=0}^m L(y_n) + N\left(\sum_{n=0}^m y_n\right) \quad (27)$$

$$\sum_{n=1}^{m+1} y_n = L(\sum_{n=0}^m y_n) + N(\sum_{n=0}^m y_n), m \geq 1$$

So that the recursive relation become

$$\sum_{n=0}^{\infty} y_n = f + L(\sum_{n=0}^{\infty} y_n) + N(\sum_{n=0}^{\infty} y_n) \quad (28)$$

Then the approximate solution of the problem follows

$$y_n = \sum_{i=0}^n y_i \quad (29)$$

V. NUMERICAL EXAMPLES

In this section, we apply the proposed semi-analytical iterative methods: Adomian decomposition method, Temimi-Ansari method and Daftardar-Jafari method to four systems of nonlinear partial differential equations to show the applicability, feasibility, and robustness of the methods.

Example 1 Consider the system of nonlinear partial differential equation

$$u_t + vu_x + u = 1$$

$$v_t + uv_x - v = 1$$

$$(30)$$

With initial conditions

$$u(x, 0) = e^x, v(x, 0) = e^{-x}$$

$$(31)$$

5.1 Implementation using ADM

Taking the inverse operator L_t^{-1} to both sides of the system in Eq. (30) using the initial conditions in Eq. (42) yield

$$\begin{aligned} u(x, t) &= e^x + t - L_t^{-1}(vu_x + u) \\ v(x, t) &= e^{-x} + t + L_t^{-1}(uv_x + v) \end{aligned} \quad (32)$$

Now, we decompose the linear terms $u(x, t)$ and $v(x, t)$ as an infinite series of the form

$$\begin{aligned} u(x, t) &= \sum_{n=0}^{\infty} u_n(x, t) \\ v(x, t) &= \sum_{n=0}^{\infty} v_n(x, t) \end{aligned} \quad (33)$$

Similarly, the nonlinear terms, vu_x and uv_x are decomposed as Adomian polynomials

$$\begin{aligned} N_1(u, v) &= \sum_{n=0}^{\infty} A_n(x, t) \\ N_2(x, t) &= \sum_{n=0}^{\infty} B_n(x, t) \end{aligned} \quad (34)$$

Where A_n and B_n are called the Adomian polynomials. Plugging Eqs. (30) and (34) into Eq. (32), we obtain

$$\begin{aligned} \sum_{n=0}^{\infty} u_n(x, t) &= e^x + t - L_t^{-1} \left(\sum_{n=0}^{\infty} A_n(x, t) + \sum_{n=0}^{\infty} u_n(x, t) \right) \\ \sum_{n=0}^{\infty} v_n(x, t) &= e^{-x} + t + L_t^{-1} \left(\sum_{n=0}^{\infty} B_n(x, t) + \sum_{n=0}^{\infty} v_n(x, t) \right) \end{aligned} \quad (35)$$

The recursive relations from the decomposition series become

$$\begin{aligned} u_0(x, t) &= e^x + t \\ u_{n+1}(x, t) &= -L_t^{-1}(A_n + u_n(x, t)), n \geq 0 \end{aligned} \quad (36)$$

and

$$\begin{aligned} v_0(x, t) &= e^{-x} + t \\ v_{n+1}(x, t) &= L_t^{-1}(B_n + v_n(x, t)), n \geq 0 \end{aligned} \quad (37)$$

5.2 Implementation by TAM

To solve the system in Eq. (32) using TAM, we proceed as follows

$$\begin{aligned} L_1(u) &= u_t, N_1(u, v) = vu_x + u, \text{ and } f_1(x, t) = -1 \\ L_2(v) &= v_t, N_2(u, v) = -uv_x - u, \text{ and } f_2(x, t) = -1 \end{aligned} \quad (38)$$

The initial problem to be solved is of the form

$$L_1(u_0(x, t)) + f_1(x, t) = 0, u_0(x, 0) = e^x \quad (39)$$

$$L_2(v_0(x, t)) + f_2(x, t) = 0, u_0(x, 0) = e^{-x} \quad (40)$$

Applying the inverse operator to Eqs. (39) and (40), using the initial condition, gives

$$u_0(x, t) = e^x + t$$

$$v_0(x, t) = e^{-x} + t$$

The next approximate solution of the problem become

$$\begin{aligned} L_1(u_1(x, t)) + N_1(u_0(x, t)) + f_1(x, t) &= 0, u_1(x, 0) = e^x \\ L_2(v_1(x, t)) + N_2(v_0(x, t)) + f_2(x, t) &= 0, u_1(x, 0) = e^{-x} \end{aligned} \quad (41)$$

Integrating both sides of Eq. (52) using the initial condition gives

$$\begin{aligned} \int_0^t u_{1t}(x, t) dt &= \int_0^t [-(v_0(x, t)u_{0x}(x, t)) - u_0(x, t) + 1] dt \\ \int_0^t v_{1t}(x, t) dt &= \int_0^t [u_0(x, t)v_{0x}(x, t) + v_0(x, t) + 1] dt \end{aligned} \quad (42)$$

Solving the system in Eq. (42) gives the solutions of the form

$$\begin{aligned} u_1(x, t) &= -2t + \frac{t^2}{2} + \left(1 + t + \frac{t^2}{2}\right)e^x \\ v_1(x, t) &= 2t + \frac{t^2}{2} + \left(1 + t - \frac{t^2}{2}\right)e^{-x} \end{aligned} \quad (43)$$

Next the third iterative solution of the problem become

$$\begin{aligned} L_1(u_2(x, t)) + N_1(u_1(x, t)) + f_1(x, t) &= 0, u_2(x, 0) = e^x \\ L_2(v_2(x, t)) + N_2(v_1(x, t)) + f_2(x, t) &= 0, u_2(x, 0) = e^{-x} \end{aligned} \quad (44)$$

Applying the inverse operator to both sides of Eq. (44), we get

$$\begin{aligned} \int_0^t u_{2t}(x, t) dt &= \int_0^t [-(v_1(x, t)u_{1x}(x, t)) - u_1(x, t) + 1] dt \\ \int_0^t v_{2t}(x, t) dt &= \int_0^t [u_1(x, t)v_{1x}(x, t) + v_1(x, t) + 1] dt \end{aligned} \quad (45)$$

Solving Eq. (56) yield the third iterative solution as

5.3 Implementation by DJM

Applying DJM to both sides of Eq. (32) and taking limits from 0 to t , we get the equation of the form.

$$\begin{aligned} u(x, t) &= f_1(x, t) + \int_0^t (1 - vu_x - u) dt \\ v(x, t) &= f_2(x, t) + \int_0^t (1 + uv_x + v) dt \end{aligned} \quad (46)$$

Now, the nonlinear terms become

$$\begin{aligned} N(u_i) &= \int_0^t (1 - v_i u_{ix} - u_i) dt \\ V(v_i) &= \int_0^t (1 + u_i v_{ix} + v_i) dt \end{aligned} \quad (47)$$

From the given initial conditions

$$f_1(x, t) = u_0(x, 0) = e^x$$

$$f_2(x, t) = v_0(x, 0) = e^{-x}$$

To obtain the preceding terms, we proceed as follows

$$\begin{aligned} u_1 &= N(u_0) = \int_0^t (1 - v_0 u_{0x} - u_0) dt = -te^x \\ u_1 &= -te^x \\ v_1 &= N(v_0) = \int_0^t (1 + u_0 v_{0x} + v_0) dt \\ v_1 &= \int_0^t (1 - 1 + e^{-x}) dt = \int_0^t e^{-x} dt \\ v_1 &= te^{-x} \end{aligned} \quad (48)$$

$$\Rightarrow u_1 = -te^x, v_1 = te^{-x}$$

Now to get the next approximate solutions, we proceed as follows

$$\begin{aligned} u_2 &= N(u_0 + u_1) - N(u_0) \\ u_2 &= \int_0^t te^x dt = \frac{t^2}{2!} e^x \end{aligned} \quad (49)$$

Similarly, $v_2 = N(v_0 + v_1) - N(v_0)$

$$\begin{aligned} v_2 &= \int_0^t te^{-x} dt = \frac{t^2}{2!} e^{-x} \\ \Rightarrow u_1 &= \frac{t^2}{2!} e^x, v_1 = \frac{t^2}{2!} e^{-x} \end{aligned}$$

Continuing in the same way, we get the succeeding terms of the problems using the form

$$\begin{aligned} u_3 &= N(u_0 + u_1 + u_2) - N(u_0 + u_1), v_2 = N(v_0 + v_1 + v_2) - N(v_0 + v_1) \\ \Rightarrow u_3 &= \frac{t^2}{3!} e^x, v_3 = \frac{t^2}{3!} e^{-x} \end{aligned} \quad (50)$$

Thus, the solution of the problem gives

$$u(x, t) = \sum_{n=1}^{\infty} u_n = u_0 + u_1 + u_2 + \dots$$

$$v(x, t) = \sum_{n=1}^{\infty} v_n = v_0 + v_1 + v_2 + \dots \quad (51)$$

$$u(x, t) = e^x \left(1 - t + \frac{t^2}{2!} - \frac{t^3}{3!} + \dots \right) = e^x \cdot e^{-t}$$

$$v(x, t) = e^{-x} \left(1 + t + \frac{t^2}{2!} - \frac{t^3}{3!} + \dots \right) = e^{-x} \cdot e^t$$

$$\Rightarrow u(x, t) = e^{x-t}, v(x, t) = e^{-x+t}$$

Example 2. Consider the system of nonlinear partial differential equation

$$u_t + vu_x - 3u = 2$$

$$v_t - uv_x + 3v = 2$$

(53)

Subject to the initial conditions

$$u(x, 0) = e^{2x}, v(x, 0) = e^{-2x} \quad (54)$$

5.4 Implementation using ADM

Taking the inverse differential operator, L_t^{-1} of bot sides of the system, we obtain

$$u(x, t) = e^{2x} - L_t^{-1}(vu_x + u)$$

$$v(x, t) = e^{-2x} + L_t^{-1}(uv_x - 3v) \quad (55)$$

Substituting the decomposition representation s for the linear and nonlinear terms, we get

$$\sum_{n=0}^{\infty} u_n(x, t) = e^{2x} - L_t^{-1} \left(\sum_{n=0}^{\infty} A_n + \sum_{n=0}^{\infty} u_n \right)$$

$$\sum_{n=0}^{\infty} v_n(x, t) = e^{-2x} + L_t^{-1} \left(\sum_{n=0}^{\infty} B_n - 3 \sum_{n=0}^{\infty} v_n \right) \quad (56)$$

Where A_n and B_n are the Adomian polynomials for the nonlinear terms, vu_x and uv_x respectively.

Now the first three terms of the Adomian polynomials are given as follows

$$A_0 = v_0 u_{0x}$$

$$A_1 = v_1 u_{0x} + v_0 u_{1x}$$

(57)

$$A_2 = v_2 u_{0x} + v_1 u_{1x} + v_0 u_{2x}$$

Similarly, for uv_x we obtain the following iterates

$$B_0 = u_0 v_{0x}$$

$$B_1 = u_1 v_{0x} + u_0 v_{1x}$$

(58)

$$B_2 = u_2 v_{0x} + u_1 v_{1x} + u_0 v_{2x}$$

Substituting the above Adomian polynomials into the recursive relation, we obtain the solution as follows.

$$(u_0, v_0) = (e^{2x}, e^{-2x})$$

$$(u_1, v_1) = (-2t - te^{2x}, -2t - 3te^{-2x}) \quad (59)$$

$$(u_2, v_2) = \left(\frac{5}{2}t^2e^{2x} + 5t^2, 6t^2 + 5t^2e^{-2x} \right)$$

Using the above iterative solution, the solution of problem in closed form become

$$(u, v) = (e^{2x+3t}, e^{-2x-3t}) \quad (60)$$

5.5 Implementation by TAM

Applying TAM to the above system, we proceed as follows

$$L_1(u) = u_t, N_1(u) = vu_x - 3u, f_1(x, t) = -2$$

$$L_2(v) = v_t, N_2(u) = -uv_x + 3v, f_2(x, t) = -2 \quad (61)$$

The initial problem to be solved is given by

$$L_1(u_0(x, t)) + f_1(x, t) = 0, u_0(x, 0) = e^{2x}$$

$$L_2(v_0(x, t)) + f_2(x, t) = 0, v_0(x, 0) = e^{-2x} \quad (62)$$

Applying the inverse operator, L_t^{-1} to both sides of the above equation, we get the form

$$\int_0^t u_{0t}(x, t) dt = \int_0^t 2 dt$$

$$\int_0^t v_{0t}(x, t) dt = \int_0^t 2 dt \quad (63)$$

In view of the above, the initial solution become

$$(u_0, v_0) = (e^{2x} + 2t, e^{-2x} + 2t) \quad (64)$$

The next approximate solution is obtain using the form

$$\begin{aligned} L_1(u_1(x, t)) + N_1(u_0(x, t)) + f_1(x, t) &= 0, u_1(x, 0) = e^{2x} \\ L_2(v_1(x, t)) + N_2(v_0(x, t)) + f_2(x, t) &= 0, v_1(x, 0) = e^{-2x} \end{aligned} \quad (65)$$

Integrating the above and taking limits from 0 to t yield the equivalent form

$$\begin{aligned} \int_0^t u_{1t}(x, t) dt &= \int_0^t (-v_0 u_{0x} - 3u_0 + 2) dt \\ \int_0^t v_{1t}(x, t) dt &= \int_0^t (u_0 v_{0x} - 3v_0 + 2) dt \end{aligned} \quad (66)$$

Solving the above equation gives the first iterative solution

$$\begin{aligned} u_1(x, t) &= -2t^2 e^{2x} - 3te^{2x} - 3t^2 \\ v_1(x, t) &= -2t^2 e^{-2x} - 3te^{-2x} - 3t^2 \end{aligned} \quad (67)$$

Continuing in the same way, the subsequent terms are found and the solution in closed form become

$$\begin{aligned} u(x, t) &= e^{2x+t} \\ v(x, t) &= e^{-2x-t} \end{aligned} \quad (68)$$

5.6 Implementation using DJM

Integrating both sides of the given system subject to the initial conditions, we obtain the form

$$\begin{aligned} u(x, t) &= f_1(x, t) + \int_0^t (2 - vu_x + 3u) dt \\ v(x, t) &= f_2(x, t) + \int_0^t (2 + uv_x - 3v) dt \end{aligned} \quad (69)$$

Now, the nonlinear terms of the problem become

$$\begin{aligned} N(u_k) &= \int_0^t (2 - v_k u_{kx} + 3u_k) dt \\ N(v_k) &= \int_0^t (2 + u_k v_{kx} - 3v_k) dt \end{aligned} \quad (70)$$

Using the given initial condition, we get

$$\begin{aligned} f_1(x, t) &= u_0(x, 0) = e^{2x} \\ f_2(x, t) &= v_0(x, 0) = e^{-2x} \end{aligned} \quad (71)$$

To obtain the subsequent terms, we proceed as follows

$$\begin{aligned} u_1 &= N(u_0) = \int_0^t (2 - v_0 u_{0x} + 3u_0) dt \\ v_1 &= N(v_0) = \int_0^t (2 + u_0 v_{0x} - 3v_0) dt \end{aligned} \quad (72)$$

Solving the above give the solution

$$\begin{aligned} (u_1, v_1) &= (3te^{2x}, -3te^{-2x}) \\ u_2 &= N(u_0 + u_1) - N(u_0) \end{aligned} \quad (73)$$

$$u_2 = \frac{3}{2} t^2 e^{2x}$$

Similarly, $v_2 = N(v_0 + v_1) - N(v_0)$ yield

$$v_2 = -\frac{3}{2} t^2 e^{-2x}$$

In view of the above the closed form solution of the problem become

$$\begin{aligned} u(x, t) &= e^{2x+3t} \\ v(x, t) &= e^{-2x-3t} \end{aligned} \quad (74)$$

Example 3. Solve the system of nonlinear partial differential equation for the unknowns

$$\begin{aligned} u_t + u_x v_x - w_y &= 1 \\ v_t + v_x w_x + u_y &= 1 \\ w_t + w_x u_x - v_y &= 1 \end{aligned} \quad (75)$$

Subject to the initial conditions

$$u(x, y, 0) = x + y$$

$$v(x, y, 0) = x - y$$

(76)

$$w(x, y, 0) = -x + y$$

5.7 Implementation using ADM

Taking the inverse operator, L_t^{-1} of both sides of the given system subject to the initial conditions yields

$$u(x, y, t) = x + y + t - L_t^{-1}(u_x v_x - w_y)$$

$$v(x, y, t) = x - y + t - L_t^{-1}(v_x w_x + u_y)$$

$$w(x, y, t) = -x + y + t - L_t^{-1}(w_x u_x + v_y) \quad (77)$$

Writing the linear terms as a decomposition series and nonlinear terms as Adomian polynomials, we obtain the recursive scheme as follows

$$\begin{aligned} \sum_{n=0}^{\infty} u_n(x, y, t) &= x + y + t - L_t^{-1} \left(\sum_{n=0}^{\infty} A_n - \sum_{n=0}^{\infty} w_n \right) \\ \sum_{n=0}^{\infty} v_n(x, y, t) &= x - y + t - L_t^{-1} \left(\sum_{n=0}^{\infty} B_n + \sum_{n=0}^{\infty} u_n \right) \\ \sum_{n=0}^{\infty} w_n(x, y, t) &= -x + y + t - L_t^{-1} \left(\sum_{n=0}^{\infty} C_n + \sum_{n=0}^{\infty} v_n \right) \end{aligned} \quad (78)$$

Where A_n, B_n and C_n are called the so-called the Adomian polynomials

The first three terms of the Adomian polynomials are given below

$$A_0 = u_{0x} v_{0x}$$

$$A_1 = u_{1x} v_{0x} + u_{0x} v_{1x}$$

$$A_2 = u_{2x} v_{0x} + u_{1x} v_{1x} + u_{0x} v_{2x} \quad (79)$$

$$B_0 = v_{0x} w_{0x}$$

$$B_1 = v_{1x} w_{0x} + v_{0x} w_{1x}$$

$$B_2 = v_{2x} w_{0x} + v_{1x} w_{1x} + v_{0x} w_{2x} \quad (80)$$

$$C_0 = w_{0x} u_{0x}$$

$$C_1 = w_{1x} u_{0x} + w_{0x} u_{1x}$$

$$C_2 = w_{2x} u_{0x} + w_{1x} u_{1x} + w_{0x} u_{2x} \quad (81)$$

Putting the above nonlinear terms into the recursive relation, we obtain the iterative solution as follows

$$(u_0, v_0, w_0) = (x + y + t, x - y + t, -x + y + t)$$

$$(u_k, v_k, w_k) = (0, 0, 0), \quad k \geq 1 \quad (82)$$

Consequently, the solution of the nonlinear system of nonlinear PDE is given by

$$(u_0, v_0, w_0) = (x + y + t, x - y + t, -x + y + t) \quad (83)$$

5.8 Implementation using TAM

Rewriting the system in the form, gives

$$L_1(u) = u_t, N_1(u) = u_x v_x - w_y, f_1(x, y, t) = -1$$

$$L_2(v) = v_t, N_2(v) = v_x w_x + u_y, f_2(x, y, t) = -1$$

$$L_3(w) = w_t, N_3(w) = w_x u_x - v_y, f_3(x, y, t) = -1 \quad (84)$$

The initial problem to be solved is given by

$$L_1(u_0(x, y, t)) + f_1(x, y, t) = 0, u_0(x, y, 0) = x + y$$

$$L_2(v_0(x, y, t)) + f_2(x, y, t) = 0, v_0(x, y, 0) = x - y$$

$$L_3(w_0(x, y, t)) + f_3(x, y, t) = 0, w_0(x, y, 0) = -x + y \quad (85)$$

Applying the inverse operator and taking the limits of integration from 0 to t , we get the initial iterative solution.

$$u_0(x, y, t) = x + y + t$$

$$v_0(x, y, t) = x - y + t$$

$$w_0(x, y, t) = -x + y + t \quad (86)$$

The next iterate approximation to the problem is obtained using the form

$$L_1(u_1(x, y, t)) + N_1(u_0(x, y, t)) + f_1(x, y, t) = 0, u_1(x, y, 0) = x + y$$

$$L_2(v_1(x, y, t)) + N_2(v_0(x, y, t)) + f_2(x, y, t) = 0, v_1(x, y, 0) = x - y \quad (87)$$

$$L_3(w_1(x, y, t)) + N_3(w_0(x, y, t)) + f_2(x, y, t) = 0, w_1(x, y, 0) = -x + y$$

Rearranging the above yield the equivalent form as follows

$$\begin{aligned} L_1(u_1(x, y, t)) &= -N_1(u_0(x, y, t)) - f_1(x, y, t), u_1(x, y, 0) = x + y \\ L_2(v_1(x, y, t)) &= -N_2(v_0(x, y, t)) - f_2(x, y, t), v_1(x, y, 0) = x - y \\ L_3(w_1(x, y, t)) &= -N_3(w_0(x, y, t)) - f_2(x, y, t), w_1(x, y, 0) = -x + y \end{aligned} \quad (88)$$

Applying the inverse operator to both sides of the above and taking limits from 0 to t , we get

$$\begin{aligned} \int_0^t u_{1t}(x, t) dt &= \int_0^t (-u_{0x} v_{0x} + w_{0y} + 1) dt \\ \int_0^t v_{1t}(x, t) dt &= \int_0^t (-v_{0x} w_{0x} - u_{0y} + 1) dt \end{aligned} \quad (89)$$

$$\begin{aligned} \int_0^t v_{1t}(x, t) dt &= \int_0^t (-w_{0x} u_{0x} - v_{0y} + 1) dt \\ u_1(x, y, t) &= \int_0^t (-u_{0x} v_{0x} + w_{0y} + 1) dt \\ v_1(x, y, t) &= \int_0^t (-v_{0x} w_{0x} - u_{0y} + 1) dt \\ w_1(x, y, t) &= \int_0^t (-w_{0x} u_{0x} - v_{0y} + 1) dt \end{aligned} \quad (90)$$

Plugging in the derivatives we obtain the first iterative solution

$$\begin{aligned} u_1(x, y, t) &= t \\ v_1(x, y, t) &= t \end{aligned} \quad (91)$$

$$w_1(x, y, t) = t$$

Continuing in the same way, the solution converges to the exact solution in the form.

$$\begin{aligned} u(x, y, t) &= x + y + t \\ v(x, y, t) &= x - y + t \end{aligned} \quad (92)$$

$$w(x, y, t) = -x + y + t$$

5.9 Implementation by DJM

Applying the DJM to the system subject to the initial condition, we obtain the form

$$\begin{aligned} u(x, y, t) &= f_1(x, y, t) + \int_0^t (1 - u_x v_x + w_y) dt \\ v(x, y, t) &= f_2(x, y, t) + \int_0^t (1 - v_x w_x - u_y) dt \\ w(x, y, t) &= f_3(x, y, t) + \int_0^t (1 - w_x u_x + v_y) dt \end{aligned} \quad (93)$$

Now, the nonlinear terms are given as follows using the routine as follows.

$$\begin{aligned} N(u_k) &= \int_0^t (1 - u_{kx} v_{kx} + w_{ky}) dt \\ N(v_k) &= \int_0^t (1 - v_{kx} w_{kx} - u_{ky}) dt \\ N(w_k) &= \int_0^t (1 - w_{kx} u_{kx} + v_{ky}) dt \end{aligned} \quad (94)$$

Using the given initial condition, we obtain the solution for the second iterate

$$\begin{aligned} f_1(x, y, t) &= x + y \\ f_2(x, y, t) &= x - y \end{aligned} \quad (95)$$

$$f_3(x, y, t) = -x + y$$

Plugging the values of $k = 0, 1, 2, 3, \dots$ We obtain the subsequent terms as follows.

$$u_1 = N(u_0) = \int_0^t (1 - u_{0x} v_{0x} + w_{0y}) dt$$

$$v_1 = N(v_0) = \int_0^t (1 - v_{0x} w_{0x} - u_{0y}) dt \quad (96)$$

$$w_1 = N(w_0) = \int_0^t (1 - w_{0x} u_{0x} + v_{0y}) dt$$

Plugging in the derivatives above and integrating, we obtain the solution as

$$u_1(x, y, t) = t$$

$$v_1(x, y, t) = t$$

$$(97)$$

$$w_1(x, y, t) = t$$

The solution of the problem in closed form is given by

$$u(x, y, t) = x + y + t$$

$$v(x, y, t) = x - y + t$$

$$(98)$$

$$w(x, y, t) = -x + y + t$$

Example 4. Solve the system of nonlinear system of partial differential equations

$$u_t + v_x w_y - v_y w_x = -u$$

$$v_t + w_x u_y + w_y u_x = v$$

$$(99)$$

$$w_t + u_x v_y + u_y v_x = w$$

Subject to the initial conditions

$$u(x, y, 0) = e^{x+y}$$

$$v(x, y, 0) = e^{x-y}$$

$$(100)$$

$$w(x, y, 0) = e^{-x+y}$$

5.10 Implementation by ADM

Taking the inverse operator, $L_t^{-1} = \int_0^t (\cdot) dt$ of both sides of the above system, we get

$$u(x, y, t) = e^{x+y} - L_t^{-1}(v_x w_y - v_y w_x + u)$$

$$v(x, y, t) = e^{x-y} - L_t^{-1}(w_x u_y + w_y u_x - v)$$

$$(101)$$

$$w(x, y, t) = e^{-x+y} - L_t^{-1}(u_x v_y + u_y v_x - w)$$

Let the linear and nonlinear terms be decomposed as an infinite series and Adomian polynomials respectively.

$$u(x, y, t) = \sum_{n=0}^{\infty} u_n(x, y, t)$$

$$v(x, y, t) = \sum_{n=0}^{\infty} v_n(x, y, t)$$

$$(102)$$

$$w(x, y, t) = \sum_{n=0}^{\infty} w_n(x, y, t)$$

$$A_n = v_x w_y$$

$$B_n = v_y w_x$$

$$C_n = w_x u_y$$

$$D_n = w_y u_x$$

$$(103)$$

$$E_n = u_x v_y$$

$$F_n = u_y v_x$$

Plugging the above into the above system yield the recursive scheme in the form

$$\sum_{n=0}^{\infty} u_n(x, y, t) = e^{x+y} - L_t^{-1} \left(\sum_{n=0}^{\infty} A_n - \sum_{n=0}^{\infty} B_n + \sum_{n=0}^{\infty} u_n \right)$$

$$\sum_{n=0}^{\infty} v_n(x, y, t) = e^{x-y} - L_t^{-1} \left(\sum_{n=0}^{\infty} C_n + \sum_{n=0}^{\infty} D_n - \sum_{n=0}^{\infty} v_n \right)$$

$$(104)$$

$$\sum_{n=0}^{\infty} w_n(x, y, t) = e^{-x+y} - L_t^{-1} \left(\sum_{n=0}^{\infty} E_n + \sum_{n=0}^{\infty} F_n - \sum_{n=0}^{\infty} w_n \right)$$

The first four terms of the Adomian polynomials are given below

$$A_0 = v_{0x}w_{0y}$$

$$A_1 = v_{1x}w_{0y} + v_{0x}w_{1y}$$

$$A_2 = v_{2x}w_{0y} + v_{1x}w_{1y} + v_{0x}w_{2y} \quad (105)$$

$$A_3 = v_{3x}w_{0y} + v_{2x}w_{1y} + v_{1x}w_{2y} + v_{0x}w_{3y}$$

$$B_0 = v_{0y}w_{0x}$$

$$B_1 = v_{1y}w_{0x} + v_{0y}w_{1x}$$

$$B_2 = v_{2y}w_{0x} + v_{1y}w_{1x} + v_{0y}w_{2x} \quad (106)$$

$$B_3 = v_{3y}w_{0x} + v_{2y}w_{1x} + v_{1y}w_{2x} + v_{0y}w_{3x}$$

$$C_0 = w_{0x}u_{0y}$$

$$C_1 = w_{1x}u_{0y} + w_{0x}u_{1y}$$

$$C_2 = w_{2x}u_{0y} + w_{1x}u_{1y} + w_{0x}u_{2y}$$

$$C_3 = w_{3x}u_{0y} + w_{2x}u_{1y} + w_{1x}u_{2y} + w_{0x}u_{3y} \quad (107)$$

$$D_0 = w_{0y}u_{0x}$$

$$D_1 = w_{1y}u_{0x} + w_{0y}u_{1x}$$

$$D_2 = w_{2y}u_{0x} + w_{1y}u_{1x} + w_{0y}u_{2x} \quad (108)$$

$$D_3 = w_{3y}u_{0x} + w_{2y}u_{1x} + w_{1y}u_{2x} + w_{0y}u_{3x}$$

$$E_0 = u_{0x}v_{0y}$$

$$E_1 = u_{1x}v_{0y} + u_{0x}v_{1y}$$

$$E_2 = u_{2x}v_{0y} + u_{1x}v_{1y} + u_{0x}v_{2y} \quad (109)$$

$$E_3 = u_{3x}v_{0y} + u_{2x}v_{1y} + u_{1x}v_{2y} + u_{0x}v_{3y}$$

$$F_0 = u_{0y}v_{0x}$$

$$F_1 = u_{1y}v_{0x} + u_{0y}v_{1x}$$

$$F_2 = u_{2y}v_{0x} + u_{1y}v_{1x} + u_{0y}v_{2x} \quad (110)$$

$$F_3 = u_{3y}v_{0x} + u_{2y}v_{1x} + u_{1y}v_{2x} + u_{0y}v_{3x}$$

Plugging the above polynomials into the recursive relations, we obtain the first iterative solution as

$$(u_0, v_0, w_0) = (e^{x+y}, e^{x-y}, e^{-x+y}) \quad (111)$$

Similarly, for the second solution we put $k = 0, 1, 2, \dots$ into the recursive schemes as follows

$$u_1 = -L_t^{-1}(A_0 - B_0 + u_0)$$

$$v_1 = -L_t^{-1}(C_0 + D_0 - v_0) \quad (112)$$

$$w_1 = -L_t^{-1}(E_0 + F_0 - w_0)$$

$$u_2 = -L_t^{-1}(A_1 - B_1 + u_1)$$

$$v_2 = -L_t^{-1}(C_1 + D_1 - v_1) \quad (113)$$

$$w_2 = -L_t^{-1}(E_1 + F_1 - w_1)$$

$$u_3 = -L_t^{-1}(A_2 - B_2 + u_2)$$

$$v_3 = -L_t^{-1}(C_2 + D_2 - v_2) \quad (114)$$

$$w_3 = -L_t^{-1}(E_2 + F_2 - w_2)$$

Evaluating the above schemes give subsequent solutions as follows

$$(u_1, v_1, w_1) = (-te^{x+y}, te^{x-y}, te^{-x+y})$$

$$(u_2, v_2, w_2) = \left(-\frac{t^2}{2!}e^{x+y}, \frac{t^2}{2!}e^{x-y}, \frac{t^2}{2!}e^{-x+y}\right) \quad (115)$$

$$(u_3, v_3, w_3) = \left(-\frac{t^3}{3!}e^{x+y}, \frac{t^3}{3!}e^{x-y}, \frac{t^3}{3!}e^{-x+y}\right)$$

Now, using the formula for the unknowns

$$u(x, y, t) = \sum_{n=0}^{\infty} u_n(x, y, t)$$

$$v(x, y, t) = \sum_{n=0}^{\infty} v_n(x, y, t)$$

$$(116)$$

$$w(x, y, t) = \sum_{n=0}^{\infty} w_n(x, y, t)$$

The exact or closed form solution of the coupled nonlinear system become

$$u(x, y, t) = e^{x+y-t}$$

$$v(x, y, t) = e^{x-y+t}$$

(117)

$$w(x, y, t) = e^{-x+y+t}$$

5.11 Implementation by TAM

Applying TAM to both sides of the system, we have

$$\begin{aligned} L_1(u) &= u_t, N_1(u) = v_x w_y - v_y w_x + u, f_1(x, y, t) = 0 \\ L_2(v) &= v_t, N_2(v) = w_x u_y + w_y u_x - v, f_2(x, y, t) = 0 \end{aligned} \quad (118)$$

$$L_3(w) = w_t, N_3(w) = u_x v_y + u_y v_x - w, f_3(x, y, t) = 0$$

The initial problem to be solved is given by

$$\begin{aligned} L_1(u_0(x, y, t)) + f_1(x, y, t) &= 0 \\ L_2(v_0(x, y, t)) + f_2(x, y, t) &= 0 \\ L_3(w_0(x, y, t)) + f_3(x, y, t) &= 0 \end{aligned} \quad (119)$$

Integrating both sides and taking limits from 0 to t yields the integrals of the form

$$\int_0^t u_{0t}(x, y, t) dt = 0$$

$$\int_0^t v_{0t}(x, y, t) dt = 0$$

(120)

$$\int_0^t w_{0t}(x, y, t) dt = 0$$

Solving the above system of integrals give the initial solution as

$$u_0(x, y, t) = e^{x+y}$$

$$v_0(x, y, t) = e^{x-y}$$

(121)

$$w_0(x, y, t) = e^{-x+y}$$

The second problem to be solved for the first iterate become

$$\begin{aligned} L_1(u_1(x, y, t)) + N_1(u_0(x, y, t)) + f_1(x, y, t), u_1(x, y, 0) &= e^{x+y} \\ L_2(v_1(x, y, t)) + N_2(v_0(x, y, t)) + f_2(x, y, t), v_1(x, y, 0) &= e^{x-y} \\ L_3(w_1(x, y, t)) + N_3(w_0(x, y, t)) + f_3(x, y, t), w_1(x, y, 0) &= e^{-x+y} \end{aligned} \quad (122)$$

Taking the inverse operator of both sides subject to the initial condition yield the set of integral equations as follows.

$$\begin{aligned} \int_0^t u_{1t}(x, y, t) dt &= \int_0^t (-v_{0x} w_{0y} + v_{0y} w_{0x} - u_0) dt \\ \int_0^t v_{1t}(x, y, t) dt &= \int_0^t (-w_{0x} u_{0y} - w_{0y} u_{0x} + v_0) dt \\ \int_0^t w_{1t}(x, y, t) dt &= \int_0^t (-u_{0x} v_{0y} - u_{0y} v_{0x} + w_0) dt \end{aligned} \quad (123)$$

In view of the above, the second iterative solution of the problem follows

$$u_1(x, y, t) = -te^{x+y}$$

$$v_1(x, y, t) = te^{x-y}$$

(124)

$$w_1(x, y, t) = te^{-x+y}$$

The third iterative problem to be solved is given as follows

$$\begin{aligned} L_1(u_2(x, y, t)) + N_1(u_1(x, y, t)) + f_1(x, y, t), u_2(x, y, 0) &= e^{x+y} \\ L_2(v_2(x, y, t)) + N_2(v_1(x, y, t)) + f_2(x, y, t), v_2(x, y, 0) &= e^{x-y} \\ L_3(w_2(x, y, t)) + N_3(w_1(x, y, t)) + f_3(x, y, t), w_2(x, y, 0) &= e^{-x+y} \end{aligned} \quad (125)$$

Taking the inverse operator of both sides and taking limits from 0 to t , we obtain

$$\begin{aligned} u_2(x, y, t) &= \int_0^t (-v_{1x} w_{1y} + v_{1y} w_{1x} - u_1) dt \\ v_2(x, y, t) &= \int_0^t (-w_{1x} u_{1y} - w_{1y} u_{1x} + v_1) dt \\ w_2(x, y, t) &= \int_0^t (-u_{1x} v_{1y} - u_{1y} v_{1x} + w_1) dt \end{aligned} \quad (126)$$

Plugging in the derivatives to be above integral equation, we obtain the iterative solution as follows

$$\begin{aligned} u_2(x, y, t) &= -\frac{t^2}{2!} e^{x+y} \\ v_2(x, y, t) &= \frac{t^2}{2!} e^{x-y} \end{aligned} \quad (127)$$

$$w_2(x, y, t) = \frac{t^2}{2!} e^{-x+y}$$

Continuing in the same way, the converging series solutions of the unknowns become

$$\begin{aligned} u(x, y, t) &= \left(1 - t + \frac{t^2}{2!} - \dots\right) e^{x+y} \\ v(x, y, t) &= \left(1 + t + \frac{t^2}{2!} + \dots\right) e^{x-y} \\ w(x, y, t) &= \left(1 + t + \frac{t^2}{2!} + \dots\right) e^{-x+y} \end{aligned} \quad (128)$$

The solution of the problem in closed form is given by

$$\begin{aligned} u(x, y, t) &= e^{x+y-t} \\ v(x, y, t) &= e^{x-y+t} \end{aligned} \quad (129)$$

$$w(x, y, t) = e^{-x+y+t}$$

5.12 Implementation by DJM

Applying DJM to both sides of the coupled nonlinear system of the given PDEs, we get

$$\begin{aligned} u(x, y, t) &= f_1(x, y, t) + \int_0^t (-v_x w_y + v_y w_x - u) dt \\ v(x, y, t) &= f_2(x, y, t) + \int_0^t (-w_x u_y - w_y u_x + v) dt \\ w(x, y, t) &= f_3(x, y, t) + \int_0^t (-u_x v_y - u_y v_x + w) dt \end{aligned} \quad (130)$$

Where the nonlinear terms are given by

$$\begin{aligned} N(u_k) &= \int_0^t (-v_{kx} w_{ky} + v_{ky} w_{kx} - u_k) dt \\ N(v_k) &= \int_0^t (-w_{kx} u_{ky} - w_{ky} u_{kx} + v_k) dt \\ N(w_k) &= \int_0^t (-u_{kx} v_{ky} - u_{ky} v_{kx} + w_k) dt \end{aligned} \quad (131)$$

Using the given initial condition, we obtain

$$\begin{aligned} f_1(x, y, t) &= u_0(x, y, 0) = e^{x+y} \\ f_2(x, y, t) &= v_0(x, y, 0) = e^{x-y} \\ f_3(x, y, t) &= w_0(x, y, 0) = e^{-x+y} \end{aligned} \quad (132)$$

Using the algorithm schemes for the subsequent terms, we obtain

$$\begin{aligned} u_1(x, y, t) &= N(u_0) = \int_0^t (-v_{0x} w_{0y} + v_{0y} w_{0x} - u_0) dt \\ v_1(x, y, t) &= N(v_0) = \int_0^t (-w_{0x} u_{0y} - w_{0y} u_{0x} + v_0) dt \\ w_1(x, y, t) &= N(w_0) = \int_0^t (-u_{0x} v_{0y} - u_{0y} v_{0x} + w_0) dt \end{aligned} \quad (133)$$

Substituting the derivatives into the above integrals, we obtain the second iterative solution in the form.

$$\begin{aligned} u_1(x, y, t) &= -te^{x+y} \\ v_1(x, y, t) &= te^{x-y} \end{aligned} \quad (134)$$

$$w_1(x, y, t) = te^{-x+y}$$

The subsequent terms are obtained using the algorithms below

$$\begin{aligned} u_2 &= N(u_0 + u_1) - N(u_0) \\ v_2 &= N(v_0 + v_1) - N(v_0) \\ w_2 &= N(w_0 + w_1) - N(w_0) \end{aligned} \quad (135)$$

In view of the above, the third iterative solution of the problem become

$$\begin{aligned} u_2(x, y, t) &= -\frac{t^2}{2!}e^{x+y} \\ v_2(x, y, t) &= \frac{t^2}{2!}e^{x-y} \end{aligned} \quad (136)$$

$$w_1(x, y, t) = \frac{t^2}{2!}e^{-x+y}$$

Thus, the closed form of the nonlinear system of PDEs is given by

$$\begin{aligned} u(x, y, t) &= e^{x+y-t} \\ v(x, y, t) &= e^{x-y+t} \end{aligned} \quad (137)$$

$$w(x, y, t) = e^{-x+y+t}$$

Example 5 Consider the coupled system partial differential equation as follows

$$u_t = uu_x + vu_y$$

$$v_t = uv_x + vv_y$$

Subject to the initial condition

$$u(x, y, 0) = x^2$$

$$v(x, y, 0) = y$$

5.13 Implementation by ADM

Taking the inverse operator of both sides of the system subject to the initial condition, we get

$$\begin{aligned} u(x, y, t) &= x^2 + L_t^{-1}(uu_x + vu_y) \\ v(x, y, t) &= y + L_t^{-1}(uv_x + vv_y) \end{aligned} \quad (138)$$

Writing the linear and nonlinear operators as infinite series an Adomian polynomials, we get

$$\begin{aligned} \sum_{n=0}^{\infty} u_n(x, y, t) &= x^2 + L_t^{-1} \left(\sum_{n=0}^{\infty} A_n + \sum_{n=0}^{\infty} B_n \right) \\ \sum_{n=0}^{\infty} v_n(x, y, t) &= y + L_t^{-1} \left(\sum_{n=0}^{\infty} C_n + \sum_{n=0}^{\infty} D_n \right) \end{aligned} \quad (139)$$

Matching both sides of the equation above we get the zeroth order components of the schemes

$$u_0(x, y, t) = x^2$$

$$v_0(x, y, t) = y$$

The respective recursive schemes of the problem become

$$\begin{aligned} u_{n+1}(x, y, t) &= L_t^{-1}(A_n + B_n) \\ v_{n+1}(x, y, t) &= L_t^{-1}(C_n + D_n) \end{aligned} \quad (140)$$

The first four terms of the nonlinear terms are given as follows

$$\begin{aligned} A_0 &= u_0 u_{0x} \\ A_1 &= u_1 u_{0x} + u_0 u_{1x} \\ A_2 &= u_2 u_{0x} + u_1 u_{1x} + u_0 u_{2x} \end{aligned} \quad (141)$$

$$A_3 = u_3 u_{0x} + u_2 u_{1x} + u_1 u_{2x} + u_0 u_{3x}$$

$$B_0 = v_0 u_{0y}$$

$$B_1 = v_1 u_{0y} + v_0 u_{1y}$$

$$B_2 = v_2 u_{0y} + v_1 u_{1y} + v_0 u_{2y} \quad (142)$$

$$\begin{aligned}
 B_3 &= v_3 u_{0y} + v_2 u_{1y} + v_1 u_{2y} + v_0 u_{3y} \\
 C_0 &= u_0 v_{0x} \\
 C_1 &= u_1 v_{0x} + u_0 v_{1x} \\
 C_2 &= u_2 v_{0x} + u_1 v_{1x} + u_0 v_{2x} \\
 (143) \\
 C_3 &= u_3 v_{0x} + u_2 v_{1x} + u_1 v_{2x} + u_0 v_{3x} \\
 D_0 &= v_0 v_{0y} \\
 D_1 &= v_1 v_{0y} + v_0 v_{1y} \\
 D_2 &= v_2 v_{0y} + v_1 v_{1y} + v_0 v_{2y} \\
 D_3 &= v_3 v_{0y} + v_2 v_{1y} + v_1 v_{2y} + v_0 v_{3y}
 \end{aligned} \tag{144}$$

Plugging the above derivatives into the recursive relation and using the preceding terms, we obtain

$$\begin{aligned}
 u_1(x, y, t) &= L_t^{-1}(A_0 + B_0) \\
 v_1(x, y, t) &= L_t^{-1}(C_0 + D_0) \\
 (145)
 \end{aligned}$$

Evaluating the above, we obtain the second iterative solution as follows.

$$(u_1, v_1) = (2tx^3, ty)$$

Similarly, the next iterative solution is obtain using the integrals

$$\begin{aligned}
 u_2(x, y, t) &= L_t^{-1}(A_1 + B_1) \\
 v_2(x, y, t) &= L_t^{-1}(C_1 + D_1) \\
 (146)
 \end{aligned}$$

In view of the above, we get the third iterative solution as follows

$$(u_2, v_2) = \left(6t^2 x^5, \frac{t^2}{2} x^2 + t^2 y \right)$$

The final solution is obtained using the sum of partial series as follows

$$\begin{aligned}
 u(x, y, t) &= x^2(1 + 2tx + 6t^2 x^2 + \dots) \\
 v(x, y, t) &= y(1 + t + t^2 + t^3 + \dots) \\
 (147)
 \end{aligned}$$

5.14 Implementation

by

TAM

To implement TAM, we first write the system in operator form as follows.

$$\begin{aligned}
 u_t - (uu_x + vu_y) &= 0 \\
 v_t - (uv_x + vv_y) &= 0 \\
 L(u) &= u_t, N(u) = -(uu_x + vu_y), f_1(x, y, t) = 0 \\
 L(v) &= v_t, N(v) = -(uv_x + vv_y), f_2(x, y, t) = 0
 \end{aligned} \tag{148}$$

The first problem to be solved is given by

$$\begin{aligned}
 L(u_0(x, y, t)) &= f_1(x, y, t), u_0(x, y, t) = x^2 \\
 L(v_0(x, y, t)) &= f_2(x, y, t), v_0(x, y, t) = y
 \end{aligned} \tag{149}$$

Integrating both sides and taking limit from 0 to t subject to the initial conditions yields

$$\begin{aligned}
 u_0(x, y, t) &= x^2 \\
 v_0(x, y, t) &= y
 \end{aligned}$$

The second iterative solution to be solved become

$$\begin{aligned}
 L(u_1(x, y, t)) + N(u_0(x, y, t)) &= 0, u_1(x, y, t) = x^2 \\
 L(v_1(x, y, t)) + N(v_0(x, y, t)) &= 0, v_1(x, y, t) = y
 \end{aligned} \tag{150}$$

Taking the inverse operator of both sides subject to the initial condition, we obtain

$$\begin{aligned}
 u_1(x, y, t) &= \int_0^t (u_0 u_{0x} + v_0 u_{0y}) dt \\
 v_1(x, y, t) &= \int_0^t (u_0 v_{0x} + v_0 v_{0y}) dt
 \end{aligned} \tag{151}$$

Plugging the derivatives into the above and solving yields the solution as

$$(u_1, v_1) = (2tx^3, ty)$$

The third iterative solution is obtained by solved by solving the equation

$$L(u_2(x, y, t)) + N(u_1(x, y, t)) = 0, u_2(x, y, t) = x^2$$

$$L(v_2(x, y, t)) + N(v_1(x, y, t)) = 0, v_2(x, y, t) = y \quad (152)$$

Integrating both sides of the above and taking limits from 0 to t yield the corresponding equations of the form.

$$u_2(x, y, t) = \int_0^t (u_1 u_{1x} + v_1 u_{1y}) dt$$

$$v_2(x, y, t) = \int_0^t (u_1 v_{1x} + v_1 v_{1y}) dt \quad (153)$$

Solving the above integrals after putting the derivatives gives the solution

$$(u_2, v_2) = \left(6t^2 x^5, \frac{t^3}{3} y \right)$$

Again, the fourth iterative solution of the problem become

$$L(u_3(x, y, t)) + N(u_2(x, y, t)) = 0, u_3(x, y, t) = x^2$$

$$L(v_3(x, y, t)) + N(v_2(x, y, t)) = 0, v_3(x, y, t) = y \quad (154)$$

Taking the inverse operator of both sides subject to the initial condition give the integral equations

$$u_3(x, y, t) = \int_0^t (u_2 u_{2x} + v_2 u_{2y}) dt$$

$$v_3(x, y, t) = \int_0^t (u_2 v_{2x} + v_2 v_{2y}) dt \quad (155)$$

Solving the above give the solution in the form

$$(u_3, v_3) = \left(36t^5 x^9, \frac{t^7}{63} y \right)$$

Therefore, taking the partial sum of the iterative solutions, we get the closed form solution of the system as

$$u(x, y, t) = x^2 (1 + 2tx + 6t^2 x^2 + \dots)$$

$$v(x, y, t) = y (1 + t + t^2 + \dots) \quad (156)$$

5.15 Implementation by DJM

Applying DJM to both sides of the system subject to the initial conditions, we get the corresponding equations.

$$u(x, y, t) = f_1(x, y, t) + \int_0^t (u u_x + v u_y) dt$$

$$v(x, y, t) = f_2(x, y, t) + \int_0^t (u v_x + v v_y) dt \quad (157)$$

Where $f_1(x, y, t) = x^2$, $f_2(x, y, t) = y$

$$N(u_i) = \int_0^t (u_i u_{ix} + v_i u_{iy}) dt$$

$$N(v_i) = \int_0^t (u_i v_{ix} + v_i v_{iy}) dt \quad (158)$$

$$u_0(x, y, t) = f_1(x, y, t) = x^2$$

$$v_0(x, y, t) = f_2(x, y, t) = y$$

$$u_1 = N(u_0) = \int_0^t (u_0 u_{0x} + v_0 u_{0y}) dt$$

$$v_1 = N(v_0) = \int_0^t (u_0 v_{0x} + v_0 v_{0y}) dt \quad (159)$$

Solving the above integral equations, we get the second iterative solution as

$$(u_1, v_1) = (2tx^3, ty)$$

Now, the succeeding terms are obtained using the following relations

$$u_2 = N(u_0 + u_1) - N(u_0)$$

$$v_2 = N(v_0 + v_1) - N(v_0) \quad (160)$$

Evaluating the above yield the solution as

$$(u_2, v_2) = \left(t^2 x^3, \frac{t^2}{2!} y \right)$$

Similarly, using the relation the next iterative solution is found

$$u_3 = N(u_0 + u_1 + u_2) - N(u_0 + u_1)$$

$$v_2 = N(v_0 + v_1 + v_2) - N(v_0 + v_1) \quad (161)$$

Solving the above, give the fourth iterative solution as

$$(u_3, v_3) = \left(\frac{t^3}{3} x^3, \frac{t^3}{3!} y \right)$$

Summing the above iterative solution for each step, the closed form solution of the problem become

$$u = x^2 \left(1 + 2tx + 6t^2x^2 + \frac{t^3}{3}x^3 \right)$$

$$v = y \left(1 + t + t^2 + \frac{t^3}{3} \right) \quad (162)$$

VI. CONCLUSION

In this research article, three semi-analytical iterative methods were proposed to solve nonlinear coupled system of partial differential equations subject to initial conditions. The applicability of these methods was demonstrated by successfully applying them to solve five systems of NLPDEs. It was found that, the methods produce rapidly converging series solution which gives the exact solution. The rate of convergence of the results obtained when compared with existing literature are found to be in excellent agreement. TAM and DJM proved to be of significant improvement to the ADM, as they give the solution with less computational work and overcome the inherent hurdle of calculating Adomian polynomials for the nonlinear term. It is recommended these methods be used for used for other highly involved problems.

REFERENCES

- [1] A.M. Wazwaz. Partial differential Equations and Solitary Waves Theory. Higher Education Press, Beijing, and Springer-Verlag Berlin Heidelberg, 2000
- [2] A.M. Wazwaz. The Variational Iteration method for solving linear and nonlinear systems of PDEs. Computer and Mathematics with Applications, 2007, 54,895-902.
- [3] M. Akbarzade. Application of Variational Iteration method to Partial Differential Equation System. International Journal of Mathematics Analysis, 2000, 5(18), 863-870.
- [4] A.M. Wazwaz. The Decomposition method Applied to Systems of Partial Differential and to Reaction-Diffusion Brusselator. Applied Mathematics and Computation, 2000, 110 (2,3,15), 251-264.
- [5] E. A, Mohammed,M. Elzali,.A Study of some Systems of Nonlinear Partial Differential Equations by using Adomian and Modified Decomposition Methods', African Journal of Mathematics and Computer Science Research, 2014, 7(6), 61-67.
- [6] M. Mohand, M. Abdelrahim,K. Abdelilah,,S. Hassan. An Efficient Method for Solving Linear and Nonlinear System of Partial Differential Equations. British Journal of Mathematics and Computer Science, 2017, 20(1): 2231-0851
- [7] J. Fadaei, J. Application of Laplace-Adomian Decomposition Method on Linear and Nonlinear System of PDEs. Applied Mathematical Sciences, 2011, 5(27), 1307 – 1315
- [8] B. Jafar., E. Mostafa. A new Homotopy perturbation method for solving systems of partial differential equations, Computers and Mathematics with Applications 2011, 62 ,225–234.
- [9] K.R. Raslan., F. Zain, A. Sheer. Differential transform method for solving non-linear systems of partial differential equations' International Journal of Physical Sciences, 2013, 8(38), 1880-1884.
- [10] V. Daftargar-Gejji,,H. Jafari. An iterative method for solving nonlinear functional equations. Journal of Mathematical. Analysis Application.2006, 316, 753 – 763
- [11] A.A. Hemeda. New Iterative Method: An Application for solving Fractional Physical Differential Equations', Abstract and Applied Analysis, 2013, 13, 231-240
- [12] K. Manoj, A.S. Shanker. New Iterative Method for solving higher order KDV equations', 4th International Conference on Science, Technology and Management (ICSTM-16): 2016, ISBN 978-81-932074-8-2.
- [13] A.S. Mohamed. New Iterative Method for Fractional Gas Dynamics and Coupled Burger's Equations. The Scientific World Journal, 2015, 2(234-240).

- [14] P.K. Gupta. Modified New Iterative Method for Solving Nonlinear Abel Type Integral Equations', International Journal of Nonlinear Science, .2012, 14(.3), 307-315.
- [15] M. Yaseem, M. Samraiz,.The Modified New Iterative Method for Solving Linear and Nonlinear Klein-Gordon Equations', Applied Mathematical Sciences, 2012, 6(60), 2979-2987.
- [16] A. Abbasbandy. Numerical solution of nonlinear Klein-Gordon equation by variational Iteration method, International Journal of Numerical methods in Engineering, 2007, 70, 876-881.
- [17] M.A. Abdou, A.A. Soliman. Variational Iteration method for solving Burgers and coupled Burgers Equations. Journal of Computational and Applied Mathematics, 2005, 181, 245-251.
- [18] M.A. Abdou, A.A. Soliman.New Applications of Variational Iteration method,Physics D, 2005, 211(1-2), 1-8.
- [19] M.A. Noor, S.T. Mohyud-Din). Homotopy Perturbation method for nonlinear higher-order boundary value problems. International Journal of Nonlinear Science and Numerical simulation, 2008, 9(2-4), 395-408.
- [20] M.A. Noor, S.T. Mohyud-Din. Modified variational Iteration method for heat and wave-like equations. Acta Appl. Math, 2018, dc:10.1007/s10440-008-9255-x
- [21] M.A. Noor, S.T. Mohyud-Din,Variational Iteration method for solving twelfth-order boundary value problem using He's polynomials. Computational Mathematics and modelling, 2018, 673-683.
- [22] S. Vandewalle, R. Piessens..Numerical Experiment with nonlinear multi-grid waveform relaxation on a parallel processor. Applied Numerical Mathematics,1991, 8, 149-161.
- [23] A.M. Wazwaz..The Variational Iteration method: A powerful scheme for handling linear and nonlinear diffusion equations. Computational Mathematics and Applications, 2007, 54, 933-939.
- [24] G.A. Afrouzi, S. Khademloo. On Adomian decomposition method for solving reaction diffusion equation. International Journal of Nonlinear Science, 2006, Vol 2, No. 1, pp. 11-15.
- [25] M. Danesh,,M. Safari. Application of Adomian decomposition method for the analytical solution of space fractional diffusion equation. APM, 2011, Vol. 1, pp. 345-350.
- [26] J.S. Dunan., R. Rach, D. Baleanu,,A.M. Wazwaz.. A review of the Adomian decomposition method and its application to fractional differential equations. Communications in Fractional Calculus, 2012, Vol. 3, pp.73-99.
- [27] S.A. El-Wakil., M. A. Abdou.,A.Elhanbaly..Adomian decomposition method for solving the diffusion-convection-reaction equations. Applied Mathematics and Computations, 2006, Vol. 177, pp.729-736.
- [28] J.M. Machado, S.L.L. Verardi, Y. Shiyu..An application of Adomian decomposition method to the analysis of MHD duct flows. IEEE Transactions on Magnetics, 2005, Vol. 41, pp.1588-1591.
- [29] M. Tatari, M. Dehghan, M.Razzaghi..Application of the Adomian decomposition method for the Fokker-Planck equation. Mathematics and computer modelling, 2007, Vol. 45, pp.639-650.
- [30] G. Adomian. A review of the decomposition method in applied mathematics. Journal of Mathematical Analysis and Applications, 1988, Vol. 135, pp.501-544.
- [31] D.J. Evans., K.R. Raslan. The Adomian decomposition method for solving delay differential equations. International Journal of Computer Mathematics, 2005, Vol. 82, pp.49-54.
- [32] Y.Q. Hassan,L.M. Zhu.Modified Adomian decomposition for singular initial value problems in the second order ordinary differential equations. Surveys in Mathematics and its Applications, 2008, Vol. 3, pp.183-193.
- [33] T.R. Ramesh.The use of Adomian decomposition method for solving generalized Riccati differential equations. Proceedings of the 6th IMT-GT Conference on Mathematics, Statistics and its Applications (ICMSA 2010), Universiti Tunku Abdul Rahman, Kuala Lumpur, Malaysia, pp. 935-941.
- [34] H. Temimi., B.M. Romdhane..Numerical solution of Falkner-Skan equation by iterative transformation method", Mathematical Modelling and Analysis, 2018, 23.1, 139-151.
- [35] H. Temimi., A.R. Ansari. A new iterative technique for solving nonlinear second order multi-point boundary value problems", Applied Mathematics and Computation, 2011, 218(4), 1457-1466.
- [36] H. Temimi., A.R. Ansari.A computational iterative method for solving nonlinear ordinary differential equations. LMS Journal of Computation and mathematics, 2015, 18(1), 730-753.

- [37] E. Liberty. Numerical Investigation of the Burgers-Fisher and FitzHugh-Nagumo Equations by Temimi and Ansari method (TAM). *International Journal of Applied Sciences and Mathematical Theory*, 2021, E-ISSN 2489-009X P-SSN 2695-1908, Vol. 7, No.2.
- [38] E. Liberty. Application of Semi-analytical Iteration Techniques for the Numerical solution of linear and nonlinear differential equations. *International Journal of Mathematics Trends and Technology*, 2012, Volume. 67, Issue 2, 146-158.
- [39] M.A. Al-Jawary. .A Semi-Analytical Iterative Method for Solving Nonlinear Thin Film Flow Problems. *Chaos Solitons and Fractals*, 2017, 99(2017) 52-56.
- [40] H. Temimi, A.R. Ansari., (2011a) A semi-Analytical Iterative Technique for solving Nonlinear Problems. *Computers and Mathematics with Applications*, 2011a, 61(2), 203-210.
- [41] M.A. AL-Jawary., S. Hatif,.A semi-analytical iterative method for solving differential algebraic equations. *Ain Shams Engineering Journal*,2017, Vol 2, 123-140.
- [42] M.M. Azeez, M.A. Weli. Semi-Analytical Iterative Methods for Nonlinear Differential Equations. *Baghdad University College of Education for Pure Science, Al-Haitham*, 2017
- [43] M.A. AL-Jawary, M.M. Azeez,G.H. Radhi. Analytical and numerical solutions for the nonlinear Burgers and advection–diffusion equations by using a semi-analytical iterative method, *Computers & Mathematics with Applications*, 2018, 76(1), 155-171, (2018).
- [44] M.A. Al-Jawary.,S.G. Al-Razaq, (2016). A semi analytical iterative technique for solving Duffing equations", *International Journal of Pure and Applied Mathematics*, 2016, 108(4), 871-885.
- [45] M.A. AL-Jawary., R.K. Raham. A semi-analytical iterative technique for solving chemistry problems", *Journal of King Saud University*, 2017, 29(3), 320-332.
- [46] M. A, Al-Jawary.,H.R. Al-Qaissy. A reliable iterative method for solving Volterra Integro-differential equations and some applications for the Lane-Emden equations of the first kind", *Monthly Notices of the Royal Astronomical Society*,2015, 448, 3093-3104.

Optimization of Dressing Conditions When External Cylindrical Grinding to Minimize Surface Roughness

Tran Phuong Thao

Center for Technical Practice
Thai Nguyen University of Technology, Vietnam

ABSTRACT

This paper studies the influence of the dressing condition on the external cylindrical grinding process to determine the optimal dressing conditions to achieve the minimum surface roughness. Six input parameters in the investigation, including depth of rough dressing, rough dressing time, depth of fine dressing, fine dressing time, non-feeding dressing time, and dressing speed. The study used the response surface method to design the experiment. The experiment results were analyzed by using Minitab R19 software. The regression equation describes the relationship between the input parameters and surface roughness was determined and the optimal dressing condition to achieve the minimum roughness was determined.

Keywords—external grinding; dressing condition; surface roughness;

I. INTRODUCTION

The surface quality of the work piece and the efficiency of the grinding process in general, and the external cylindrical grinding process, in particular, much depends on the dressing condition [1, 2]. However, the introduction of the dressing condition in the practice is also limited in general guidelines [3].

Currently, there are some studies of dressing conditions to improve the efficiency and quality of the grinding process. The research results show a clear influence of the dressing condition on the quality and productivity of the grinding process [4]. The study of Haoyan Cao indicated the grinding conditions should be selected in conjunction with wheel dressing conditions. The constraint of textural gouge shape depends on grinding contact length and dressing conditions [5]. Xun Chen also presents a study about the relation of grinding force and grinding power to the dressing operation by considering the effective density of the cutting edges on the wheel surface [6]. In addition, the relationship between the dressing parameters and the radial wear has been studied by Puerto [7].

The study of Tran Ngoc Giang and Tran Thi Hong study the effect of dressing parameters on surface roughness and Flatness tolerance when surface grinding. In these studies, the six input dressing parameters were investigated and the results have shown the dressing condition has a great impact on surface roughness and flatness tolerance, the optimization of dressing condition to reach minimum surface roughness or flatness tolerance was also presented [8, 9]. The multi-objective optimization of dressing conditions when surface grinding has been studied [10, 11]. The other study about internal cylindrical grinding has been presented by Le Xuan Hung [12].

In the external cylindrical grinding process, the effect of dressing conditions on the surface roughness, material removal rate, or roughness tolerance has been investigated. These studies applied the Taguchi method to design the experiment and determined the optimum dressing conditions [13-15]. However, the Taguchi method could only determine the optimal dressing condition at the investigated levels. Therefore, in this study, we study the effect of dressing parameters on surface roughness when external cylindrical grinding 90CrSi using the response surface method.

II. EXPERIMENTAL DESIGN

As literature review above, in this section, an experiment design using response surface Box-Behnken method was applied to investigate the effect of six input parameters including depth of rough dressing, rough dressing time, depth of fine dressing, fine dressing time, non-feeding dressing time, and dressing speed on surface roughness when external grinding 90CrSi. The input parameters and their levels were shown in table 1.

TABLE 1.INPUT PARAMETERS AND INVESTIGATED LEVELS

No.	Input parameters	Symbol	Unit	Level of investigating	
				Low	High
1	Depth of rough dressing	a_r	mm	0.02	0.04
2	Rough dressing time	n_r	-	1	5
3	Depth of fine dressing	a_f	mm	0.005	0.015
4	Fine dressing time	n_f	-	0	4
5	Non-feeding dressing time	n_0	-	0	4
6	Feed speed	S_d	m/min	1	2

The experiments were conducted using the following fixed grinding conditions and equipment: The Cantex Aquatex 3810 with a concentration of 3% and a flow-rate of 10 l/min was used for coolant condition; the grinding condition is: feed rate at 1.8 m/min, depth per cut is 0.005 per single stroke, total depth of cut is 0.05 mm and the speed of grinding wheel is 29.3 m/s; Grinding machine: CONDO-Hi-5 HTS (Japan origin); grinding wheel: Ct80MV1-G 400x40x203 35m/2 (Vietnam origin); dressing tool: 3908-0088C type 2 (Russian origin); surface roughness tester: Mitutoyo 178-923-2A SJ201 (Japan origin). The workpiece properties are described in table 2.

TABLE 2.90CrSi STEEL PROPERTIES

Steel grade: 90CrSi						
C	Si	Mn	Cr	P	S	Co
0.85-0.95	12-1.6	0.3-0.6	0.95-1.25	≤0.03	≤0.03	≤1

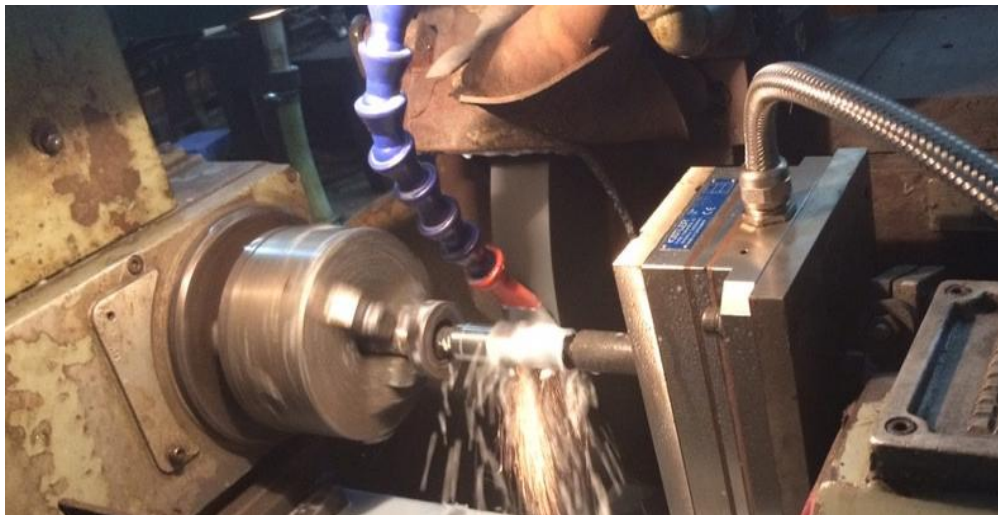


Fig 1. Experiment setup

According to the response surface method, the experiment design is calculated based on the input data in table 1. By using Minitab R19, the experiment design table with 54 experiments is listed in table 3. The surface roughness of each run is described in table3 either.

TABLE 3.EXPERIMENT DESIGN AND MEASUREMENT RESULTS

Std Order	Run Order	Pt Type	Blocks	a _r	n _r	a _f	n _f	n ₀	S _d	Mean of Ra(μm)
30	1	2	1	0.04	3	0.01	0	4	1.5	0.233
46	2	2	1	0.04	3	0.005	2	2	2	0.331
37	3	2	1	0.03	1	0.01	2	0	2	0.252
16	4	2	1	0.03	5	0.015	2	4	1.5	0.264
...
20	51	2	1	0.03	3	0.015	4	2	1	0.359
17	52	2	1	0.03	3	0.005	0	2	1	0.411
48	53	2	1	0.04	3	0.015	2	2	2	0.379
15	54	2	1	0.03	1	0.015	2	4	1.5	0.355

III. RESULT AND DISCUSSIONS

In order to find the optimum set of dressing parameters, the ANOVA method is conducted by using Minitab R19 to determine the influence of input parameters on the surface roughness.

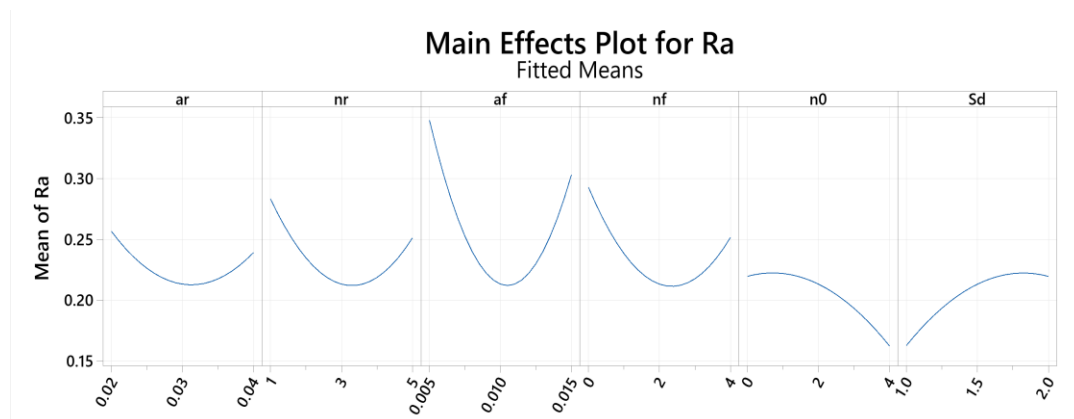


Fig2.Effect of input factors on surface roughness

Observing the analysis result in figure 2 shows all of the input parameters affect the response in the quadratic form. This result indicated that investigated area has extreme value and the optimal value of the input parameter can be determined.

The influence degree of input factors is described in the Pareto chart in figure 3.

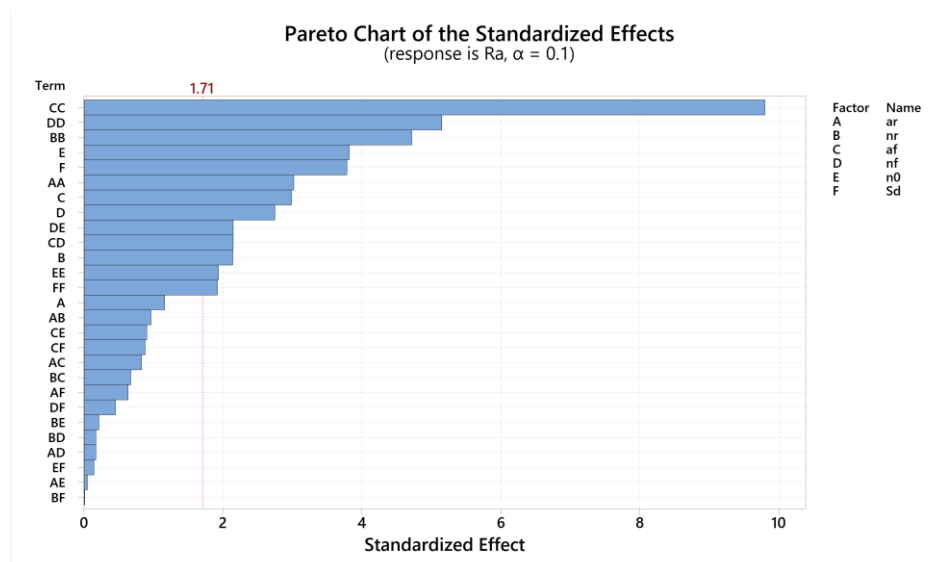


Fig 3. The influence degree of input factor on surface roughness

The figure shows clearly that the quadratic effect of CC ($a_f \cdot a_f$) is largest, then followed by the effect of DD ($n_f \cdot n_f$), BB ($n_r \cdot n_r$), E (n_0), F (S_d), AA ($a_r \cdot a_r$), C (a_f), D (n_f), DE ($n_f \cdot n_0$), CD ($a_f \cdot n_f$), B (n_r), EE ($n_0 \cdot n_0$) and FF ($S_d \cdot S_d$).

After determining the influence of the input factor on surface roughness and then remove the negligible influence factors. The regression equation coefficients are determined by using Minitab R19 software. The calculated results are shown in Table4.

TABLE 4.THE ESTIMATED COEFFICIENTS OF INPUT PARAMETERS AND THEIR INTERACTION

Coded Coefficients

Term	Coef	SE Coef	T-Value	P-Value	VIF
Constant	0.2135	0.0132	16.14	0.000	
a_r	-0.00871	0.00661	-1.32	0.196	1.00
n_r	-0.01604	0.00661	-2.43	0.020	1.00
a_f	-0.02238	0.00661	-3.38	0.002	1.00
n_f	-0.02058	0.00661	-3.11	0.003	1.00
n_0	-0.02858	0.00661	-4.32	0.000	1.00
S_d	0.02833	0.00661	4.28	0.000	1.00
$a_r \cdot a_r$	0.0346	0.0101	3.42	0.001	1.30
$n_r \cdot n_r$	0.0540	0.0101	5.34	0.000	1.30
$a_f \cdot a_f$	0.1122	0.0101	11.10	0.000	1.30
$n_f \cdot n_f$	0.0589	0.0101	5.83	0.000	1.30
$n_0 \cdot n_0$	-0.0221	0.0101	-2.19	0.034	1.30
$S_d \cdot S_d$	-0.0220	0.0101	-2.17	0.036	1.30
$a_f \cdot n_f$	0.0279	0.0115	2.43	0.020	1.00
$n_f \cdot n_0$	0.0279	0.0115	2.43	0.020	1.00

Model Summary

S	R-sq	R-sq(adj)	R-sq(pred)
0.0324025	86.82%	82.09%	74.33%

The regression equation of surface roughness is described by the following model:

Regression Equation in Uncoded Units

$$Ra = 1.076 - 21.61a_r - 0.0890n_r - 99.77a_f - 0.1110n_f - 0.0061n_0 + 0.320S_d + 346a_r \cdot a_r + 0.01350n_r \cdot n_r + 4486a_f \cdot a_f + 0.01474n_f \cdot n_f - 0.00553n_0 \cdot n_0 - 0.0879S_d \cdot S_d + 2.79a_f \cdot n_f + 0.00697n_f \cdot n_0$$

Based on the determined regression equation, the calculate the optimal value of the input parameters to achieve the minimum surface roughness is determined by Minitab R19 software.

TABLE 5.THE CALCULATED OF THE OPTIMAL VALUE OF THE INPUT PARAMETERS

Solution

Solution	a_r	n_r	a_f	n_f	n_0	S_d	Ra Fit	Composite Desirability
1	0.03131	3.3030	0.01056	1.8182	4	1	0.1092	1

From the optimal calculation results in table 5, an optimal set of dressing condition parameters can be obtained to achieve the smallest surface roughness based on the adjustment range of the machine are $a_r = 0.03$ mm, $n_r = 3$ times, $a_f = 0.01$ mm, $n_f = 2$ times, $n_0 = 4$ times and $S_d = 1$ m/min. The predicted value of Ra corresponding to optimum dressing condition is 0.1123 μ m.

IV. CONCLUSION

The current study presents the optimization to achieve the minimum surface roughness with the optimum dressing condition when external cylindrical grinding. The response surface method and ANOVA are applied to find the orthogonal array for the experimental plan. The following conclusions can be made:

- All of the dressing parameters investigated affect surface roughness. Among them, the quadratic effect of CC ($a_f \cdot a_f$) is largest, and then followed by the effect of DD ($n_f \cdot n_f$), BB ($n_r \cdot n_r$), E (n_0), F (S_d), AA ($a_r \cdot a_r$), C (a_f), D (n_f), DE ($n_f \cdot n_0$), CD ($a_f \cdot n_f$), B (n_r), EE ($n_0 \cdot n_0$) and FF ($S_d \cdot S_d$).
- The regression equation for the relationship between dressing parameters and surface roughness is determined as follows:

$$Ra = 1.076 - 21.61a_r - 0.0890n_r - 99.77a_f - 0.1110n_f - 0.0061n_0 + 0.320S_d + 346a_r \cdot a_r + 0.01350n_r \cdot n_r + 4486a_f \cdot a_f + 0.01474n_f \cdot n_f - 0.00553n_0 \cdot n_0 - 0.0879S_d \cdot S_d + 2.79a_f \cdot n_f + 0.00697n_f \cdot n_0$$

- The optimum dressing condition is determined to be $a_r = 0.03$ mm, $n_r = 3$ times, $a_f = 0.01$ mm, $n_f = 2$ times, $n_0 = 4$ times and $S_d = 1$ m/min. And the optimum value of surface roughness is $0.1123 \mu\text{m}$.

ACKNOWLEDGMENT

The authors wish to thank Thai Nguyen University of Technology for supporting this work.

REFERENCES

- [1] Jackson, M.J. and J.P. Davim, "Machining with abrasives". 2011: Springer.
- [2] Malkin, S. and C. Guo, "Grinding technology: theory and application of machining with abrasives". 2008: Industrial Press Inc.
- [3] King, R.I. and R.S. Hahn, "Handbook of modern grinding technology". 2012: Springer Science & Business Media.
- [4] Koeshardono, F. and S. Khairunnisa. "Effect of feeding and depth of cut on surface roughness in truing and dressing process using cylindrical grinding machine". in AIP Conference Proceedings. 2019. AIP Publishing LLC.
- [5] Cao, H., X. Chen, and H.J.T.I.J.o.A.M.T. Li, "Dressing strategy and grinding control for cylindrical microstructural surface". 2018. **99**(1): p. 707-727.
- [6] Chen, X., et al., "A grinding power model for selection of dressing and grinding conditions". 1999.
- [7] Puerto, P., et al., "Evolution of surface roughness in grinding and its relationship with the dressing parameters and the radial wear". 2013. **63**: p. 174-182.
- [8] Giang, T.N., et al. "Studying the Influence of Dressing Parameters on the Surface Roughness when Conducting the External Grinding of SKD11 Steel". in Solid State Phenomena. 2021. Trans Tech Publ.
- [9] Tran, T.H., et al. "Optimizing Dressing Conditions for Minimum Flatness Tolerance when Grinding SKD11 Tool Steel". in Materials Science Forum. 2021. Trans Tech Publ.
- [10] Hong, T.T., et al. "Multi Response Optimization of Dressing Conditions for Surface Grinding SKD11 Steel by HaiDuong Grinding Wheel Using Grey Relational Analysis in Taguchi Method. in International Conference on Engineering Research and Applications". 2020. Springer.
- [11] Tung, L.A., et al. "Optimization of dressing parameters of grinding wheel for 9CrSi tool steel using the Taguchi method with grey relational analysis". in IOP Conference Series: Materials Science and Engineering. 2019. IOP Publishing.
- [12] Hung, L.X., et al., "Multi-objective optimization of dressing parameters of internal cylindrical grinding for 9CrSi Alloy steel using Taguchi method and grey relational analysis". 2019. **18**: p. 2257-2264.
- [13] Nguyen, T.T., et al. "Influence of Dressing Parameters on Roundness Tolerance in Cylindrical External Grinding SKD11 Tool Steel". in Materials Science Forum. 2021. Trans Tech Publ.
- [14] Tu, H.X., "Investigation the Effect of Dressing Condition on Material Removal Rate in External Cylindrical Grinding 90CrSi Harden Steel", 2021, International Journal of Innovation Engineering and Science Research, volume 5 issue 2, IJIESR.
- [15] Tu, H.X., et al. "Influence of dressing parameters on surface roughness of workpiece for grinding hardened 9XC tool steel". in IOP Conference Series: Materials Science and Engineering. 2019. IOP Publishing.

Thermal Properties of Chemically Prepared Emeraldine-Base Form Polyaniline

AMER N. J AL-DAGHMAN

Department of Physics, Materials of Science, Polymer Research Center,
University of Basrah, Basrah, Iraq
amer.jarad@uobasrah.edu.iq

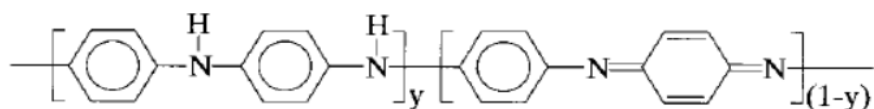
ABSTRACT

In this work, pure emeraldine base (EB)-form of Polyaniline (PANI) powder was chemically prepared in 1M HCl aqueous solution. The thermal characteristics and chemical structures of this powder were studied by differential scanning calorimetric (DSC), thermo gravimetric analysis (TGA), Fourier transform infrared spectroscopy (FTIR), and X-ray diffraction (XRD). A polarizing optical microscope was also used to examine the morphology of this sample. The results show that the EB-PANI powder had observable moisture content. Moreover, in the first run of DSC thermal analysis, the exothermic peak about 170–345°C was due to the interlocking reaction occurring among the EB-PANI molecular chains. X-ray and FTIR examinations further confirmed the chemical interlocking reaction during thermal treatment. TGA results provided that there were two major stages of weight loss for EB-PANI sample. The first weight loss, at the lowest temperature, resulted from an evaporation of moisture. The other weight loss, at the highest temperature, was due to the chemical structure degradation of the sample. Degradation temperature of the pure PANI powder was around 450°C. The degradation temperature of emeraldine salt ES-PANI was lower than 360–400°C, than that of the EB-form. From TGA results, we approximately estimated that 2.7 Aniline of repeat units, on average, were doped with 1MHCl molecule in the ES-PANI. Single crystal morphology found of EB-PANI, mostly like a conifer leaf.

Keywords-Thermal characteristics, EB-PANI, XRD, DSC, morphology

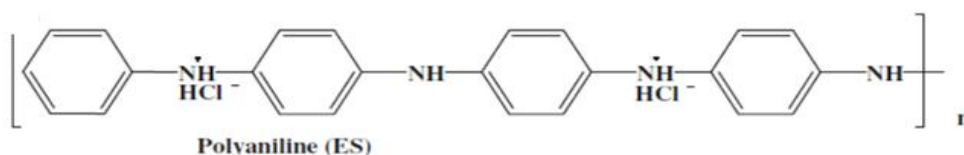
I. INTRODUCTION

Polyaniline (PANI) is one of very important member in the family of conducting polymers materials (CPs). MacDiarmid [1], a first one exemplified that the chemical structure of Polyaniline could be diagramed by the following formula:



Where the value $(1 - y)$ represents the chemical oxidation of PANI. The value of y can be varied from $y \sim 1$ (leucoemeraldine base LB) to $y \sim 0$ (pernigraniline base PB). If $y \sim 0.5$, the PANI is referred to as (emeraldine base EB). This form of EB-PANI cannot be dissolved in the common organic solvents. However, it can be dissolved in inorganic solvents as Chloroform and NMP. Then, pure form of PANI films can be cast from the NMP solution [2,3]. Furthermore, EB-PANI can be doped in a protonic acid, such as HCl or H₂SO₄, and transferred to emeraldine salt form as (ES-PANI), with a moderately high level conductivity up to 10–100 S.cm⁻¹. Generally, chemical oxidation method synthesis is the major way for the fabrication of PANI [4,5]. Chemical oxidation polymerization process is particularly important because this synthesis is the most feasible method for making PANI powder on a micro-scale. Due to PANI has a good environmental stability and unusually electrochemical characteristics, many of scientific applications of PANI have been studied and developed, such as rechargeable batteries [6,7] biosensors [8,9] protections of corrosion [10,11] and antistatic materials [12]. However, due to its poor thermal processing properties the commercial applications of PANI have been limited. There have been several reports focusing on the thermal and mechanical character of Polyaniline PANI. Wei [3, 4], investigated the thermal transitions and mechanical properties of films of chemical fabricated PANI. They also studied the thermal characteristics of chemical oxidative synthesized PANI with

variant dopants [13]. Chen [5] discussed the thermal analysis, chemical structure, and doping behavior of prepared PANI plasticized with HCl solvent. Stevenson [14] investigated the thermal degradation of HCl-doped EB-PANI. Gregory [15] studied thermal properties of chemical prepared PANI. Chandrakanth and Careem [16] presented study on thermal properties to examine the thermal stability of polymers material and to identify the optimum processing. In the previously studies, the polymerization method by strong of salt ionic media were almost 1M HCl Hydrochloride acid aqueous solution. Therefore, in this study, we used 1M HCl aqueous solution as the acidic polymerization media to prepare EB-PANI. A chemical structure of the ES-PANI (doped by salt ionic) can be schematically represented by the following formula:



The charged Cl⁻ group of HCl associates with the positively charged backbone of polymer chain. ES-PANI is not soluble in common organic solvents. In this work, we also estimated how many repeating units of aniline, in average, doped with 1M HCl in doped form of PANI. The results of thermogravimetric analysis (TGA). The thermal properties of the PANI were studied with differential scanning calorimetric (DSC). Then studied the crystallinity and chemical microstructure of thermally undoped and undoped PANI with x-ray diffraction (XRD) and Fourier transform infrared spectroscopy (FTIR), respectively. Through these studies, the thermal stability of EB-PANI could be estimated in more detail. Moreover, to our knowledge, study morphology of EB-PANI crystalline from solution was not to show. Therefore, in this study, we fabricated 0.1wt % EB-PANI in HCl acid and observed the crystalline structure of EB-PANI. Three-necked flat-bottomed reactor was used to fabricate the PANI polymer. A stirrer was put in the reactor to ensure proper mixing. After that, solution A was placed into an ice bath, which contained salt and was equipped with a thermometer. After that temperature of solution A was cooled to 0°C, solution B was then slowly added drop by drop into solution A over a period of 3h. The oxidation process of aniline is highly an exothermic; the addition rate of solution B was properly controlled to prevent any sharp temperature increase because of the polymerization reaction. After 24 h, the precipitated dark green ES-form of Polyaniline was recovered from the reaction mixture. Furthermore, the precipitate was filtered and washed again with methanol until the methanol filtrate was colorless to remove any other byproducts. Then, the prepared ES-PANI was converted to EB-form PANI by stirring with 1M NH₄OH Hydroxide Ammonium solution at room temperature overnight. At the end of the stirring, the material was filtered and dried under a vacuum oven for 48 h. Finally, 6.41 g of the dark blue EB-PANI powder.

II. MATERIALS AND REQUIREMENTS

We have used the following chemical materials for synthesis Polyaniline. All chemicals materials used here were the highest purity available, which their supplier companies and the purpose for used were listed in Table (1).

Table 1: Chemicals materials and their supplier companies.

No.	Chemical Materials	Molecular weight (g/Mole)	The Origin Company
1-	Aniline hydrochloric (C ₆ H ₅ NH ₂ .HCl)	93.13	Merck Schuchardt, Germany
2-	Ammonium persulphate (NH ₄) ₂ S ₂ O ₈	228.20	Merck KGaA, Germany
3-	Hydrochloride Acid (HCl)	36.46	BRIGHTCHEM, Penang, Malaysia

III. EXPERIMENTAL PROCEDURES

In this work, EB-PANI was prepared by chemical oxidative method with ammonium persulphate as oxidative agent on the procedure described [2, 5]. Two solutions were prepared previously. Solution 1 was of 1M HCl aqueous solution containing 0.46M of aniline. Solution 2 was 1M HCl aqueous solution

containing 20g of ammonium persulphate (0.44M). A 1000ml of four-necked flat-bottomed reactor was used to prepare the PANI. A stirrer was put in the reactor to ensure proper mixing. Then, the reactor was kept under vigorously stirring. After that, solution A was poured into this reactor, which was placed into an ice-bath, which contained salt and was equipped with a thermometer. After the temperature of solution A was cooled to 0°C, solution 2 was then slowly added drop by drop into solution 1 over a period of 3 h. Because the oxidation of aniline is highly exothermic, the addition rate of solution 2 was properly controlled to prevent any sharp temperature increase because of the polymerization reaction. After 24 h, the precipitated dark green ES-PANI was recovered from the reaction mixture. Then, this material was filtered and washed with 400 mL of 0.1M HCl solution followed by 400 mL of distilled water until the filtrate was colorless. Furthermore, the precipitate was washed again with methanol until the methanol filtrate was colorless to remove oligomers and other byproducts. Then, the prepared ES-PANI was converted to EB-PANI by stirring with 400 mL of 1M NH₄OH solution at room temperature for another 24 h. At the end of the stirring, the material was filtered and dried under a vacuum oven for 48 h. Finally, 6.48 g of the dark blue EB-PANI powder was obtained.

IV. INSTRUMENTS AND MEASUREMENTS

To study morphological examination of EB-PANI powder (0.01 g) was dissolved in 10ml of Chloroform to form a dark blue solution. For polarizing optical examination, a drop of Chloroform solution containing the EB-PANI was placed onto a slide. Then, this slide was dried under a vacuum oven at 60°C for 48 h. Morphological study of the thin films of PANI was carried out using field effect scanning electron microscopy (FESEM) (Model: FEI Nova Nano SEM 450) operating at 20 kV, was used to examine the crystalline morphology of the EB-PANI. X-ray diffraction study (Model: PANalytical Xpert Pro MRD PW3040) was used to analyze different EB-PANI powder samples. Thin films samples were annealed at 350, and 450°C for 1 h, respectively, and were then left at room temperature. XRD results were obtained in a range from 10-70° (2θ position). XRD patterns were recorded with a step width of 0.02° and step time 1.25 sec by using (CuKα) radiation (λ=1.5406 Å). The patterns were analyzed by matching the observed peaks with the standard pattern provided by JCPDS file data reference. Thermal analysis studies by DSC. A differential scanning calorimeter (Shimadzu model DSC-60, USA) was used to study the thermal characters of the EB-PANI powder in a temperature range from room temperature 25-350°C at a heating rate of 30°C/min. After the first run finished, the sample pan containing the EB-PANI powder was cooled to room temperature naturally 25°C. Thermograms for these two conditions were recorded, analyzed, and compared. FTIR analysis examination for the chemical structure of EB-PANI powder was identified by FTIR (Model: Perkin Elmer Spectrum Gx, USA) in the wavenumber range 400–4000 cm⁻¹ with the number of scans equal to 10. Also, to examine the influence of thermal treatment on the chemical structure of the EB-PANI, the sample analyzed by DSC was also examined by FTIR. I prepared all of the EB-PANI samples for FTIR analysis by grinding powdery samples with KBr powder (weight ratio 1:99) and then pressing the mixture into tablets. TGA (Perkin Elmer model TGA 7, USA) was used to measure the weight loss of the EB-PANI powder in a temperature range from room temperature 25°C to 700°C at a heating rate of 30°C/min under a nitrogen stream. The weight loss of ES-PANI (HCl- doped) PANI powder in a temperature range from room temperature to 700°C at a heating rate of 30°C/min under a nitrogen stream was also examined.

V. RESULTS AND DISCUSSION

A. Morphological Examination:

Studies the morphological of chemically synthesized Polyaniline are important for investigating the intrinsic characteristics of the polymer [17]. Many of the studies [18-21] are rudimentary and exploratory in nature. The dependence of morphology upon variables such as different anions employed in the synthesis and difference in chemical procedures need to be investigated in detail. Fig 1 (a, b) shows the morphology of Polyaniline pure Emeraldine base (EB) form of powder polymer which synthesized at 0° C. FESEM photo samples taken at deep magnifications at 5µm and 10µm.

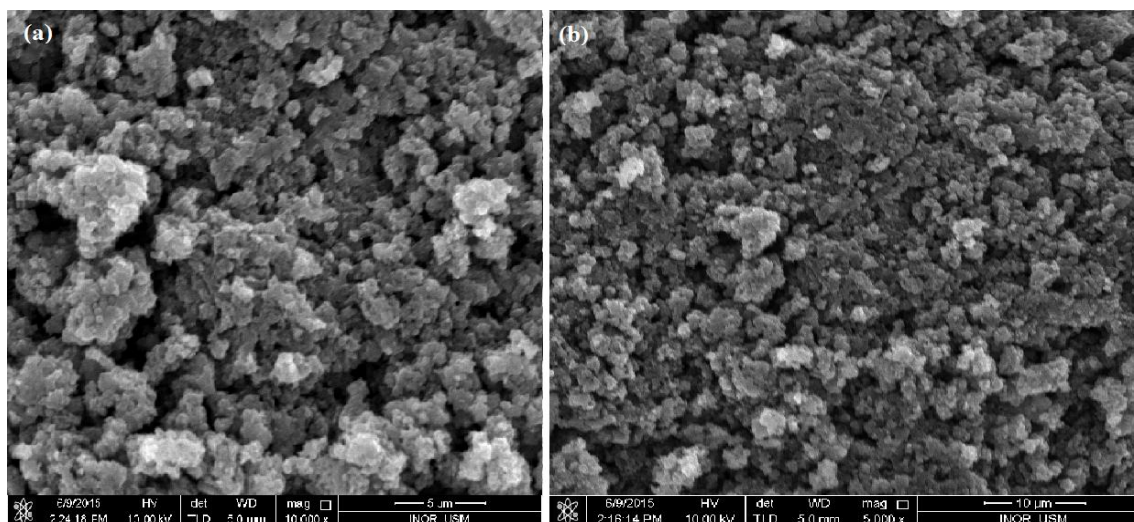


Figure1. FESEM micrographs of PANI-EB powders synthesized at
Magnification (a) 5 μm (b) 10 μm .

FESEM shows typical features of the polymer material. All photographs are mainly composed of irregularly arranged granular. Moreover, the structure behavior more porosity. FESEM aside from pictures shown in Fig. 1, illustrate the morphology of Polyaniline (EB) synthesized at 0° C. It can be seen that the Polyaniline particles have highly micro porous type morphology and is able to increase the liquid–solid interfacial area. The highly porosity nature of the polymer material and the clumped spherical morphology was confirmed with a FESEM study [22, 23].

B. XRD Analysis:

XRD patterns studies were done by using high resolution x-ray diffraction (PAN Analytical X-PERKY Pro MRD PW3040). XRD patterns were recorded in the range 2θ from 10°–70° with step width 0.02° using $\text{CuK}\alpha 1$ radiation at $\lambda = 1.5406 \text{ \AA}$. The observed diffraction peaks agreed well with the standard card of polymer with orthorhombic structure. Fig 2, representing the x-ray diffraction of immaculate Polyaniline (pure) PANI-EB demonstrates a peak at 22.73°; this means the PANI is an amorphous nature material, these outcomes are in agreement with previous studies [24– 26].

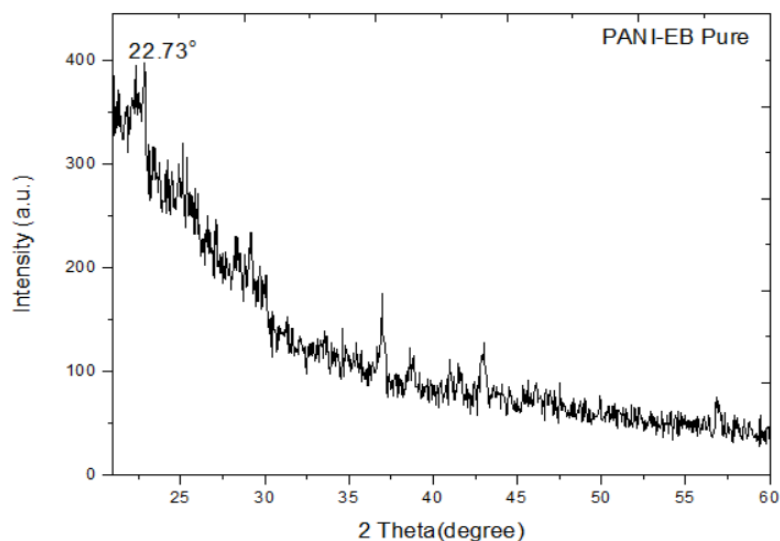


Figure2. XRD pattern of Polyaniline EB.

For polymer structure as an orthorhombic crystal can be estimated from the XRD information of all

planes at 2θ values taking into account d -dispersing values. For the specimens, the constants have been resolved and are recorded in Table 2. The interplanar crystallinity distance d and crystal size were calculated by Bragg's and Scherer Debye equations:

$$D = \frac{k\lambda}{\beta \cos \theta}$$

Where β is the full width half maximum (FWHM). The crystalline size D of the polymer is assessed with the full width half maximum FWHM intensity of the x-beam diffraction peaks at 2θ values utilizing Debye Scherer formula.

Table2: X-ray diffraction parameters of Polyaniline Samples.

Polymer	2θ (Degree)	FWHM $\beta(^{\circ})$	(hkl)	d (\AA)	D (nm)
PANI-EB	22.75	0.45	(021)	3.9	18.8

X-ray diffraction of PANI-EB and doped prepared at 0°C showed the partial crystalline state increased as the molecular weight grew. The increase was more obvious for the samples prepared at low temperature. This may indicate that chains under lower temperature conditions have less structural defects.

C. DSC Thermal Analysis:

DSC thermal analysis we have two curves are shown in Fig3. Fig 3(a) is the DSC thermogram of the EB-PANI in the first run. There were two peaks in Fig 3(a), an endothermic peak at $50^{\circ}\text{--}160^{\circ}\text{C}$ and an exothermic peak at $180\text{--}340^{\circ}\text{C}$. Therefore, the endothermic peak was most likely due to the vaporization of water. This was in agreement with the TGA results. The chemical process related to the exothermic peak was due to a crosslinking reaction. This crosslinking reaction resulted from a coupling of two neighboring -N=Q=N- groups (where Q represents the quinoid ring) to give two -NH-B-NH- groups (where B represents the benzenoid ring) through a link of the N with its neighboring quinoid ring, as suggested by Scherer et al [27]. Fig 3(b) shows the DSC thermogram of the EB-form PANI powder in the second run. There were almost no significant endothermic or exothermic peaks, as shown in Fig 3(b), because no apparent moisture existed in the sample. Moreover, a crosslinking reaction occurred during the first run DSC thermal treatment and resulted in a three dimensional chemical structure of EB-PANI. Therefore, no apparent exothermic peak was observed.

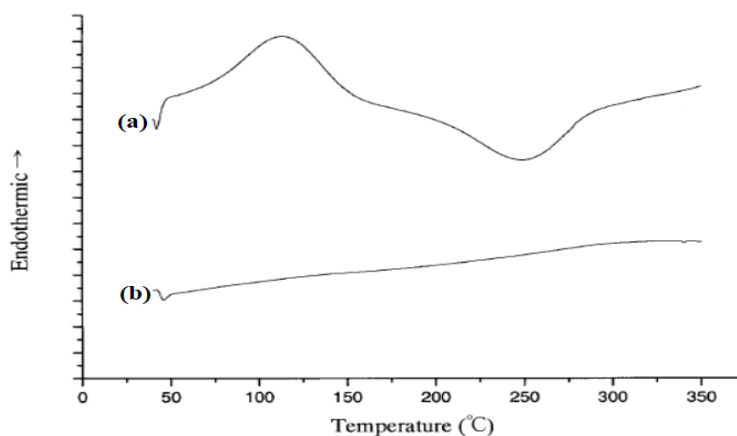


Figure 3. DSC thermal analysis curves of EB-PANI powder under N_2 gas: (a) first run, and (b) second run (Heating rate $\sim 20^{\circ}\text{C}/\text{min}$).

D. FTIR Analysis:

To investigate whether the crosslinking reaction really occurred, the FTIR examination was conducted at room temperature. Two of EB-PANI samples were examined untreated and treated by DSC thermal analysis. The results are illustrated in Fig 4. Fig 4(A) shows the FTIR results of the EB-PANI without DSC thermal analysis. Fig 4(B) shows the FTIR results of the EB-PANI powder treated by DSC thermal analysis (first run). The intensity ratios of the FTIR absorption of the C=C stretching vibration of quinoid rings (1592 cm^{-1}) to that of benzenoid rings (1508 cm^{-1}) and the electronic like absorption peak of $-N=Q=N-$ (1150 cm^{-1}) both decreased when the EB-PANI powder was treated by DSC thermal analysis. These results proved the occurrence of the crosslinking reaction from quinoid rings to benzenoid rings. Figure 3 illustrates the thermal crosslinking reaction among EB-form PANI, molecular chains [27].

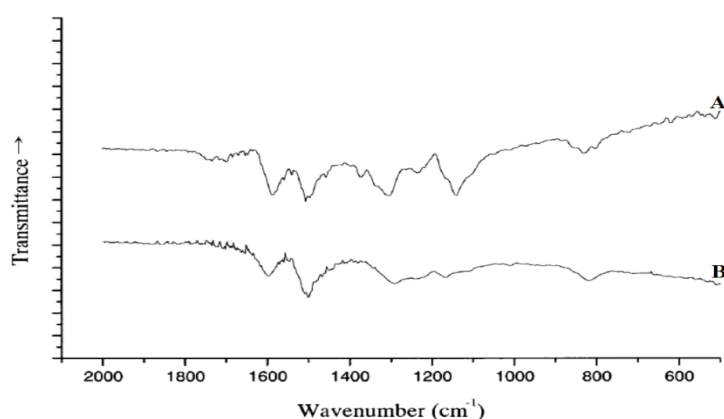


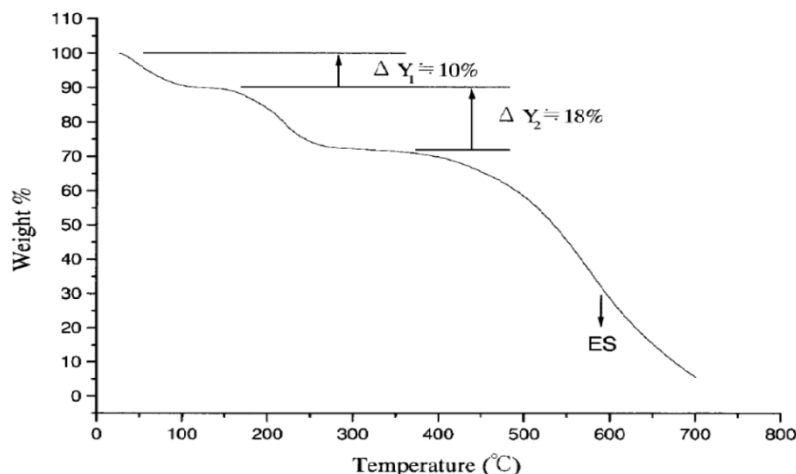
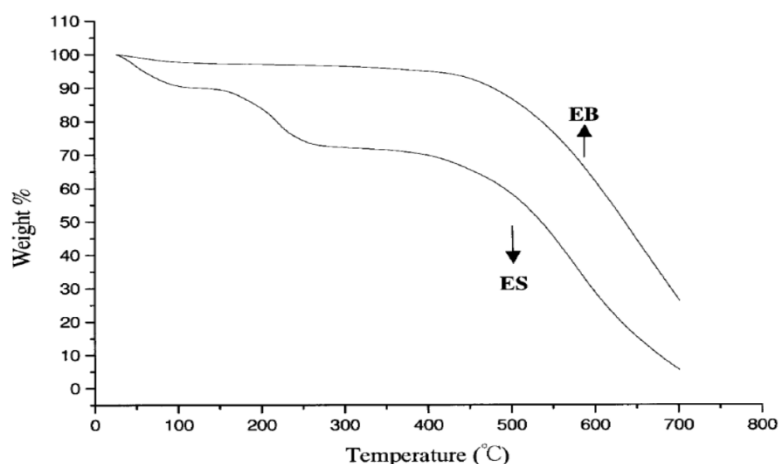
Figure 4: FTIR of EB-pure PANI: (A) unanalyzed and (B) analyzed by DSC at first run.

E. TGA Analysis:

Fig.5, shows that the moisture and HCl contents of ES-form PANI were around 10% (ΔY_1) and 18% (ΔY_2), respectively. Therefore, the weight percentage of PANI should have been around 70%. To find how many monomer aniline repeating units doped with 1 molecule in PANI, we set up eq. (1):

$$\frac{100 - \Delta Y_1 - \Delta Y_2}{\Delta Y_2} = \frac{M_1 \cdot X}{M_2 \cdot 1} \dots \dots \dots (1)$$

Where (ΔY_1) and (ΔY_2) are the weight losses of moisture and HCl, respectively; M_1 and M_2 are the molecular weights of aniline and HCl, respectively; and X is the number of aniline repeating units. Therefore, according to Eq. (1), I substituted ΔY_1 , ΔY_2 , M_1 , and M_2 with 10, 18, 92, and 63, respectively. Then, we obtained the value of X at around 2.74. This implied that there were roughly 2.8 aniline repeat units, on average, doped with 1 HCl molecule in the ES-PANI form. Fig 5 shows the TGA results of the EB-form and ES-form PANI powders under a N_2 atmosphere. For the EB-form, there were two major stages for the weight loss of the PANI sample. The first weight loss, at around 100°C , resulted from the evaporation of moisture, which was consistent with the DSC result [15]. The second weight loss, at the higher temperature, indicated chemical structure degradation of the PANI molecule; the degradation temperature was around $400\text{--}450^\circ\text{C}$. For the ES-PANI powder, there were three major stages for weight loss, around 100 , 200 , 360 and 410°C , which were assigned to the removal of moisture, HCl, and the degradation of the PANI molecule, respectively. This apparently indicated that the degradation temperature of the EB-PANI was higher than that of ES form. This may have been caused from the HCl, gas formed during the heating process; this strong acid vapor accelerated the degradation of the ES-PANI. Also, this showed that the moisture content of the ES-PANI powder was higher than that of the EB form, as shown in Fig 5.

Figure 5. TGA curve of ES-doped PANI powder under aN₂ gas (heating rate ~20°C/min).Figure 6. TGA curves of EB and ES form PANI samples under N₂ gas (heating rate ~20°C/min).

VI. CONCLUSION

FESEM images indicated that the particle size of the polymer within the micro-scale and with the presence of acid. The XRD results showed that the EB-PANI had a small amount of crystallinity. However, the annealed EB-PANI powder sample (at 250°C for 1h), there was only a broad amorphous nature as semi-crystalline structure. This phenomenon again illustrated that if the thermal energy was high enough, the chemical crosslinking reaction occurred among the EB-PANI polymer chains. The polarizing micrograph of the crystalline EB-PANI was successfully revealed. We found the single and the more complex multi-layered branched crystalline morphologies of the EB-PANI. DSC thermal analysis curves indicated that the EB-PANI had discernible moisture content. This phenomenon was in agreement with TGA results. Moreover, at the first run of the DSC thermal analysis, an exothermic peak around 170–340°C was found. This peak was due to the chain crosslinking, resulting from a coupling of two neighboring -N=Q=N- groups to give two -NH-B-NH- groups through a link of the N with its neighboring quinoid ring. The FTIR examinations further confirmed the chemical crosslinking reaction among the pure polymer chains. TGA results illustrated that the degradation temperature of the EB-PANI powder was around 450°C. Also, from the TGA curve of the ES-form PANI, we calculated that 2.74 aniline repeating units, on average, doped with HCl acid.

REFERENCES

- [1] MacDiarmid, A. G.; Chiang, J. C.; Huang, W.; Humphery, B. D.; Somasir, N. L. D. *MolCrystLiqCryst* 1985, 125, 309.
- [2] Cao, Y.; Andreatta, A.; Heeger, A. J.; Smith, P. *Polymer* 1989, 30, 2305.
- [3] Wei, Y.; Jang, G. W.; Hsueh, K. F.; Scherr, E. M.; MacDiarmid, A. G.; Epstein, A. J. *Polymer* 1992, 33, 314.
- [4] Pouget, J. P.; Laridjani, M.; Jozefowicz, M. E.; Epstein, A. J.; Scherr, E. M.; MacDiarmid, A. G. *Synth Met* 1992, 51, 95.
- [5] Chen, S. A.; Lee, H. T. *Macromolecules* 1993, 26, 3254.
- [6] Venkatachalam, S.; Prabhakaran, P. V. *Synth Met* 1998, 97, 141.
- [7] Ryu, K. S.; Kim, K. M.; Kang, S. G.; Lee, G. J.; Joo, J.; Chang, S. H. *Synth Met* 2000, 110, 213.
- [8] Parente, A. H.; Marques, E. T. A., Jr.; Azevedo, W. M.; Diniz, F. B.; Melo, E. H. M.; Lima Filho, J. L. *ApplBiochemBiotechnol* 1992, 37, 267.
- [9] Leite, V.; Dasilva, V. L.; Azevedo, W. M.; Melo, E. H. M.; Lima, Filho, J. L. *Biotechnol Tech* 1994, 8, 133.
- [10] Li, P.; Tan, T. C.; Lee, J. Y. *Synth Met* 1997, 88, 237.
- [11] Pud, A. A.; Shapoval, G. S.; Kamarchik, P.; Ogurtsov, N. A.; Gromovaya, V. F.; Myronyuk, I. E.; Kontsur, Y. V. *Synth Met* 1999, 107, 111.
- [12] Subramaniam, C. K.; Kaiser, A. B.; Gilberd, P. W.; Wessing, B. J. *PolymSci Part B: PolymPhys* 1993, 31, 1425.
- [13] Yen, W.; Kesiyin, F. H. *J PolymSci Part A: PolymChem* 1989, 27, 4351.
- [14] Traore, M. K.; Stevenson, T. K.; McCormick, B. J.; Dorey, R. C.; Shao, W.; Meyers, D. *Synth Met* 1991, 40, 137.
- [15] Ding, L. L.; Wang, X. W.; Gregory, R. V. *Synth Met* 1999, 104, 73.
- [16] Chandrakanthi, N.; Careem, M. A. *Polym Bull* 2000, 44, 101.
- [17] T.L.A.Campos,D.F.Kersting, C.A.Ferreira, *SurfaceandCoatingsTech- nology*,122, p.3(1999).
- [18] B.Wang,J.TangandF.Wang,*Synthetic Metals*,13,p.329(1986).
- [19] S.A.Chen,andT.S.Lee,*Journal of PolymerScience,PolymerLetter Edi- tion*,25,p.455(1987).
- [20] Kang,S.I.TsujiokaandK.Sakaki,*Journal ofPolymerSci- ence,PartA:PolymerChemistry*, 26,p.1531(1988).
- [21] Y.Lu,J.Li,andW.Wu,*Synthetic Metals*,30,p.87(1989).
- [22] DW Hatchett, M Josowicz, J Janata, *J. Phys. Chem. B*, 1999, 103, 10992.
- [23] “Conducting Polymers: Polyaniline Its State of the Art and Applications” Thesis master Himani Sharma, School of physics and Materials Science, Patiala, Punjab,2006
- [24] Kroschwitz, J.I., (1988),*Electrical and electronic properties ofpolymers:Astate-of-the-artcompendium*.Wiley,New York.
- [25] SinglaSajeelaAwssth, M. L.; Alooksrivava, D.V. join, S. (2007) *J. sensors and Actuators A*136, p 604.
- [26] Reka Devi, M. Lawrence, B. Prithivikumaran, N. Jeyaku, N. (2014) *International Journal of Chen Tech Research* vol.6, No.13, 5400-5403.
- [27] Scherr, E. M.; MacDiarmid, A. G.; Manohar, S. K.; Masters, J. G.; Sun, Y.; Tang, X.; Druy, M. A.; Glatkowski, P. J.; Cajipe, V. B.; Fischer, J. E.; Cromack, K. R.; Jozefowicz, M. E.; Ginder, J. M.; McCall, R. P.; Epstein, A. J. *Synth Met* 1991, 41, 735.